

**CHARACTERIZATION OF AN ULTRA-HIGH
PERFORMANCE CONCRETE**

BY

IBRAHIM YAHYA AHMED HAKEEM

A Thesis Presented to the
DEANSHIP OF GRADUATE STUDIES

KING FAHD UNIVERSITY OF PETROLEUM & MINERALS

DHAHRAN, SAUDI ARABIA

In Partial Fulfillment of the
Requirements for the Degree of

MASTER OF SCIENCE

In

CIVIL ENGINEERING

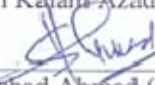
MAY, 2011

KING FAHD UNIVERSITY OF PETROLEUM & MINERALS
DHAHRAN 31261, SAUDI ARABIA
DEANSHIP OF GRADUATE STUDIES

This thesis, written by **Ibrahim Yahya Ahmed Hakeem** under the direction of his thesis advisor and approved by his thesis committee, has been presented to and accepted by the Dean of Graduate Studies, in partial fulfillment of the requirements for the degree of **MASTER OF SCIENCE IN CIVIL ENGINEERING**

Thesis Committee


Prof. Abul Kalam Azad (Advisor)



Dr. Shamshad Ahmad (Co-Advisor)


Dr. Husain J. Al-Gahtani (Member)


Dr. Muhammed Maslehuddin (Member)


Dr. Ahmad S. Al-Gahtani (Member)


30 MAY 2011
Dr. Nedal T. Ratrouf
(Department Chairman)


Dr. Salam A. Zummo
(Dean of Graduate Studies)



13/6/11
Date



Dedicated

to

My beloved parents, wife and children

For their love, sacrifices and prayers

ACKNOWLEDGMENT

Praise and thanks a lot Allah Almighty, for giving me the health, knowledge and patience to complete this work. I acknowledge the financial support given by Aden University and by KFUPM's Civil Engineering Department during my graduate studies.

My sincerest gratitude goes to my advisor Prof. Abul Kalam Azad and co-adviser Dr. Shamshad Ahmad. I am also grateful to my Committee Members, Dr. Husain Jubran Al-Gahtani, Dr. Mohammed Maslehuddin and Dr. Ahmad S. Al-Gahtani, for their constructive guidance and support. Thanks are also to the department's Chairman Dr. Nedal T. Ratrouf and his secretary for providing aid, and to other staff members of the department especially the lab supervisor, Dr. Essa, and the technicians: Mr. Omar, Mr. Mukaram, and Mr. Emran, for their help.

Deep thanks are to the research institute team, the researchers: Mr. Shameem, Mr. Bary, and Mr. Ibrahim, for their help and supplying with needed instruments.

Special thanks are due to my 'real' brother Dr. Nazih Fadel at Aden University for his continuous moral support, encouragement and guidance during all my study.

My heartfelt gratitude is given to my beloved wife, and my children, who always support me with their love, patience, encouragement and constant prayers. I would like to thank brother, sisters, and all members of my family in Yemen.

TABLE OF CONTENTS

ACKNOWLEDGMENT	iv
List of Tables	viii
List of Figures.....	x
THESIS ABSTRACT (English).....	xiv
THESIS ABSTRACT (Arabic).....	xvii
CHAPTER 1 INTRODUCTION.....	1
1.1 General.....	1
1.2 Principles of Developing UHPC	4
1.3 Ductal	5
1.4 Applications	11
1.5 Scope and Objectives	12
CHAPTER 2 LITERATURE REVIEW	15
2.1 Mechanical Properties	15
2.1.1 <i>Compressive Strength</i>	15
2.1.2 <i>Flexural Strength and Toughness</i>	16
2.1.3 <i>Drying Shrinkage</i>	18
2.1.4 <i>Fracture Energy</i>	19
2.2 Durability Performance.....	20
2.2.1 <i>Porosity</i>	20
2.2.2 <i>Chloride Ions Penetration</i>	21
CHAPTER 3 EXPERIMENTAL PROGRAM.....	23
3.1 General.....	23
3.2 Test Program Details	23
3.2.1 <i>Cyclic Exposure</i>	25
3.2.2 <i>Test Schedule</i>	25
3.3 Ductal Mixing Procedure	30
3.4 Casting and Curing.....	33
3.5 Compressive Strength and Modulus of Elasticity Testing.....	34
3.5.1 <i>Compressive Strength</i>	34

3.5.2	<i>Modulus of Elasticity</i>	35
3.6	Tensile Properties of Ductal	36
3.6.1	<i>Flexural Properties</i>	36
3.6.2	<i>Mortar Briquette (Direct Tension Test)</i>	44
3.6.3	<i>Split Tensile Strength</i>	45
3.7	Drying Shrinkage	46
3.8	Water Absorption	47
3.9	Water Permeability	48
3.10	Rapid Chloride Ion Penetrability	49
3.11	Chloride Diffusion	51
3.12	Fracture Toughness	52
3.12.1	<i>General</i>	52
3.12.2	<i>Fracture Parameters</i>	55
3.12.3	<i>Fracture Energy</i>	60
CHAPTER 4 RESULTS AND DISCUSSION		62
4.1	Compressive Strength and Modulus of Elasticity	62
4.1.1	<i>Compressive Strength</i>	62
4.1.2	<i>Modulus of Elasticity</i>	69
4.2	Tensile Properties of Ductal	73
4.2.1	<i>Flexural Properties</i>	73
4.2.1.1	<i>Effect of Curing</i>	73
4.2.1.2	<i>Effect of Exposure Conditions</i>	78
4.2.1.3	<i>Effect of Fiber</i>	80
4.2.2	<i>Mortar Briquette Test (Direct Tension Test)</i>	89
4.2.3	<i>Split Tensile Strength</i>	91
4.3	Drying Shrinkage	93
4.4	Water Absorption	94
4.5	Water Permeability (DIN Test)	95
4.6	Rapid Chloride Ion Penetrability Testing	95
4.7	Chloride Diffusion	96
4.8	Fracture Toughness Test Results	98
4.8.1	<i>Fracture Energy</i>	103
CHAPTER 5 MICROSTRUCTURAL INVESTIGATION OF DUCTAL		106

5.1	General.....	106
5.2	Scanning Electron Microscope (SEM)	106
5.3	X-ray Diffraction (XRD).....	111
CHAPTER 6 UTILIZATION OF DUCTAL CONCRETE		113
CHAPTER 7 CONCLUSIONS AND RECOMMENDATIONS.....		115
7.1	Conclusions	115
7.2	Recommendations for Future Studies	117
CHAPTER 8 REFERENCES.....		118
APPENDICES		125
APPENDIX A	Compressive Strength and Modulus of Elasticity Results.....	126
APPENDIX B	Fracture Toughness Test Results	130
APPENDIX C	Flexural Strength Test Results	146
VITAE		160

LIST OF TABLES

	Title	Page
Table 1.1:	Properties of UHPC compared with high strength concrete (Lubbers, 2003).....	3
Table 1.2:	Ductal mix proportions	11
Table 3.1:	Details of specimens required for various tests on Ductal® concrete	24
Table 3.2:	Exposure conditions.....	25
Table 3.3:	Testing schedule	27
Table 3.4:	Ductal mix proportions	30
Table 4.1:	Average compressive strength results of Ductal with different percentage of fibers and curing time and methods	63
Table 4.2:	Compressive strength of Ductal subjected to three exposure conditions (6.2% steel fibers).....	63
Table 4.3:	Modulus of elasticity of Ductal at different curing time and exposure conditions.....	69
Table 4.4:	Modulus of elasticity of Ductal at different fiber content and curing methods.....	71
Table 4.5:	Average flexural toughness parameter for water-cured specimens (6.2% fibers)	75
Table 4.6:	Average flexural toughness parameter for exposure specimens (6.2% fibers)	80
Table 4.7:	Average flexural toughness parameter for 28 days water- cured specimens with different percentage of fibers	83
Table 4.8:	Comparison of the average first peak strength of different ages and different fiber contents and different exposure conditions	85
Table 4.9:	Average flexural properties of Ductal cured in water for 7 and 28 days	86
Table 4.10:	Average flexural properties of specimens contained different fiber contents and cured in water for 28 days	86
Table 4.11:	Average flexural properties of Ductal subjected to different curing conditions for 6 months after curing in water for 28 days	87
Table 4.12:	Average mortar briquette test for Ductal at 28 days water curing	89

Table 4.13:	Average splitting tensile strength of Ductal.....	91
Table 4.14:	Average water absorption of Ductal specimens.....	94
Table 4.15:	Average rapid chloride ion penetrability results.....	95
Table 4.16:	Average water soluble chloride contents of Ductal	96
Table 4.17:	Average fracture toughness test results for 28-day water-cured specimens.....	101
Table 4.18:	Average fracture toughness test results for heat-cool cycled and control specimens of Ductal (6.2% fibers).....	101
Table 4.19:	Average critical energy release rate (G_f) and total fracture energy (GF) for Mode I at 28 days water curing	103
Table 4.20:	Average critical energy release rate (G_f) and total fracture energy (GF) for Mode I of Ductal (6.2% fibers).....	104

LIST OF FIGURES

	Title	Page
Figure 1.1:	Evolution of the resistance of concrete over the last century (Lafarge website)	6
Figure 1.2:	A comparison of Ductal matrix to normal concrete and high performance concrete matrices (Lafarge website)	7
Figure 1.3:	A comparison of the differences in matrix structures between conventional concrete and Lafarge’s Ductal North America, Inc. (Woodworth, 2008).....	9
Figure 1.4:	Effect of short and long fibers on micro and macro cracks (presentation of Walraven, 2007)	10
Figure 1.5:	Sherbrooke footbridge, Canada, 1997	12
Figure 1.6:	Seonyu footbridge, Korea, 2003 (8th Hitachi EU Science and Technology Forum, Athens, May 20-22, 2005) Arch span 120 m deck thickness 3 cm.....	13
Figure 1.7:	LRT Train Station, Shawnessy, Canada, 2003 (Images from Lafarge) Canopies 5×6 m, 2 cm thick, supported on single columns.....	13
Figure 2.1:	Typical flexural strength test curves of four types of concrete (Lukasik, 2005).....	17
Figure 3.1:	HOBART planetary mixer.....	31
Figure 3.2:	a) Ductal premix powder inside the mixer; b) Ductal after addition of water and half of super plasticizer(first turning point); c) Ductal after addition of another half of superplasticizer (second turning point); during addition of steel fibers; e) casting of Ductal in cubes; casting of Ductal in prism.....	32
Figure 3.3:	Impact table measurement of Ductal flow	33
Figure 3.4:	Ductal cylinders after failure under compression test.....	35
Figure 3.5:	Specimens of Ductal with strain gauges for measuring modulus of elasticity	36
Figure 3.6:	Schematic of the loading and measuring system for four-point bending	38
Figure 3.7:	Flexural strength test using four-point bending	39
Figure 3.8:	Definition of toughness index according to ASTM C 1609	40

Figure 3.9:	Flexural toughness description according to PCS method	43
Figure 3.10:	Mortar Briquette specimens of Ductal after testing	44
Figure 3.11:	Mortar briquette setup including test grips and specimen	45
Figure 3.12:	Split cylinder tensile test on Ductal	46
Figure 3.13:	Drying shrinkage measurements by multi-length dial gauge.....	47
Figure 3.14:	Water penetration test setup.....	49
Figure 3.15:	Experimental setup to determine the Rapid Chloride Ion Penetrability	50
Figure 3.16:	Coated specimens utilized for chloride diffusion test.....	51
Figure 3.17:	Details of attaching clip gauge to Ductal prism which measures crack mouth opening displacement (CMOD).....	54
Figure 3.18:	Complete test setup for measuring fracture toughness of Ductal prisms.....	55
Figure 3.19:	Loading and unloading compliance C_i and C_u	58
Figure 3.20:	Close-up view of fracture toughness test.....	59
Figure 3.21:	Bridging effect of fibers during the fracture test	59
Figure 4.1:	Evolution of compressive strength	65
Figure 4.2:	Failure mode of Ductal without fiber (0% fibers).....	66
Figure 4.3:	Failure mode of Ductal (6.2% fibers)	67
Figure 4.4:	Average compressive strength after 6 months of exposure	68
Figure 4.5:	Effect of curing time and exposure conditions on the modulus of elasticity of Ductal	70
Figure 4.6:	Effect of fiber contents on the modulus of elasticity of Ductal	71
Figure 4.7:	Selected stress-strain responses for 28 days water-cured Ductal (6.2% fibers) specimens.....	72
Figure 4.8:	Load-deflection curves for three similar specimens tested after 7 days water curing	74
Figure 4.9:	Load-deflection curves for three similar specimens tested after 28 days water curing	74
Figure 4.10:	MOR of Ductal cured in water for 7 and 28 days.....	77

Figure 4.11:	Flexural toughness of Ductal cured in water for 7 and 28 days.....	77
Figure 4.12:	Load-deflection plots for three specimens tested after 6 months of normal exposure (control).....	78
Figure 4.13:	Load-deflection plots for three specimens tested after 6 months of wet-dry cycles.....	79
Figure 4.14:	Load-deflection plots for three specimens tested after 6 months of heat-cool cycles.....	79
Figure 4.15:	MOR of Ductal subjected to different exposure conditions for 6 months after 28 days of water-curing.....	81
Figure 4.16:	Flexural toughness of Ductal subjected to different exposure conditions for 6 months after 28 days of water-curing.....	81
Figure 4.17:	Load-deflection curves for three similar specimens of Ductal (with 3.1% fiber) tested after 28 days water curing.....	82
Figure 4.18:	Load-deflection curves for three similar specimens of Ductal (with 0% fiber) tested after 28 days water curing.....	82
Figure 4.19:	MOR of specimens with different fiber contents and cured in water for 28 days.....	84
Figure 4.20:	Flexural toughness of specimens with different fiber contents and cured in water for 28 days.....	84
Figure 4.21:	Residual flexural strength (ASTM C 1609) of Ductal (6.2% fibers) cured in water for 7 and 28 days.....	88
Figure 4.22:	Residual flexural strength (ASTM C 1609) of specimens with different fiber contents and cured in water for 28 days.....	88
Figure 4.23:	Residual flexural strength (ASTM C 1609) of Ductal subjected to different exposure conditions for 6 months after 28 days of water-curing....	89
Figure 4.24:	Load-cross head displacement plots for 28 days water-cured (6.2% steel fibers).....	90
Figure 4.25:	Load-cross head displacement plots for 28 days air-cured (6.2% steel fibers).....	90
Figure 4.26:	Average splitting strength against exposure conditions.....	92
Figure 4.27:	Mode of failure after splitting tensile test.....	93
Figure 4.28:	Drying shrinkage in micro strain with time after 28-day water curing.....	94

Figure 4.29:	Chloride concentrations Cl% of Ductal mass versus depth from the exposed face after 4 months.....	97
Figure 4.30:	Chloride concentrations Cl% of Ductal mass versus depth from the exposed face after 6 months.....	97
Figure 4.31:	Selected loading and unloading deflections for 28-day water-cured (6.2% fibers)	99
Figure 4.32:	Selected loading and unloading deflections for 28-day water-cured (6.2 % fibers)	99
Figure 4.33:	Critical stress intensity factor (K_{ic}) vs. fiber content after 28 days water curing	102
Figure 4.34:	Critical stress intensity factor (K_{ic}) vs. exposure condition of Ductal (6.2% fibers)	103
Figure 4.35:	Total fracture energy vs. percentage of fibers	105
Figure 4.36:	Total fracture energy vs. exposure condition of Ductal (6.2% fibers).....	105
Figure 5.1:	SEM image for heat-cool cycle specimen around the fiber	107
Figure 5.2:	SEM image for non-heat treated specimen around the fiber	108
Figure 5.3:	SEM image for cementitious matrix of heat-cool treated specimen (100 μ m \times 150)	109
Figure 5.4:	SEM image for cementitious matrix of non -heat-treated specimen (100 μ m \times 160)	109
Figure 5.5:	SEM image for cementitious matrix of heat-cool treated specimen (10 μ m \times 1000)	110
Figure 5.6:	SEM image for cementitious matrix of non-heat treated specimen (10 μ m \times 1000)	110
Figure 5.7:	X-RD results of Ductal matrix	112

THESIS ABSTRACT

NAME: IBRAHIM YAHYA AHMED HAKEEM

TITLE: *CHARACTERIZATION OF AN ULTRA-HIGH PERFORMANCE CONCRETE*

DEPARTMENT: CIVIL ENGINEERING

DATE: May, 2011

Ductal® is a proprietary ultra-high performance concrete (UHPFRC) cooperatively developed by three companies Lafarge, Bouygues, and Rhodia in France. Ductal is claimed to be a technological breakthrough UHPFRC, offering very high compressive strength exceeding 200 MPa and flexural tensile strength exceeding 30 MPa, ductility like plastic or wood, durability like stone, and the aesthetic like ceramics. This new technology offers the possibility to build structural elements without passive reinforcements and to combine innovative applications, lightness, and excellent durability.

Ductal concrete is produced using materials commonly found in concrete: cement, silica fume, sand, superplasticizer and water, as well as some materials unique to Ductal: ground quartz and fibers. The various Ductal formulations are all based on an optimized proportioning, combining homogeneity and granular compacted density to satisfy rheological criteria (excellent workability and self-placing capability), mechanical criteria (very high compressive strength and non-brittle tensile behavior) and durability criteria (near-total invulnerability to all conventional aggressions).

In the light of this new development in concrete, an exploratory work was undertaken to study this material and examine its potential use as a construction and repair material in Saudi Arabia. An experimental program was planned to prepare Ductal concrete using imported Ductal materials and measure its basic mechanical properties and durability. The findings of this study are presented in this thesis work, which covers in detail all aspects of work carried out.

The experimental work focused on measuring properties and performance on two fronts: (a) physical and mechanical properties and (b) properties and performance related to durability. With regard to physical and mechanical properties, the following were obtained:

- Compressive strength: 28-day strength exceeds 160 MPa. Strength increases in heat-cool cycles.
- Flexural tensile strength determined from four-point bend tests shows a value of about 31 MPa.
- Splitting tensile strength shows a value of 12.6 MPa after 28 days of water curing.
- Modulus of elasticity is about 57 GPa.
- Stress intensity factor, $K_{Ic} = 16.8 \text{ MPa}\sqrt{\text{m}}$ and fracture energy = 31.6 kN/m.
- Drying shrinkage = 300×10^{-6} after 28-day water curing.
- Water absorption is almost negligible at about 0.1%.
- Water permeability measured using DIN test showed virtually no depth of water penetration.
- Rapid chloride permeability tests showed negligible readings.

Durability of Ductal was examined by using three exposure conditions for a period of 6 months: (a) exposure to laboratory conditions, (b) exposure to alternate heat-cool cycles (heating at 60°C for 2 days and then cooling at room temperature for 2 days), and (c) exposure to alternate wet-dry cycles (wetting for 2 days in sabkha type solution and then drying at 30°C for 2 days).

The tests conducted on the cycled specimens showed the following results:

- There is a slight gain in compressive strength for specimens subjected to heat-cool cycles.
- Heat-cool cycles also increased stress intensity factor (K_{ic}) and fracture energy, and reduced water absorption.
- Cyclic exposure did not show any noticeable change in water permeability and rapid chloride permeability.

The study affirms the claim by the manufacturers that Ductal has excellent physical and mechanical properties and it is a highly durable material in aggressive environment. The drawbacks for this material for a widespread application are its relatively much higher cost, controlled mixing and difficulty in finishing the surface by conventional trowelling and floating operation. The product can be utilized in special construction where weight and durability are major concerns.

MASTER OF SCIENCE DEGREE
KING FAHD UNIVERSITY OF PETROLEUM AND MINERALS
DHAHRAN, SAUDI ARABIA

ملخص الرسالة

الإسم : ابراهيم يحي احمد حكيم

عنوان الرسالة : توصيف الخرسانه العاليه الاداء
التخصص : الهندسة المدنية

تاريخ التخرج : مايو 2011م

يعتبر Ductal® ملكيه مسجله من الخرسانه العاليه الاداء و الجوده (UHPC) وقد طور بالتعاون بين ثلاث شركات , Rhodia و Bouygues, Lafarge في فرنسا. Ductal® هو انجاز تكنولوجي للخرسانه العاليه الاداء والجوده (UHPC) حيث يعطي قوه ضغط عاليه جدا تتجاوز 200 ميجاباسكال وقوه شد الانحناء تزيد عن 30 ميجاباسكال، و الليونه مثل البلاستيك او الخشب، وديمومه مثل الصخر، ومظهرا جماليا كالسيراميك.

هذه التكنولوجيا الجديده توفر امكانيه بنا العناصر الانشائيه بدون حديد تسليح و تجمع بين التطبيقات المبتكره، و الخفه و الديمومه الممتازه. ويتم انتاج هذه الخرسانه باستخدام مواد شائعه في الخرسانه : مثل الاسمنت، وغبار السيليكيا، و الرمل، و المضاف العالي الملدن، والماء فضلا عن بعض المواد الفريده والخاصه ب Ductal® مثل الكوارتز المسحوق والالياف. و تستند جميع صيغ Ductal® على التناسب الامثل و الجمع بين التجانس و الكثافه المدكوكه وذلك لتلبيه معايير الريولوجيه (قابليه تشغيل ممتازه وقدره وضع ذاتيه)، ومعايير ميكانيكيه (قوه ضغط عاليه جدا وسلوك شد غير هش)، و معايير الديمومه (مقاومه شبه كامله لجميع الاعتداءات التقليديه).

و في ضوء هذا التطور الجديد في الخرسانه، فقد تم تنفيذ هذا العمل الاستكشافي لدراسه هذه ماده و النظر في استخدامها كماده انشاء واصلاح في المملكه العربيه السعوديه. و قد تم عمل برنامج اختبارات لاعداد خرسانه Ductal® وذلك باستخدام مواد مستورده وقياس الخواص الميكانيكيه و الديمومه. و قد تم عرض نتائج هذه الدراسه في هذه الرساله، والتي تغطي بالتفصيل جميع جوانب العمل المنجز.

وقد تركز برنامج الاختبارات على قياس الخواص والاداء على جبهتين : (ا) الخواص الفيزيائية و الميكانيكية، (ب) الخصائص والاداء المتعلق بقياس الديمومه. و فيما يتعلق بالخصائص الفيزيائية و الميكانيكية، فقد تم الحصول على مايلي:

- قوه الضغط تجاوزت 160 ميجاباسكال بعد 28 يوما. وتزداد القوه في دورات الحراره-البروده.
- قوه شد الانحناء من اختبارات التحميل على اربع نقاط اظهرت حوالي 31 ميجاباسكال.
- قوه شد الفصل اظهرت قيمه 12.6 ميجاباسكال بعد 28 يوما . وتزداد القوه في دورات الحراره-البروده.
- معامل المرونه حوالي 57 ميجاباسكال بعد 28 يوما.
- معامل شده الاجهاد، Kic كان 16.8 ميجاباسكال بعد 28 يوما و طاقه الكسر 31.6 كيلونيوتن/متر.
- الانكماش الجاف اظهر قيمه 300×10^{-6} بعد 28 يوما.
- امتصاص الماء يكاد لا يذكر، حوالي 0.1 %.
- قياس نفاذيه الماء باستخدام اختبار DIN اظهر عمليا ان لا وجود لاختراق الماء.
- اختبار نفاذيه الكلوريد السريع اظهر قراءات ضئيله جدا.

تم فحص ديمومه Ductal® وذلك باستخدام ثلاث حالات تعريض لمدته سته اشهر: (ا) التعرض لظروف المختبر، (ب) التعرض لدورات حراره – بروده متعاقبه (تسخين بدرجه حراره 60 درجه مئوية لمدته يومين ثم التبريد بدرجه حراره الغرفه ليومين)، (ج) التعرض لدورات ترطيب – جفاف متعاقبه (ترطيب لمدته يومين بمحلول السبخه ثم التجفيف بدرجه حراره 30 درجه مئوية لمدته يومين) .

و قد اظهرت التجارب التي اجريت على عينات الدورات النتائج التاليه:

- هناك ارتفاع في قوه الضغط للعينات المعرضه لدورات الحراره – البروده.
- دورات الحراره – البروده ايضا زادت من معامل شده الاجهاد (Kic) وطاقه الكسر، وانخفاض في امتصاص الماء.

- لم تظهر دورات التعرض اي تغير ملحوظ في نفاذيه المياه و نفاذيه الكلوريد السريع.

تؤكد هذه الدراسه الادعاء من قبل الشركات المصنعه ان Ductal® يمتلك خصائص فيزيائيه و ميكانيكيه ممتازه و هي ماده ذات ديمومه عاليه في البيئه العدوانيّه. عيوب هذه الماده لاستخدامها على نطاق واسع هو ارتفاع الكلفه نسبيا، التحكم بالخلط و صعوبه تسويه السطح باستخدام الادوات التقليديه. يمكن استخدام المنتج في المنشآت الخاصه حيث الوزن و الديمومه هما الاهتمام الاكبر.

درجة الماجستير في العلوم
جامعة الملك فهد للبترول والمعادن
31261 – الظهران
السعودية العربية المملكة

CHAPTER 1

INTRODUCTION

1.1 General

Ultra-High Performance Concrete (UHPC), also referred to as Ultra-High Performance Fiber Reinforced Concrete (UHPFRC), is a new generation of cement-based materials that was developed in France in the 1990s (Moallem, 2010).

UHPC is relatively a new generation of concretes optimized at the nano and micro-scale to provide superior mechanical and durability properties compared to conventional and high performance concretes. Improvements in UHPC are achieved through: limiting the water-to-cementitious materials ratio (i.e., $w/cm < 0.20$), optimizing particle packing, eliminating coarse aggregate, using specialized materials, and implementing high temperature and high pressure curing regimes. In addition, and randomly dispersed and short fibers are typically added to enhance the material's tensile and flexural strength, ductility, and toughness (Yanni, 2009).

The range of performances and characteristics that are today covered by concrete have been expanded in various directions from ordinary concrete up, ultra-high-performance concrete to self-compacting concrete. The type of high-strength concrete, developed thus far is basically a brittle material requiring the use of passive reinforcement. A technological breakthrough took place in the 90's with the

development of the said Reactive Powder Concrete (RPC) (Richard and Cheyrezy, 1994), offering compressive strength exceeding 200 MPa and flexural tensile strength of over 40 MPa, showing limited ductility. Based on the RPC initial research, the Ductal technology was then developed by the combined effects of three companies in France, LAFARGE, the construction materials manufacturer, BOUYGUES, contractor in civil and structural engineering, and RHODIA, chemical materials manufacturer. With this joint effort through intensive research and development, the material was patented, industrialized and commercialized. The attractive features of this new concrete are that it has both high compressive and tensile strengths requiring no passive reinforcement and has excellent material properties with some ductility.

The outstanding properties of Ductal encouraged the authors to undertake an exploratory work to examine its potential use as an ultra-high performance concrete (UHPC) in the aggressive exposure conditions of Saudi Arabia. This research covers the work carried out in evaluating the mechanical properties and durability of Ductal. A comparison between properties of UHPC and high strength concrete (HPC) is shown in Table 1.1.

Table 1.1: Properties of UHPC compared with high strength concrete (Lubbers, 2003)

Material Characteristic	UHPC Compared with HPC
Compressive Strength	2–3 times greater
Flexural Strength	2–6 times greater
Elastic Modulus	1.5 times greater
Total Porosity	4–6 times lower
Micro-porosity	10–50 times lower
Permeability	50 times lower
Water Absorption	7 times lower
Chlorine Ion Diffusion	25 times lower
Abrasive Wear	2.5 times lower
Corrosion Velocity	8 times lower

1.2 Principles of Developing UHPC

Improving the homogeneity, increasing the dry-compacted density, and enhancing the microstructure of regular concrete are the main principles of development of UHPC matrices.

There are two main kinds of UHPC concerning the basic development principles, following the idea of improving the homogeneity of the row mix, a class of concretes known as densified small particle concrete (DSP) has been developed. The matrix of this concrete has a very compact granular packing, with high content of super plasticizers and silica fume, and hard aggregates (Richard, Cheyrezy 1995; Rossi 2001). Another approach was oriented towards improving the strength of the paste, based on the concept of the so called macro-defect-free concretes (MDF). This material comprises a paste that is modified by the addition of water-soluble polymers and, from the manufacturing point of view, is highly demanding.

DUCTAL that is currently used in construction has been developed according to the concept of DSP concretes. Several researchers have defined some of the principles used in Ductal, which can be summarized as follows:

- Enhancement of homogeneity by elimination of coarse aggregate,
- Enhancement of compacted density by optimization of the granular mixture, i.e. the reason for the high silica fume content and use of fine quartz sand as the only aggregate,
- Optional enhancement of the microstructure by post-set heat-treatment, i.e. the quartz sand may become reactive at these elevated temperatures,

- Enhancement of ductility by incorporating small-sized steel fibers,

The application of the first three principles produces a matrix with very high compressive strength, without any improvement in ductility. The addition of the steel fibers noted in the last principle helps to improve both tensile strength and ductility (Richard and Cheyrezy 1995).

1.3 Ductal

Ductal concrete is produced using materials commonly used in concrete: cement, silica fume, sand, superplasticizer and water, as well as other materials, like ground quartz and fibers. Ductal is proportioned with particle sizes ranging from a maximum of approximately 600 μm , down to less than 0.1 μm to obtain a very dense mixture to minimize void spaces in the concrete. Steel fibers used in Ductal concrete are typically 13–15 mm long and 0.2 mm in diameter. The various Ductal formulations are all based on an optimized proportioning combining homogeneity and granular compacted density to satisfy rheological criteria (excellent workability and self-placing capability), mechanical criteria (very high compressive strength and non-brittle tensile behavior) and durability criteria (near-total invulnerability to all conventional aggressions). To enhance performances, especially mechanical ones, the heat treatment may be applied to Ductal by subjecting to temperatures between 60 to 90°C for 48 to 72 hours after completion of setting. As compared to normal concrete, Ductal concrete is found to be more fire-resistant (Acker and Behloul, 2004). Figure 1.1 shows the evolution of the resistance of concrete over the last century (Lafarge website).

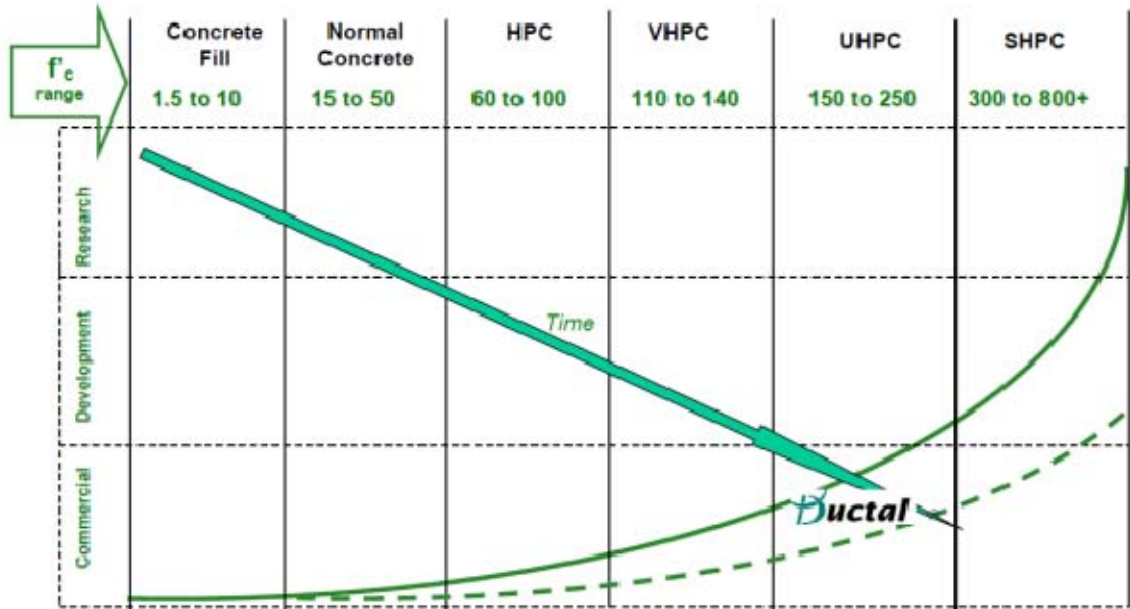


Figure 1.1: Evolution of the resistance of concrete over the last century (Lafarge website).

A comparison of Ductal's matrix to normal concrete and high performance concrete matrices (Lafarge website) is shown in Figure 1.2.

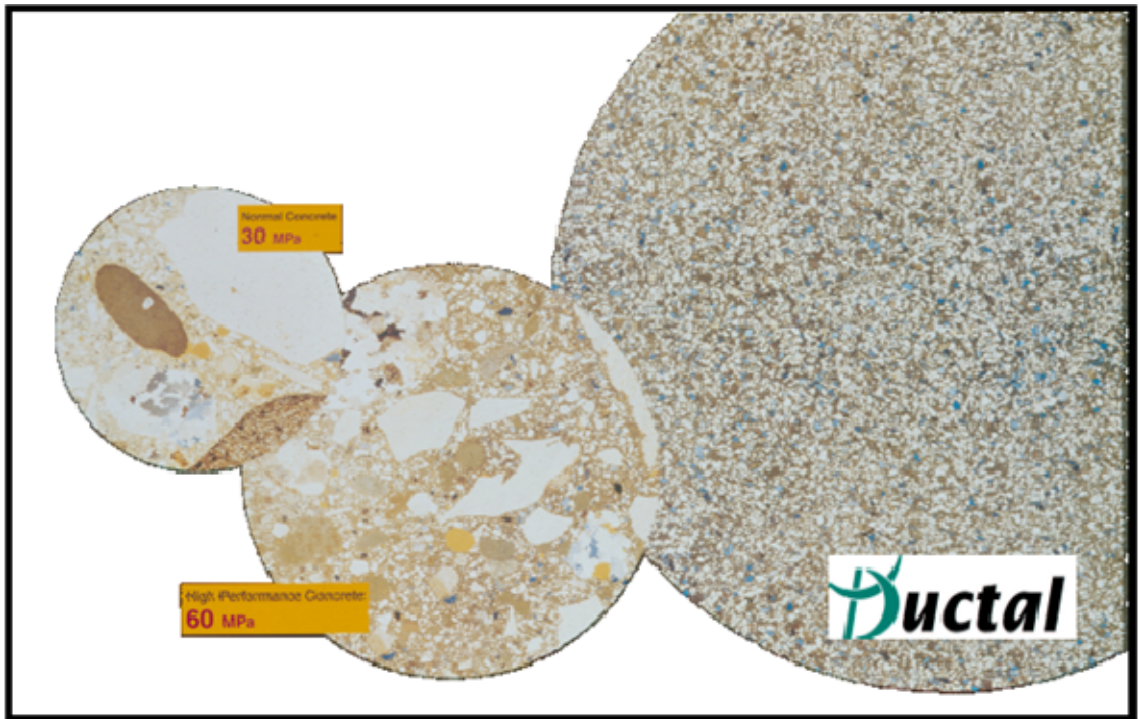


Figure 1.2: A comparison of Ductal matrix to normal concrete and high performance concrete matrices (Lafarge website).

The constituents of Ductal include Portland cement, silica fume, quartz powder (also referred as quartz flour), sand, superplasticizer, water, and fibers. Each of the components in UHPC aids in optimizing the material properties, thus contributing to its extraordinary strength.

According to VandeVoort et al. (2008), silica fume in Ductal has three main functions:

- Filling the voids in the next larger granular class (cement);

- Enhancing lubrication of the mix due to the perfect sphericity of the basic particles;
- Production of secondary hydrates by pozzolanic reaction with the products from primary hydration of cement (Richard and Cheyrezy, 1995).

Quartz powder has an average diameter of 10–15 μm , approximately the same granular size as cement particles. Since quartz powder is a reactive material, it acts as an excellent paste-aggregate interface. For cases where heat-treatment is employed, quartz powder demonstrates even higher reactivity. Other advantages of it include extreme hardness and availability.

Sand forms the largest portion of Ductal with about 41 percent by weight. To obtain a highly homogeneous matrix as well as minimum void, UHPC contains finely graded sand between 150 μm to 600 μm .

To create a gradation of particle sizes that result in a tightly packed matrix of materials the fine aggregates are carefully selected in order to minimizing voids. This has the effect of creating a very durable material with low porosity and permeability. As stated by many researchers the dense microstructure also eliminates shrinkage and limits creep when heat treated during curing. The difference between UHPC and other concretes' gradation is illustrated by this image used in promotion of Ductal (Figure 1.3).

Since Ductal uses a small w/c ratio, superplasticizer is needed to make the mixture flow and consolidate. Today's high performance superplasticizers having either a polycarboxylate (PC), NapthaleneSulfonate (NS), or Melamine Sulfonate (MS) base allow the dense, highly homogeneous mixture to be poured with the concerns of

segregation being lessened. The development of such admixtures is a welcomed addition.

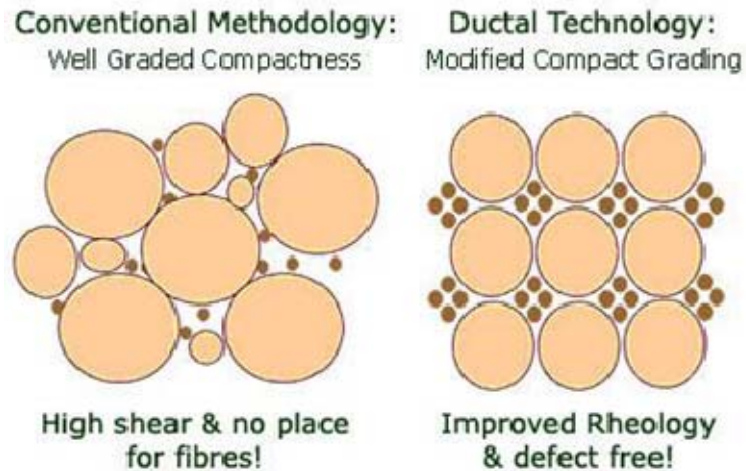


Figure 1.3: A comparison of the differences in matrix structures between conventional concrete and Lafarge’s Ductal North America, Inc. (Woodworth, 2008).

The addition of a superplasticizer can help compensate for the workability, but the percentage of liquid portion is still much lower as opposed to that in conventional concrete.

Ductal without fibers is very strong but very brittle. Fibers are included to increase tensile capacity and improve ductility. Studies using different fiber materials, contents, sizes, and shapes have been conducted by various researchers (e.g. Skazlic’ and Bjegovic’, 2009).

Dimensionally, the largest constituent in the mix is the steel fibers. In this study, the fibers in the mix had a diameter of 0.2 mm and a length of 12.7 mm. Given the relative sizes of the sand and the fibers, the steel fibers are able to reinforce the concrete matrix on the micro level (Graybeal, 2006).

The addition of steel fibers helps in preventing the propagation of microcracks and macrocracks and thereby limits crack width and permeability (Figure 1.4). This is the largest particle in the mix and is added at 6.2 percent by weight to the mix. Because of its size relative to the other constituents, it reinforces the concrete on the micro level and eliminates the need for secondary reinforcement in prestressed bridge girders (Graybeal, 2005).

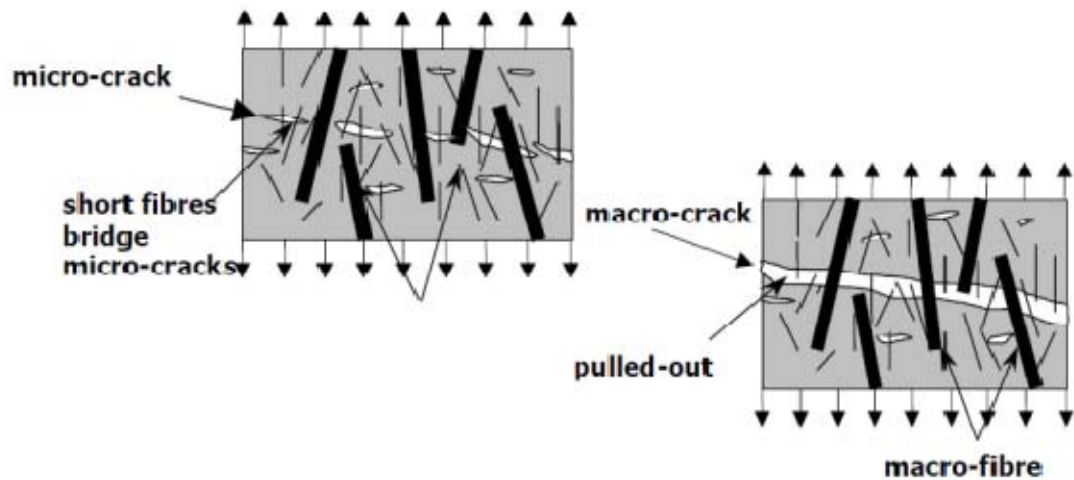


Figure 1.4: Effect of short and long fibers on micro and macro cracks (presentation of Walraven, 2007).

A typical composition of Ductal is listed in Table 1.2. The material is available in premixed packages.

Table 1.2: Ductal mix proportions

Ductal Mix Component	Weight (kg/m³)	Percent by weight
Premix	2202	87.2
Water	136	5.4
Superplasticizer	30	1.2
Steel Fibers	157	6.2

1.4 Applications

Ductal can be used for any applications, either structural or architectural, for which concrete would normally be specified. Ductal may be best suited for use in prestressed bridge superstructures in the transportation field. Because of its very high mechanical properties, Ductal technology gives access to very thin slender and elegant structures like footbridges. A very wide range of texture and colors effects are accessible to Ductal. Such properties provide architects with very high potential of innovative design in all elements that build up new architecture.

Ductal concrete has been used in a number of applications worldwide. Mention can be made of Sherbrooke footbridge 1997 in Canada (Figure 1.5), the Seonyu

footbridge 2003 in Korea (Figure 1.6), and LRT Train Station, Shawnessy, Canada, 2003 (Figure 1.7).

1.5 Scope and Objectives

The scope of this study was to conduct an exploratory research work on UHPC in the light of new developments in concrete technology. Ductal product was procured from Lafarge Company in France and concrete samples were prepared for its performance evaluation under local environmental conditions. Only Ductal FM (with steel fibers only) was used in this work.

The primary objective of this study is to prepare the Ductal concrete samples and then to determine the physical and mechanical properties and measure durability characteristics after a planned period of exposure cycles.

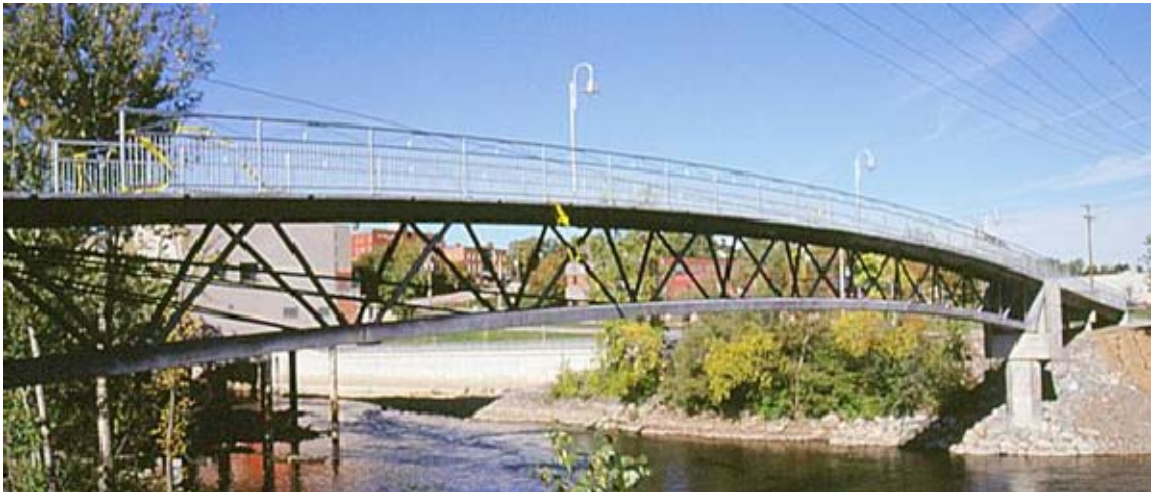


Figure 1.5: Sherbrooke footbridge, Canada, 1997.



Figure 1.6: Seonyu footbridge, Korea, 2003 (8th Hitachi EU Science and Technology Forum, Athens, May 20-22, 2005) Arch span 120 m deck thickness 3 cm.



Figure 1.7: LRT Train Station, Shawnessy, Canada, 2003 (Images from Lafarge) Canopies 5×6 m, 2 cm thick, supported on single columns.

The broad objectives of this study were the following:

- To procure Ductal product from Lafarge Company in France, as this is the only proprietary product available in the market.
- To cast test specimens which will include cylinders, cubes, and prisms required for various mechanical and durability tests.
- To subject the test specimens to a period of heat-cool and wet-dry cycles.
- To carry out the planned mechanical and durability tests on specimens after the completion of the exposure cycles and record the degradation in properties, if any.

CHAPTER 2

LITERATURE REVIEW

A review of literature covering the past work has been presented in two broad sections:

- Mechanical Properties
- Durability Performance

2.1 Mechanical Properties

2.1.1 Compressive Strength

One of the most significant properties of Ductal is its high compressive strength. Lafarge North America claims that the compressive strength of Ductal after thermal treatment ranges between 158 and 228 MPa, which has been confirmed by Perry and Zakariassen (2004). The increase in compressive strength, over normal concrete or high performance concrete, can be attributed to the particle packing and selection of specific constituents, and thermal curing of Ductal.

Graybeal and Hartmann (2003) conducted series of tests and found that the curing method yielded significant variations in compressive strength, up to a 65% difference between steam curing and ambient air curing. While various curing methods can be used, the quality control on curing methods makes Ductal more suitable for precast operations.

The results reported for both heat treated and untreated Ductal in several references (e.g. Heinz and Ludwig, 2004; Graybeal, 2005; Soutsos et al., 2005) have shown that the compressive strength of Ductal generally appears to increase with increasing heat treatment temperature. The compressive strength of Ductal, when heat treated at 90°C, increases by about 33 percent of the strengths obtained for untreated specimens.

2.1.2 Flexural Strength and Toughness

Several researchers have attempted to characterize the flexural strength of Ductal with single or two-point bending tests on small prisms. Ductal North America claims that the flexural strength of Ductal after heat treatment ranges from 27–50 MPa.

Research by Cheyrezy et al. (1995) shows that Ductal is capable of reaching a flexural strength up to 48 MPa and a toughness of 250 times that of normal strength concrete. Perry and Zakariassen (2004) showed that UHPC exhibited flexural strengths ranging from 34–48 MPa which confirmed Cheyrezy's findings. Dugat et al. (1996) also reported an ultimate flexural strength of 32 MPa.

The increase in the flexural behavior of Ductal attributed to the particle packing and the addition of fibers which hold the cement matrix together after cracking has occurred. UHPC with steel fibers exhibits ductility because as the specimen begins to microcrack the small scale fibers reinforce the matrix causing smaller, less damaging cracks to form (Graybeal and Hartmann, 2003).

The typical flexural strength test curves for Ductal and another three types of concrete shown in Figure 2.1 indicates that the equivalent stress of Ductal is more than 47 MPa, compared to about 13 MPa for FRC 80.

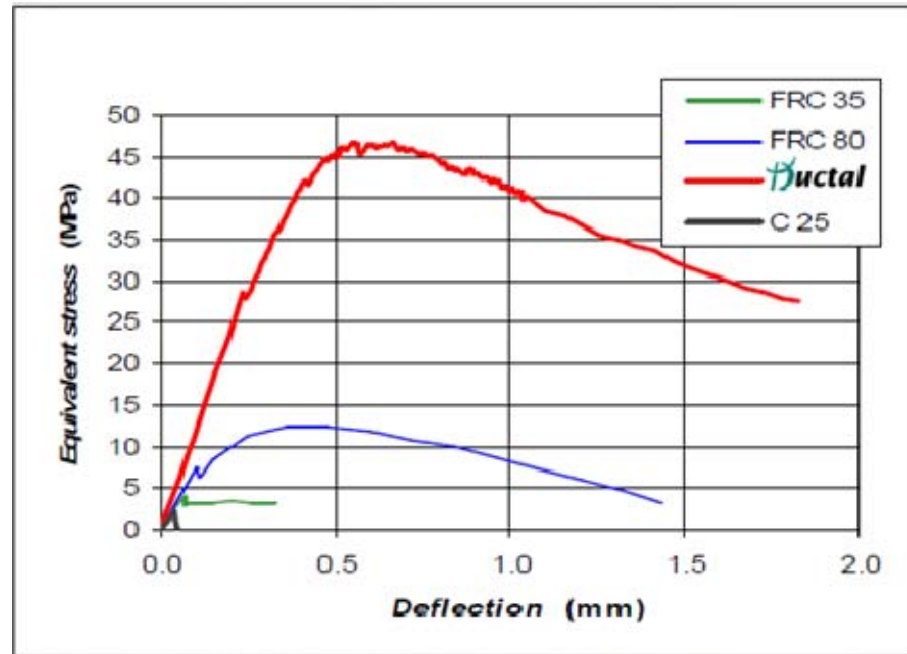


Figure 2.1: Typical flexural strength test curves of four types of concrete (Lukasik, 2005).

Graybeal (2005) conducted flexural testing of 71 specimens utilizing the procedure outlined in ASTM C 1018, which controls the rate of deflection of the prism. Specimens had span lengths of 6 in., 9 in., 12 in., and 15 in. with a cross section of 2 × 2 in. and a 12 in. span with a 3 × 4 in. cross section. Corrections were applied to calculate a more representative tensile strength from the first-crack strength. Ultimate load and toughness values based on the procedure outlined in ASTM C 1018 were reported. The flexural testing results appear to show that the flexural tensile strength of Ductal depends heavily on the size of the prisms used in the test. The results of flexural strength of steam

curing specimens was 35.4 MPa and that of untreated specimens of the same size was 29.9 MPa.

Reineck and Greiner (2004) have reported the average values of flexural strength for a wider range of prism sizes, showing the size effect. The recorded higher strengths for smaller beams are largely due to local alignment of fibers in small prisms. The local alignment leads to relatively more fibers oriented parallel to the long direction of the prism, making a greater proportion of the fibers effective to bridge flexural cracks (VandeVoort et al., 2008).

2.1.3 Drying Shrinkage

Drying shrinkage refers to the volume reduction in the cement matrix resulting from an overall loss of water to the environment through evaporation. Habel et al. (2006) investigated the drying shrinkage of Ductal and he found that drying shrinkage in Ductal is most intense during the first 20 days, reaching a magnitude of 40×10^{-6} at day 20 and 80×10^{-6} by day 90. They noted that, after 20 days, the dense matrix of Ductal largely prevents moisture exchange with the environment except in a localized zone at the surface. Cheyrezy and Behloul (2001) found a somewhat higher drying shrinkage of 170×10^{-6} at 90 days.

In 2006, Graybeal used embedding vibrating wire strain gage in a Ductal prism to capture some of the early-age behavior. He found that the total shrinkage of untreated Ductal at 40 days was 790×10^{-6} . Loukili et al. in 1999 also confirm this estimate of shrinkage with reported autogenous shrinkage (including early-age behavior) of

approximately 875×10^{-6} at 40 days and 890×10^{-6} at 90 days after casting. Based on Acker and Behloul (2004) and Graybeal (2006a, b), much of the shrinkage will take place during the first 48 hours at 90°C heat treatment.

2.1.4 Fracture Energy

Fracture energy represents the total amount of work that must be done on a concrete beam to achieve complete failure. The large amount of energy required to pull out or fracture the steel fibers in the matrix gives UHPC much greater fracture energy than normal concrete. Fracture energy in Ductal subjected to standard heat treatment ranges from $20,000 \text{ J/m}^2$ to $47,300 \text{ J/m}^2$ (Gowripalan and Gilbert, 2000; Dugat et al., 1996).

Tanaka et al. (2002) reported that the bending fracture energy of Ductal is $36,000 \text{ J/m}^2$ compared to normal concrete ranging from 50 J/m^2 to 200 J/m^2 . This was supported by Cavill (2005), who found the total fracture energy in the range of $20,000 \text{ J/m}^2$ to $30,000 \text{ J/m}^2$.

The rate of development of fracture energy is slower than the rates of development of the elastic modulus, compressive strength, and tensile strength. This slow development is most likely due to the fact that fracture energy depends largely on bond strength, which is affected by the tensile strengths and elastic modulus of the Ductal mix (VandeVoort et al., 2008).

Normal concrete and HPC exhibit virtually no post-cracking flexural strength, but the fracture energy of Ductal is relatively much higher because of fiber. The fracture energy of Ductal was estimated by Gilliland (1996) to be 250 times that of typical HPC.

2.2 Durability Performance

Durability of concrete is defined as the resistance of concrete to the attack of physical or chemical aggressive agents. Concrete can experience deterioration from either physical attack (abrasion, freezing and thawing, fire, or salt crystallization) or chemical agents (alkali-silica reaction, chloride ingress causing corrosion of embedded steel and sulfate attack, etc.) (Theresa et al., 2008).

2.2.1 Porosity

The improved microstructure of UHPC not only results in higher compressive strength but also leads to superior durability properties. This makes Ductal both a high strength and a high performance material. The low porosity of UHPC, particularly capillary porosity, leads to great improvements in the durability properties of UHPC. The superior durability characteristics of UHPC are due to the low and disconnected pore structure, which is generated as a result of the use of a combination of fine powder materials.

Schmidt et al. (2003) and Acker (2001) stated that the total porosity of Ductal appears to depend on the curing process applied to the material. Measurements of the total porosity range from 4.0 percent to 11.1 percent for Ductal without heat treatment.

Cwirzen (2007) and Herold and Müller (2004) reported that when the standard heat treatment is used, Ductal has total porosity ranging from 1.1 percent to 6.2 percent.

Based on the work of Cheyrezy et al. (1995), the total porosity of the untreated Ductal in their study is approximately 8.4 percent, but heat treatment reduces the total porosity of the UHPC sample to only 1.5 percent. Literature review shows that there is a wide range in values reported. This is however not usual, as porosity depends to some extent on the preparation and curing.

2.2.2 Chloride Ions Penetration

The chloride ion penetration through concrete by means of capillary absorption, hydrostatic pressure, or diffusion is one of the most problematic durability issues associated with high permeability concretes (Stanish et al., 2000). The presence of chloride ions near metallic reinforcement is a major cause of corrosion. Roux et al. (1996) and Australian publications also reported chloride diffusion coefficient of Ductal to be around 2.0×10^{-10} cm²/sec compared to 1.1×10^{-8} cm²/sec for normal concrete.

Rapid chloride permeability test (RCPT) is another method to evaluate chloride ion permeability is by measuring the total electric charge passed through a test sample. Additional research by Graybeal (2006a, b) demonstrated that measured 18 Coulombs as the total charge passed through a 51-mm thick Ductal sample subjected to the standard heat treatment and 360 Coulombs for an untreated Ductal sample (over a six-hour period). Bonneau et al. (1997) reported that the total charge passed through a 51-mm thick when thermally treated Ductal sample was 10 Coulombs. These amounts which are relatively small indicated relatively high chloride impermeability of Ductal.

CHAPTER 3

EXPERIMENTAL PROGRAM

3.1 General

The experimental work, the core component of this study, was designed to examine the preparation method and provide some informative properties of Ductal concrete. As the primary interest of this work was to examine the durability of Ductal under local exposure conditions, its performance under repeated thermal and moisture cycles and resistance against water and chloride ingress, were studied in addition to the mechanical properties.

3.2 Test Program Details

The Ductal concrete specimens were cast using the materials supplied by Lafarge Company adopting the recommended preparation procedure. Specimens required for various types of tests conducted to determine the mechanical and durability properties are presented in Table 3.1.

The test program involves testing of prepared specimens at certain ages to determine the mechanical properties and durability under preset exposure conditions.

Table 3.1: Details of specimens required for various tests on Ductal® concrete

Test	Test Standard	Specimen
1. Compressive strength	ASTM C 39	75 × 150 mm cylinder
2. Modulus of elasticity	ASTM C 469	75 × 150 mm cylinder
3. Flexural strength and flexural toughness (using 4-point bending test)	ASTM C 78 and ASTM C 1609	100 × 100 × 400 mm prism
4. Mortar briquette	AASHTO T-132	76 mm long, and thickness of 25 mm
5. Split tensile strength	ASTM C 496	75 × 150 mm cylinder
6. Drying shrinkage	ASTM C 356	100 × 100 × 400 mm prism
7. Water absorption, 30 min	BS 1881:Part 122	75 × 150 mm cylinder
8. Water permeability using penetration test	DIN 1048	150 mm cube
9. Chloride permeability	ASTM C 1202	75 × 150 mm cylinder
10. Chloride diffusion	Based on Fick's second law	75 × 150 mm cylinder
11. Fracture toughness	RILEM Committee on Fracture Mechanics (1990) and Jenq and Shah (1985)	100 × 100 × 400 mm prism (notched)

3.2.1 Cyclic Exposure

The specimens, following moist curing for 28 days, were exposed to the three exposure conditions for a period of six months, as detailed in Table 3.2. The sabkha solution was chosen for wet-dry cycle in view of its more aggressive chemical attack and also several areas of Saudi Arabia, notably the eastern coastal zones, have sabkha terrains. The solution was prepared by adding sodium chloride (NaCl), sodium sulfate (Na_2SO_4) and magnesium sulfate (MgSO_4) to obtain 15.7% Cl^- and 0.55% SO_4^{--} concentrations.

Table 3.2: Exposure conditions

Exposure	Duration
Control specimens at lab environment	6 months
Heat-cool cycles (Heating at 60°C for 2 days and then cooling at room temperature for 2 days)	6 months
Wet-dry cycles (Wetting for 2 days in a sabkha type solution and then drying at 30°C for 2 days)	6 months

3.2.2 Test Schedule

The test schedule is shown in Table 3.3, which includes all tests that were conducted in this study. Testing of cyclic specimens was carried out at the completion of their exposure cycles. Table 3.3 lists the type of test, specimen size and the number of specimens used for each test. Three specimens were used for a test as repetition except chloride diffusion and fracture toughness tests, for which only two specimens were used.

Table 3.3: Testing schedule

Test	Specimen	Number of specimens and age at the time of testing	Total number of specimens
Compressive strength	75 × 150 mm cylinder	6 cylinders after 3 days curing 3 in water and 3 in air	24 cylinders All this repeated 3 times for 6.2%, 3.1% and 0% steel fibers. Total 72 cylinders
		6 cylinders after 7 days curing 3 in water and 3 in air	
		6 cylinders after 14 days curing 3 in water and 3 in air	
		6 cylinders after 28 days curing 3 in water and 3 in air	
		3 control cylinders after 6 months of normal laboratory exposure (6.2% fibers)	9 cylinders Total cylinders tested 81 cylinders
		3 cylinders after 6 months of heat-cool cycles (6.2% fibers)	
		3 cylinders after 6 months of wet-dry cycles (6.2% fibers)	
Modulus of elasticity	75 × 150 mm cylinder	3 cylinders after 7 days water curing (6.2% fibers)	30 cylinders
		6 cylinders after 28 days curing (6.2% fibers) 3 in water and 3 in air	
		6 cylinders after 28 days curing (3.1% fibers) 3 in water and 3 in air	
		6 cylinders after 28 days curing (0% fibers) 3 in water and 3 in air	
		3 control cylinders after 6 months of normal laboratory exposure (6.2% fibers)	
		3 cylinders after 6 months of heat-cool cycles (6.2% fibers)	
		3 cylinders after 6 months of wet-dry cycles (6.2% fibers)	

Table 3.3: (continued)

Test	Specimen	Number of specimens and age at the time of testing	Total number of specimens
Flexural strength and flexural toughness (using 4 point bending test)	100 × 100 × 400 mm prism	3 prisms after 7 days curing(6.2% fibers)	21 prisms
		3 prisms after 28 days curing(6.2% fibers)	
		3 prisms after 28 days curing(3.1% fibers)	
		3 prisms after 28 days curing(0% fibers)	
		3 control prisms after 6 months of normal laboratory exposure(6.2% fibers)	
		3 prisms after 6 months of heat-cool cycles (6.2% fibers)	
		3 prisms after 6 months of wet-dry cycles(6.2% fibers)	
Mortar briquette	76 mm long, and thickness of 25 mm	6 cubes at 28 days water curing	12 cubes
		6 cubes at 28 days air curing	
Split tensile strength	75 × 150 mm cylinder	3 cylinders after 28 days water curing	12 cylinders
		3 control cylinders after 6 months of normal laboratory exposure	
		3 cylinders after 6 months of heat-cool cycles	
		3 cylinders after 6 months of wet-dry cycles	
Drying shrinkage	100×100×400mm prism	3 prisms up to 2 months of normal dry laboratory exposure	3 prisms
Water absorption	75 × 150 mm cylinder	3 control cylinders after 6 months of normal laboratory exposure	9 cylinders
		3 cylinders after 6 months of heat-cool cycles	
		3 cylinders after 6 months of wet-dry cycles	

Table 3.3: (continued)

Test	Specimen	Number of specimens and age at the time of testing	Total number of specimens
Water permeability (DIN test)	150 mm cube	3 control cubes after 6 months of normal laboratory exposure	9 cubes
		3 cubes after 6 months of heat-cool cycles	
		3 cubes after 6 months of wet-dry cycles	
Chloride permeability	75 × 150 mm cylinder	3 control cylinders after 6 months of normal laboratory exposure	9 cylinders
		3 cylinders after 6 months of heat-cool cycles	
		3 cylinders after 6 months of wet-dry cycles	
Chloride diffusion	75 × 150 mm cylinder	2 cylinders after 4 months of immersion in chloride solution	4 cylinders
		2 cylinders after 6 months of immersion in chloride solution	
Fracture toughness	100 × 100 × 400 mm prism (notched)	3 prisms after 28 days of curing (6.2% fibers)	15 prisms
		3 prisms after 28 days of curing (3.1% fibers)	
		3 prisms after 28 days of curing (0% fibers)	
		3 prisms after 6 months of heat-cool cycles (6.2% fibers)	
		3 prisms after 6 months of heat-cool cycles (6.2% fibers)	

3.3 Ductal Mixing Procedure

The Ductal material, purchased from Lafarge, was received in four components:

- 1- Ductal premix G3: 48 containers of 25 kg each, total 1200 kg
- 2- A container of 20 liters of superplasticizer F2
- 3- One container of 20 liters of accelerator A2 (not used)
- 4- Chopped steel fibers

Table 3.4 provides information about the Ductal mix used throughout this study.

The premix packages included: Portland cement, silica fume, quartz powder and sand.

The mix proportions were used following the manufacturer's recommendation.

Table 3.4: Ductal mix proportions

Ductal Mix Component	Weight (kg/m ³)	Percent by weight
G3 Premix Material	2202	87.2
Water	136	5.4
Plasticizer F2	30	1.2
Steel Fibers	157	6.2

Mixing of Ductal requires special equipment and procedures to develop consistency in batching, casting, and curing in a timely fashion. A high shear capacity mixer along with vibratory table is required. Mixing of Ductal was carried out in the Civil Engineering Department's laboratory, using a HOBART planetary mixer (Figure 3.1).



Figure 3.1: HOBART planetary mixer.

From experience gained from trial mixes, the following mixing procedure for Ductal was adopted:

- Weigh all constituent materials. Add half of superplasticizer to water.
- Place premix in mixer pan and mix for 2 minutes.
- Add all the water and half of the superplasticizer to premix slowly.
- Mix for 8-10 minutes until the powder becomes granules
- Then add the rest of the superplasticizer.

- Continue mixing until the mix is completely homogenous and fluid. The time for this process is about 5 minutes, but it can vary a bit.
- Add the fibers to the mix slowly in small amounts over the course of the next 2 minutes.
- After the fibers have been added, continue running mixer for further 3 minutes to ensure that the fibers are well dispersed.

It is worth mentioning that the total time of mixing of Ductal varies between 20-25 minutes. It should be noted that this mixing time is relative and is only specifically applicable to the pan mixer used in this study.

The important stages of the mixing of Ductal are shown in Figure 3.2.

As soon as mixing was completed, Ductal mix was tested for consistency. ASTM C 1437 standard test method for measuring flow of hydraulic cement was used to comply with the recommendations outlined in Ductal reference T006 (Operating Procedure – Flow Test). In this test, mini slump cone is filled with Ductal mix (Figure 3.3) then removed slowly to allow the Ductal to flow evenly on the table and then the flow table is dropped 20 times and its average diameter is recorded.

The average flow diameter of Ductal mix ranged from 200 to 240 mm, which is classified under Domain B according to Ductal reference (T002 Cylinder and Prism Preparation).

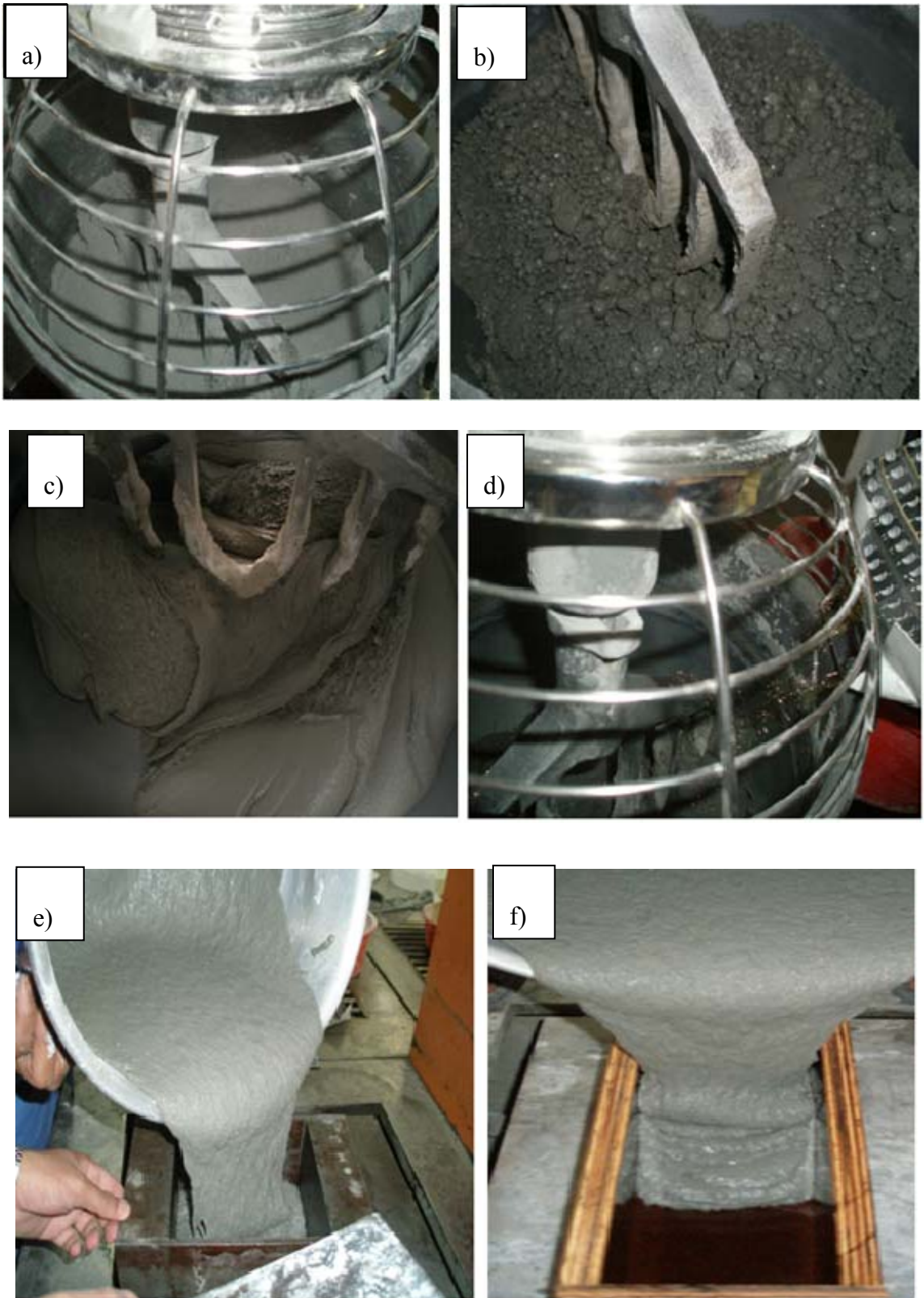


Figure 3.2: a) Ductal premix powder inside the mixer; b) Ductal after addition of water and half of super plasticizer(first turning point); c) Ductal after addition of another half of superplasticizer (second turning point); d) during addition of steel fibers; e) casting of Ductal in cubes; f) casting of Ductal in prism



Figure 3.3: Impact table measurement of Ductal flow.

3.4 Casting and Curing

After completion of mixing, all specimens were cast within 20 minutes by pouring the material into molds on a vibrating table and vibrating them for about 30 seconds after filling to consolidate the mix. The specimens in molds were covered with plastic to prevent moisture loss (Graybeal, 2006a, b). They were demolded after one day of casting.

Ductal concrete is cured using different curing conditions: normal laboratory moist curing; steam curing (normal, tempered and delayed); and self-curing in normal laboratory conditions.

For the purpose of this study, only 28-day water curing at room temperature was used. Even for exposure period of 6 months, all the specimens were moist-cured for 28 days. The reasons behind this choice of curing method are: (i) water curing has not been

used in the past work, and (ii) the use of in-situ cast-in-place concreting would prefer water curing or self-curing in air, as heat treatment or steam curing would be undesirable.

3.5 Compressive Strength and Modulus of Elasticity Testing

The test procedures for compressive strength and modulus of elasticity are presented in the following subsections.

3.5.1 Compressive Strength

The compressive tests were carried out following the standard test method of ASTM C 39 for cylinders. For all cylinders, the standard size had a diameter of 3 in. and pre-end preparation length of 6 in. The cylinders had their trowled end prepared by cutting because of rough surface, and their final lengths were approximately 1.95 times their diameter. The cylinders were tested under a 3000 kN capacity compression testing machine.

Figure 3.4 shows failure of cylinders after compression testing. Unlike normal concrete, the failure occurs due to development of multiple vertical cracks due to the presence of fibers.



Figure 3.4: Ductal cylinders after failure under compression test.

3.5.2 Modulus of Elasticity

As specified in ASTM C 469 standard test method for static modulus of elasticity and Poisson's ratio of concrete in compression, the elastic portion of the compressive stress-strain curve up to 40 percent of the ultimate compressive strength ($0.40 f_c'$) was used to determine modulus of elasticity.

The modulus of elasticity was measured by recording strain using electrical strain gauges fixed to cylinders (Figure 3.5).



Figure 3.5: Specimens of Ductal with strain gauges for measuring modulus of elasticity.

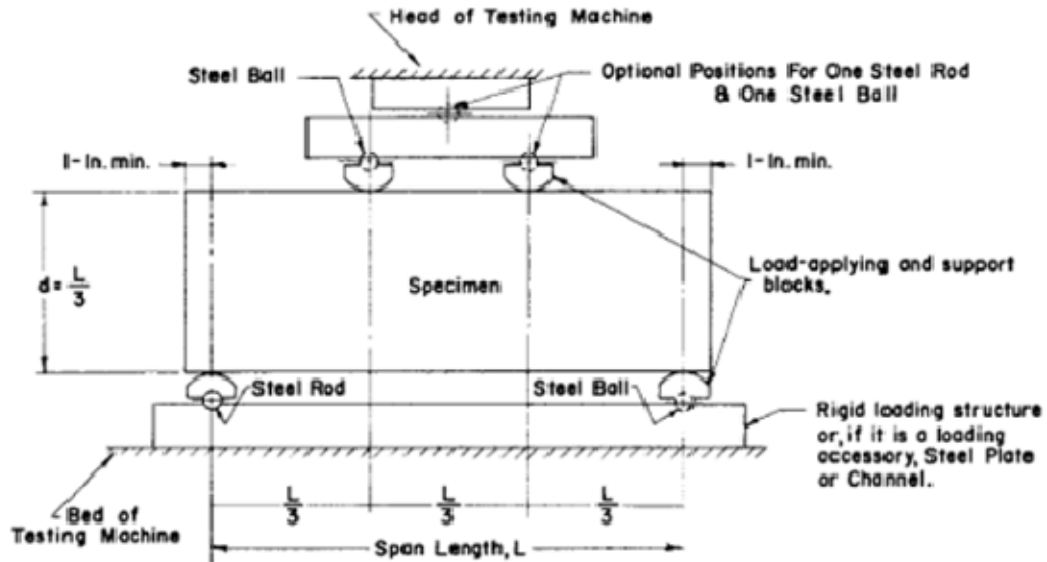
3.6 Tensile Properties of Ductal

In the present work, the tensile strength of Ductal was determined using all three tests, flexural test, direct tension test and split tensile test. Prisms were cast for flexural testing to determine the modulus of rupture, flexural toughness, and residual flexural strength (i.e., post-cracking flexural strength). Standard ASTM specified briquettes were used to find axial tensile strength testing and cylinders were used for determining the split tensile strength.

3.6.1 Flexural Properties

The standard four-point flexural test to determine the modulus of rupture (MOR) according to ASTM C 78 is the most common method for obtaining flexural tensile strength of normal as well as high-performance concretes (Figure 3.6). The flexural

toughness can be determined as equal to the area under the load-deflection curve obtained from the four-point load test. However, the method for the determination of residual flexural strength, which is crucial to ultra-high performance concrete, like Ductal, is not covered by ASTM C 78. For more than a decade, the ASTM C 1018 standard has been used for flexural toughness of fiber reinforced concrete (Marijan Skazlic 2009). However, this method evaluates the flexural toughness in terms of dimensionless parameters, such as toughness index and residual strength factor. In the year 2005, the ASTM C 1018 standard was replaced with a new standard, ASTM C 1609, for determination of MOR at peak flexural strength, flexural toughness, and residual flexural strength. The ASTM C 1609 (titled “Standard Test Method for Flexural Performance of Fiber-Reinforced Concrete using Beam with Third-Point Loading”) is now being commonly used to determine the flexural properties of ultra-high performance concrete such as Ductal. This test involves the four-point flexural loading of small-scale concrete prisms (100×100×400 mm). During the test, the load and the mid-span deflection of the prism are monitored. These data are then used to determine the MOR and flexural toughness. Flexural toughness is calculated as area under load-deflection curve up to 2 mm deflection. The residual flexural strength is also determined using the same load-deflection curve. Other standard method used to determine flexural toughness is JSCE-SF4. Also a new method, called Post Crack Strength (PCS) method (Banthia and Trottier, 1995) is used under the present work to determine the residual flexural strength. This method uses similar test specimens and testing procedure as that of ASTM C 1609 method.



I. Calculations of MOR and Flexural Toughness according to ASTM C 1609

Twenty one prisms were tested, six prisms after 7 and 28 days water curing and nine prisms for all exposure conditions: control specimens, wet-dry cycles and heat-cool cycles, respectively, and additional six prisms after 28 days water curing for 3.1% and 0% steel fibers as shown in Table 3.3. Testing of prisms was conducted on a 600 kN INSTRON machine with a loading rate of 0.5 mm/min and the deflection was measured using one LVDT at mid span of the prisms (Figure 3.7).

The load-deflection data was recorded by using a data logger. The reading from the data logger was transferred to a computer to plot the load-deflection curve during testing.



Figure 3.7: Flexural strength test using four-point bending.

From each set of the load-deflection curve, the following parameters were recorded for each specimen of Ductal.

- First-Peak Strength
- Peak strength or MOR
- $P_{100,0.5}$, $F_{100,0.5}$, $P_{100,2}$, and $F_{100,2}$
- Flexural toughness, $T_{100,2}$

where, $P_{100,0.5}$, $F_{100,0.5}$ are the residual load and strength at deflection of 0.5 mm in the load deflection curve, respectively, and $P_{100,2}$, and $F_{100,2}$ are the residual load and strength at deflection of 2 mm in the load deflection curve, respectively. $T_{100,2}$ is the flexural toughness which is equal to the area under load deflection curve up to 2 mm according to ASTM C 1609 (Figure 3.8).

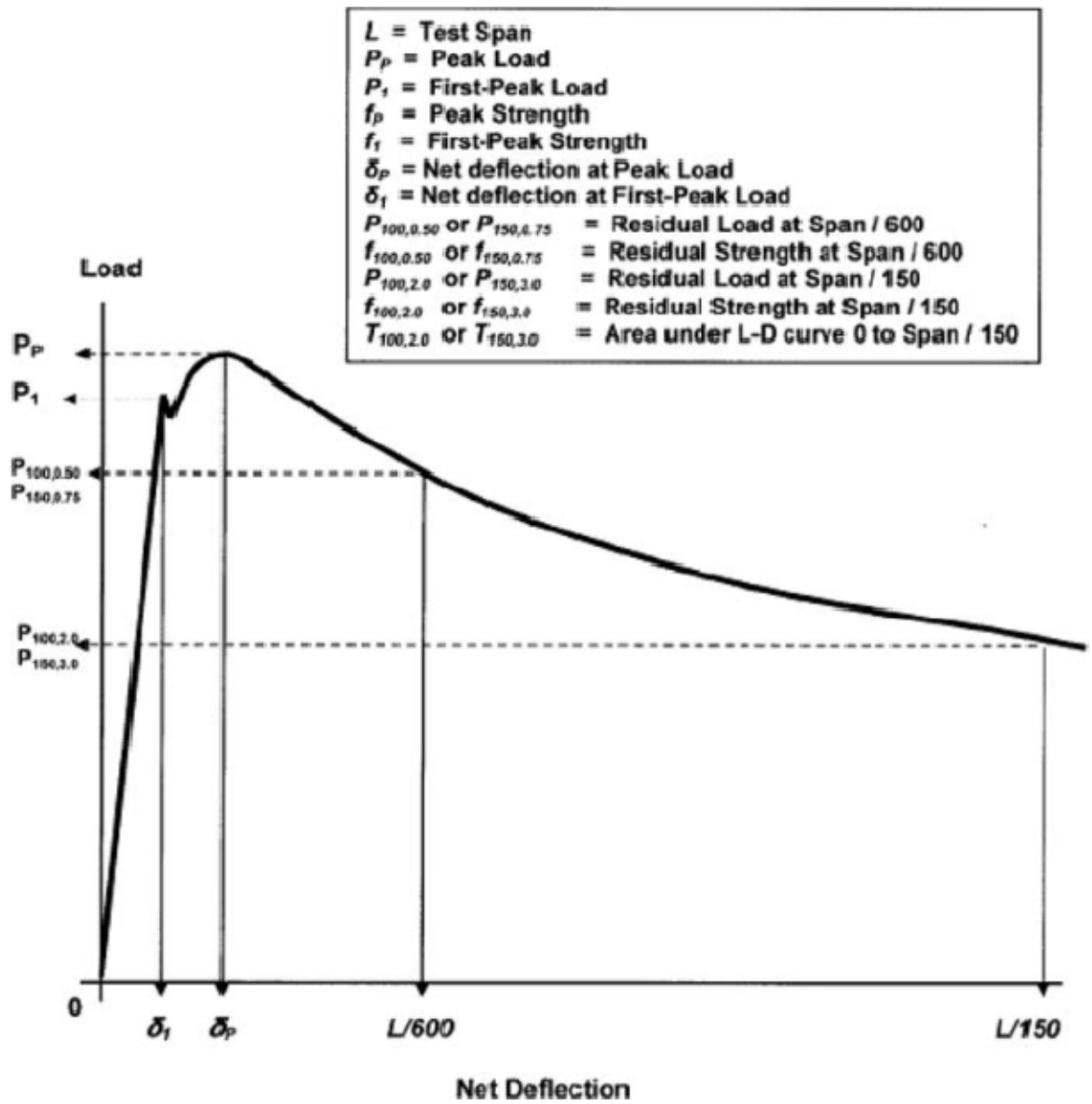


Figure 3.8: Definition of toughness index according to ASTM C 1609

II. Calculation of Residual Flexural strength (Post-Cracking Flexural Strength)

The procedure for calculation of residual flexural strength according to ASTM C1609, JSCE-SF4 and PCS methods is described below:

a) ASTM C 1609 Method

The residual post-peak behavior is described in terms of two parameters: the residual flexural strength $f_{100,2}$, and the flexural toughness $T_{100,2}$.

As mentioned earlier, the flexural toughness $T_{100,2}$ is taken as the area under load-deflection curve up to a 2 mm of mid-span deflection. The expression for calculating residual flexural strength $f_{100,2}$ is given by Bordelon (2007) as follows:

$$f_{100,2} = \frac{P_{100,2} * L}{b * d^2} \quad (3.1)$$

where:

$f_{100,2}$ = equivalent residual flexural strength,

$P_{100,2}$ = residual load to a deflection of span in mm/150,

L = span of the beam,

b = breadth of the beam, and

d = depth of the beam.

b) JSCE SF-4 Method

The expression for calculating the residual flexural strength $f_{100,2}$ as given in JSCE SF-4, is as follows:

$$f_{e,2} = \frac{T_{100,2} L}{\delta_{tb} b d^2} \quad (3.2)$$

where,

$f_{e,2}$ = equivalent residual flexural strength or flexural toughness factor

$T_{100,2}$ = the absolute toughness which is defined as the area under the load-deflection curve to a deflection of span/150, and

δ_{tb} = deflection at span/150

c) PCS Method

In order to simplify the approach, a new method has been proposed by Banthia and Trottier (1995) wherein identification of first crack is not required. The procedure according to them is as follows:

1. Obtain the load-deflection curve with accurate deflection measurements.
2. Locate the peak load and divide the curve into two regions: the pre-peak region (before the occurrence of the peak load) and the post-peak region (after the peak load). Note the value of the load at the peak and measure the area under the curve up to the peak load. This measure of energy is termed as pre-peak energy and denoted as E_{pre} .
3. Locate points on the curve in the post-peak region with specimen deflections equal to various fractions of the span L/m_1 , L/m_2 , etc. The suggested

fractions are between $L/3000$ and $L/150$. Measure the areas under the curve up to these deflections, denoted as $E_{total,m}$ (measured at a deflection of L/m). According to this method L/m should be taken as 0.1, 0.2 etc. up to 2. For our calculation, L/m of 2 was taken to calculate the flexural toughness.

4. Subtract the pre-peak energy E_{pre} from the various values of $E_{total,m}$ to obtain the post-peak energy values to a deflection of L/m , $E_{post,m}$.
5. Calculate the post-crack strength (PCS_m) in the post peak region at the various deflections. The PCS_m at a deflection of L/m , is defined as

$$PCS_m = \frac{(E_{post,m})L}{\left(\frac{L}{m} - \delta_{peak}\right)bh^2} \quad (3.3)$$

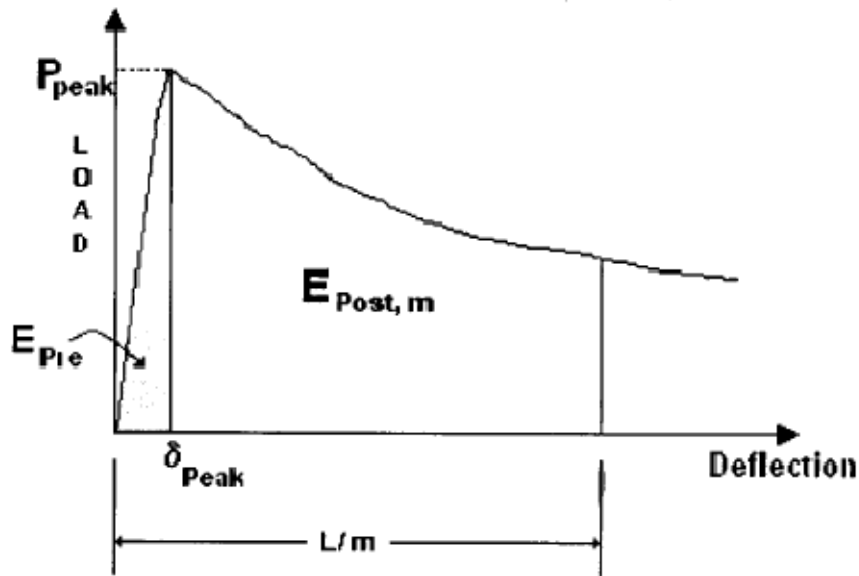


Figure 3.9: Flexural toughness description according to PCS method.

3.6.2 Mortar Briquette (Direct Tension Test)

Mortar briquette test is another means of determination of the tensile strength of concrete. The test normally involves measuring the direct tension of a small briquette cast from cement mortar, as described in AASHTO T-132. The dogbone-shaped briquette is 76 mm (3 inches) long, and 25 mm (1 inch) thick with cross section at mid length of 645 mm² (1 in²) as shown in Figure 3.10.

The test was completed using a constant displacement rate of 0.5 mm/min in an INSTRON machine (Figure 3.11).

A total of 10 briquette cubes were made, 5 briquettes for 28 normal water curing and the other 5 for ambient air curing. All the specimens contained 6.2% steel fibers by weight of Ductal.



Figure 3.10: Mortar Briquette specimens of Ductal after testing.



Figure 3.11: Mortar briquette setup including test grips and specimen.

3.6.3 Split Tensile Strength

Split cylinder is another means of measuring indirectly the tensile strength of concrete using ASTM C 496 (Figure 3.12). Three inch diameter cylinders of approximately six inch length were tested for 28 days water cured specimens at the age of 28 days and six- month exposure at laboratory condition (control specimens), wet-dry cycles and heat-cool cycles. All contained samples of 6.2% steel fibers by weight. A total of 12 specimens, three for each exposure condition, were used.

The maximum tensile strength was calculated based on Equation (3.1) (ASTM C 496), where P is load applied to the cylinder and l , d are the length and diameter and f_t is the tensile strength.

$$f_r = 2P/\pi l d \quad (3.4)$$

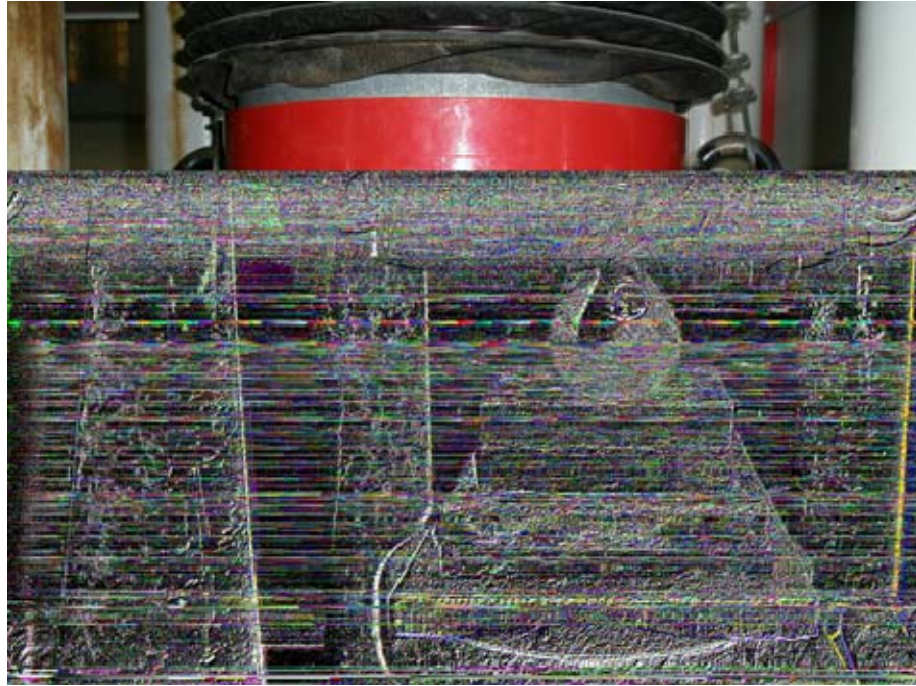


Figure 3.12: Split cylinder tensile test on Ductal.

3.7 Drying Shrinkage

A total of three prisms of $100 \times 100 \times 400$ mm were used in measuring the drying shrinkage of Ductal. Each prism was fitted with demec gauges and the shrinkage strain was measured using multi-length dial gauge (Figure 3.13). Drying shrinkage was measured after 28 days of water curing and leaving the specimens in normal laboratory conditions (temperature $21\text{--}24^\circ\text{C}$ and humidity about 40%).

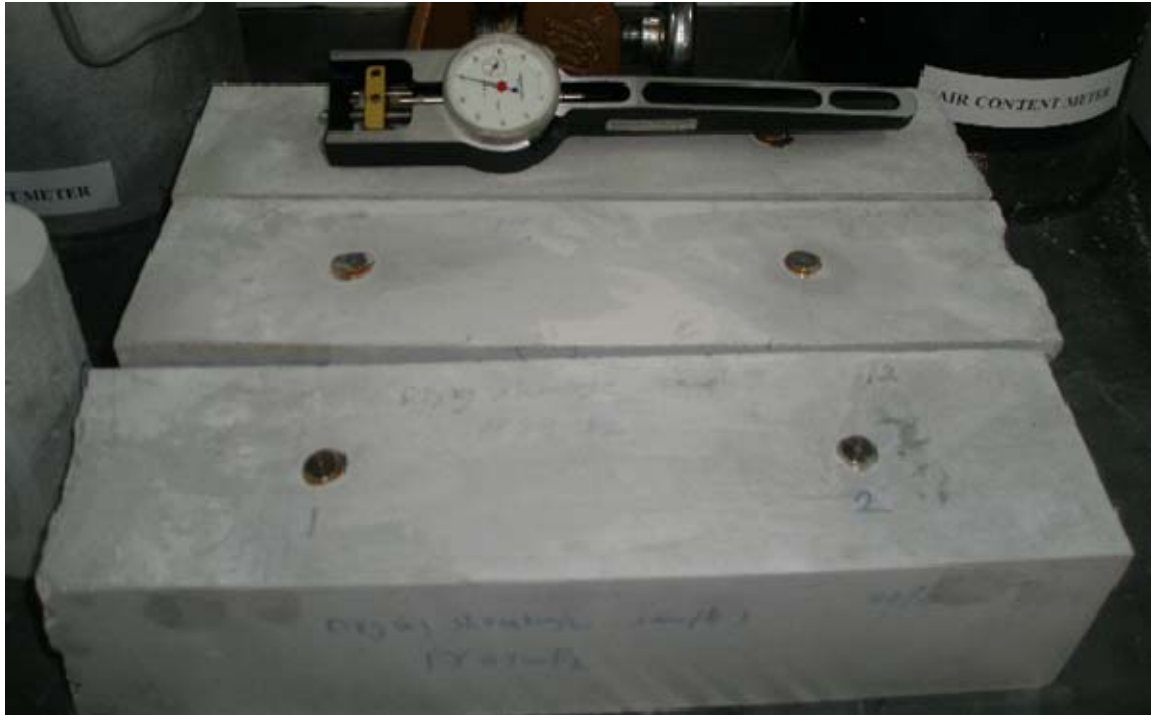


Figure 3.13: Drying shrinkage measurements by multi-length dial gauge.

3.8 Water Absorption

The water absorption of the concrete cylindrical specimens was determined according to BS 1991: Part 122. The test was conducted on 9 3×6 in. cylinders under different exposure conditions: control specimens, wet-dry cycles and heat-cool cycles. The test procedure is as follows:

The specimens were dried in an oven at 105°C for 72 hours. Then they were cooled in a dry airtight vessel for 24 hours and weighed and immediately immersed in a tank containing water at 20°C with the longitudinal axis of the specimens kept horizontal,

and with 25 mm depth of water over the specimens for 30 min. Thereafter, the specimens were removed, shaken, and surface dried, then reweighed. The water absorption is calculated as the increase in the mass resulting from immersion expressed as a percentage of the dry mass.

3.9 Water Permeability

The depth of water penetration was determined according to DIN 1048. The test was conducted on 150 mm cube, three specimens for each exposure conditions of Ductal after 6 months of exposure to laboratory (lab temperature), wet-dry and heat-cool cycles. Figure 3.14 shows the experimental test setup to determine the depth of water penetration using Zwick/Roell instrument.

The specimens were exposed to a constant water pressure of 5 bars for a period of 72 hours. After the completion of the test, the specimens were taken out and split open into two halves with the face which was exposed to water facing down.



Figure 3.14: Water penetration test setup.

3.10 Rapid Chloride Ion Penetrability

The ability of concrete to resist ingress of chloride ions can result in a durable concrete. The electrical indication of concrete's ability to resist chloride ion penetration was determined according to ASTM C 1202. The test was conducted by using PROOVE IT instrument (Germann Instruments) as shown in Figure 3.15.



Figure 3.15: Experimental setup to determine the rapid chloride ion penetrability.

The tests were conducted for three exposure conditions: control specimens, wet-dry and heat-cool cycles exposures for 6 months. Nine specimens were used, three for each exposure. The test method involved obtaining 75×150 mm cylinders. A 50 mm thick disk was cut from the center of the specimens, then coated with epoxy and put in a vacuum chamber for 3 hours after the epoxy dried. The specimens were then saturated with water and kept for 24 hours following which they were clamped between two cells, the negative side of the test cell filled with 3% NaCl solution and the positive cell was filled with 0.3 NaOH solution. The system was connected to the PROOVE IT instrument for 6 hours, after which the specimens were removed from the cell. The total charge passed and the class of permeability is displayed on the computer screen.

3.11 Chloride Diffusion

After 28 days of water curing, the specimens were coated with an epoxy resin on the curved surface and on one end face to ensure unidirectional flow of chloride ions through the uncoated surface (Figure 3.16). The coated specimens were immersed in a 10% sodium chloride solution for a period of 6 months. After this period, the specimens were cleaned and dried to remove the surface moisture and slices of 5 mm were obtained at depths of 5, 15, 25, 35, 45, and 55 mm from the exposed surface by drying cutting. The slices were ground to a fine powder, passing through ASTM No.100 sieve by using a pulverizer.



Figure 3.16: Coated specimens utilized for chloride diffusion test.

The specimens were chemically analyzed to determine the water soluble chloride concentration. The chloride concentration was determined by the spectrophotometric method. The chloride concentration was plotted against the concrete depth for each specimen. Chloride diffusion coefficient was calculated using Fick's second law of diffusion given as:

$$C_x = C_s \left[1 - \operatorname{erf} \frac{x}{2\sqrt{D_e/t}} \right] \quad (3.5)$$

in which:

C_x = chloride concentration at a depth x from exposed surface, %

C_s = chloride concentration at the surface, %

x = depth from concrete surface, cm

erf = error function

D_e = effective diffusion coefficient, cm^2/sec

t = exposure time (elapsed time), sec.

3.12 Fracture Toughness

3.12.1 General

Ductal concrete is reported to have excellent fracture properties besides its very high strength and elasticity. The fibers added to Ductal make it able to resist the fracture by its ductility. The ductile behavior of Ductal was tested through cyclic loading and unloading. The data generated through this test was utilized to study the fracture properties

of Ductal in terms of various parameters such as: critical stress intensity factor (K_{ic}), critical crack tip opening displacement ($CTOD_c$), and fracture energy.

In the present study, fracture properties of Ductal were determined using fracture toughness test developed by Jenq and Shah (1985). For this testing, prism specimens, having dimensions of 100×100×400 mm with a notch created at center point, were used. The specimens were cast for conducting fracture toughness tests after 28 days normal water curing of specimens with different fiber contents. The specimens were also cast for fracture toughness testing after exposing the specimens to heat-cool cycles and control exposure (laboratory environment) for six months followed by 28 days of water curing. This way a total of 15 prisms were cast for conducting fracture toughness test to evaluate the fracture properties of Ductal.

Fracture toughness test developed by Jenq and Shah (1985) uses a single-edge notched beam (SEN) specimen (dimensions 100×100×400 mm) to determine the fracture properties of the concrete. Two-Parameter Fracture Model (TPFM) is used to determine fracture properties. For TPFM: a span-to-depth ratio (S/d) of 3; initial notch depth (a_0) as one-third of the total depth of the beam (~30 mm), and the notch width of 4 mm are used. Three-point bending with the load (P) and crack mouth opening displacement (CMOD) are measured for single edge notched beam specimen as shown in Figure 3.17. TPFM is used to determine the critical stress intensity factor (K_{ic}) and critical crack tip opening displacement ($CTOD_c$) of a monolithic beam based on an effective elastic crack approach. The nonlinear fracture behavior was accounted for by using linear elastic fracture mechanics equations to calculate the effective elastic crack length based on the measured

loading and unloading compliance of the beam. Geometric factors were included in the calculations to account for the geometry and size of the beams.

The test was conducted on INSTRON machine of 600 kN capacity (Figure 3.18).

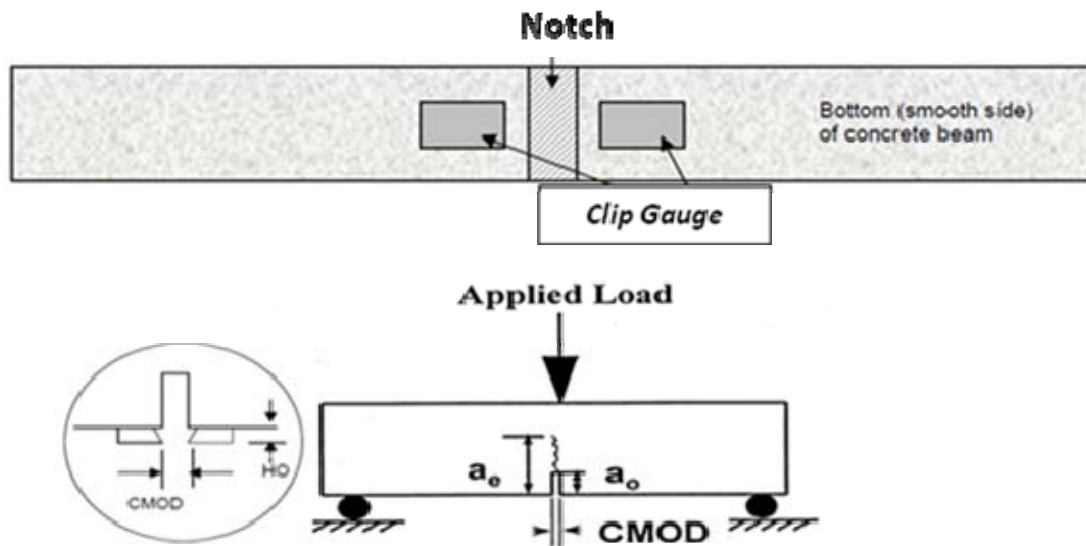


Figure 3.17: Details of attaching clip gauge to Ductal prism which measures crack mouth opening displacement (CMOD).



Figure 3.18: Complete test setup for measuring fracture toughness of Ductal prisms.

3.12.2 Fracture Parameters

The two fracture parameters determined using the TPFM are the K_{ic} and $CTOD_c$. These are computed by first obtaining the critical effective crack length (a_c). By equating, the concrete's modulus of elasticity from the loading and unloading curves ($E = E_i = E_u$) as shown in equations below, the critical effective crack length (a_c) could be determined as follows:

$$E_i = \frac{6Sa_0g_2(\alpha_0)}{C_id^2b} \quad (3.6)$$

$$E_u = \frac{6Sa_cg_2(\alpha_c)}{C_ud^2b} \quad (3.7)$$

With

$$\alpha_0 = \frac{(a_0 + HO)}{(D + HO)} \quad (3.8)$$

$$\alpha_c = \frac{(a_c + HO)}{(D + HO)} \quad (3.9)$$

where S is the span, d is the depth, b is the width, a_0 is the initial notch depth of the beam, α_0 is the initial notch/depth ratio, α_c is the critical notch/depth ratio, HO is the thickness of the clip gauge holder (Figure 3.18), and $g_2(\alpha)$ is the opening displacement geometric factor for the Three-Point Bending (TPB) specimen given by:

$$g_2(\alpha) = 0.76 - 2.28\alpha + 3.87\alpha^2 - 2.04\alpha^3 + \frac{0.66}{(1-\alpha)^2} \quad (3.10)$$

Once the a_c is computed, then the critical stress intensity factor (K_{ic}) could be calculated from the following:

$$K_{ic} = 3(P_c + 0.5W_0S/L) \frac{S\sqrt{\pi a_c} g_1(a_c/d)}{2d^2b} \quad (3.11)$$

where, (P_c) is the peak load, W_0 is the weight of the specimen, L is the length of the specimen and (g_1) is the stress intensity factor geometric function for the beam specimen defined as follows

$$g_1\left(\frac{a_c}{d}\right) = \frac{1.99 - (a_c/d)(1 - a_c/d)[2.15 - 3.93(a_c/d) + 2.70(a_c/d)^2]}{\sqrt{\pi}[1 + 2(a_c/d)][1 - (a_c/d)]^{2/3}} \quad (3.12)$$

Finally, the $CTOD_c$ could be computed using equation:

$$CTOD_c = 6(P_c + 0.5W_0S/L) \times \frac{Sa_c g_2(a_c/d)}{Ed^2 d} \times \left[(1 - (a_c/a_0))^2 + \left[1.081 - 1.149 \left(\frac{a_c}{d} \right) \right] * \left[(a_c/a_0) - (a_c/a_0)^2 \right] \right]^{1/2} \quad (3.13)$$

where

$$g_2\left(\frac{a_c}{d}\right) = 0.76 - 2.28\left(\frac{a_c}{d}\right) + 3.87\left(\frac{a_c}{d}\right)^2 - 2.04\left(\frac{a_c}{d}\right)^3 + \frac{0.66}{\left(1 - \frac{a_c}{d}\right)^2} \quad (3.14)$$

The loading compliance (C_i) is calculated as the inverse of the slope from 10% of the peak load until 50% of the peak load. This is estimated to be in the linear elastic range ignoring any initial seating load discontinuities in the curve. The unloading compliance (C_u) is the inverse of slope of the unloading curve. C_u should be calculated between 10% and 80% of the peak load on the unloading curve. The criteria for determination of C_i and C_u , as given by Bordelon (2007), are shown in Figure 3.19.

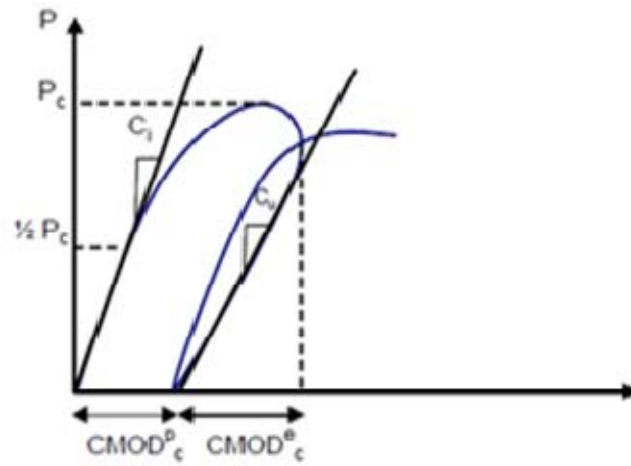


Figure 3.17. Loading and unloading compliance C_I and C_{II} .

Figures 3.20 and 3.21 show the close-up view of the fracture toughness test and the bridging effect of fibers during fracture testing, respectively.



Figure 3.20: Close-up view of fracture toughness test.

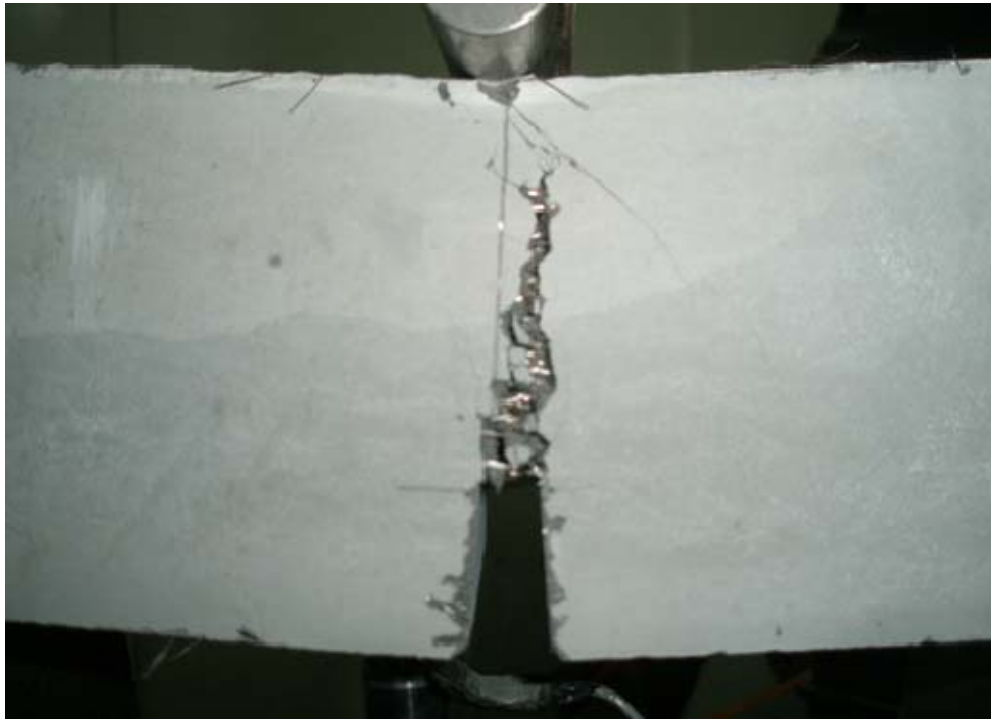


Figure 3.21: Bridging effect of fibers during the fracture test.

3.12.3 Fracture Energy

Fracture energy represents the total amount of work that must be done on a concrete beam to achieve complete failure. The large amount of energy required to pull out or fracture the steel fibers in the matrix gives UHPC much greater fracture energy than normal concrete. According to Gowripalan and Gilbert (2000) and Dugat et al. (1996), the fracture energy in UHPC subjected to standard heat treatment ranges from 20,000 N/m to 47,300 N/m.

There is little information in the literature focused on the fracture energy of Ductal concrete. In this study, the specimens were tested to determine the critical energy release rate and the total fracture energy on Ductal as discussed below.

Critical Energy Release Rate (G_f)

By using a thin TPB (Three-Point Bending) beam, plane stress was assumed and the critical energy release rate (G_f), or also known as the initial fracture energy, was related to K_{ic} and the modulus of elasticity, E , by equation

$$G_f = \frac{K_{ic}^2}{E} \quad (3.15)$$

Total Fracture Energy (GF)

The total fracture energy (GF) or specific fracture energy is based on Hillerborg's work-of-fracture method (Hillerborg's, 1985), which is defined as the ratio between the total energy (W_t), and the area of concrete fracture, $(d - a_0)b$. The total energy (W_t) is

calculated as the summation of the area (W_0) under the raw load (P_a) versus CMOD (crack mouth opening displacement) curve and $P_w\delta_o$, where P_a is the raw load applied by the testing machine (without considering self-weight). P_w is the equivalent self weight force, and δ_o is the CMOD displacement corresponding to $P_a = 0$ (Shah et al., 1995). The equivalent self weight force is calculated as $P_w = (S/2L) mg$, where S is the testing span, L is the length and mg is the mass (m) times gravity (g) weight of the beam. The total fracture energy was calculated as

$$GF = \frac{W_t}{(d - a_o)b} = \frac{W_o + 2P_w\delta_o}{(d - a_o)b} \quad (3.16)$$

CHAPTER 4

RESULTS AND DISCUSSION

In this work, several properties of Ductal were investigated including compressive strength, modulus of elasticity, flexural tensile strength, , mortar briquette test, split tensile strength, drying shrinkage, water absorption, water permeability, rapid chloride ion penetrability, chloride diffusion, and finally fracture toughness. The experimental data developed in this study are discussed. The results are also compared with published literature.

4.1 Compressive Strength and Modulus of Elasticity

4.1.1 Compressive Strength

Table 4.1 lists the average values of compressive strength of Ductal specimens for different ages and curing methods with different percentage of steel fibers. Also, Table 4.2 lists the average values of compressive strength of Ductal specimens for different exposure conditions after 6 months.

Table 4.1: Average compressive strength results of Ductal with different percentage of fibers and curing time and methods

Fiber content by weight %	Specimen age at testing (days)	Water-cured	Air-cured
		Average compressive strength (MPa)	Average compressive strength (MPa)
6.2%	3	108	107
	7	130	128
	14	147	134
	28	163	149
3.1%	3	106	104
	7	114	108
	14	127	126
	28	155	137
0%	3	92	84
	7	111	109
	14	116	110
	28	130	112

Table 4.2: Compressive strength of Ductal subjected to three exposure conditions (6.2% steel fibers)

Exposure Conditions	Average Compressive Strength (MPa)
6 months control	164
6 months wet-dry	161
6 months heat-cool	194

For exposure conditions, all specimens had a fiber content of 6.2%, first water-cured for 28 days and then exposed to air, heat-cool and wet-dry cycles for 6 months.

The results in Table 4.1 show that the compressive strength is much greater than that reported for HSC and conventional concrete. The compressive strength is about 163 MPa for 28-day water-cured specimens.

a) Effect of Curing Time and Method

As can be seen from Figure 4.1, the compressive strength increases with the length of curing for both types of curing. At any age, concrete cured in the air achieved slightly lesser strength than concrete subjected to water curing. However, the difference in strength is negligible at early age of 3 and 7 days between water and air curing.

Ductal (6.2% fibers) after 28 days of water curing exhibited 8% higher strength than similar specimens cured in air. Water-cured Ductal with 3.1% fibers had 11% more strength than same concrete cured in air. The increase in strength due to water curing over air curing was 14% for Ductal with 0% fibers. This indicates that the benefit of water curing as compared to air curing is more with less fiber content.

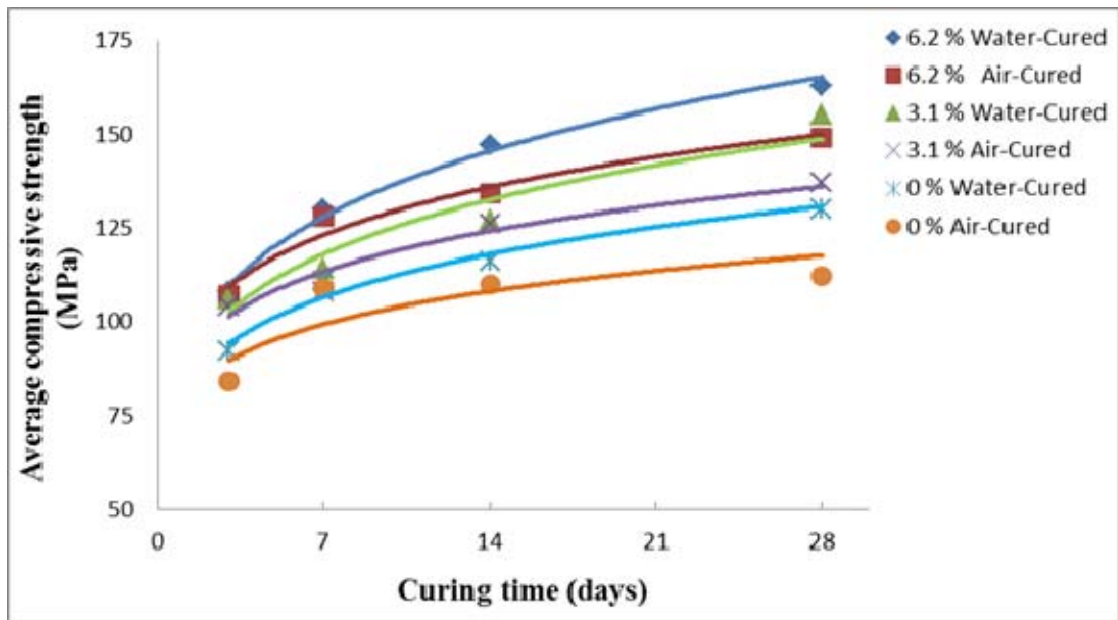


Figure 4.1: Evolution of compressive strength.

b) Effect Fiber Content

From the data in Table 4.1, it is found that there is no significant decrease in compressive strength with decrease in fiber content up to 50% below the standard value of 6.2% fiber in Ductal concrete.

After 28 days of water curing, the reduction in compressive strength is 5% when the fiber content was reduced from 6.2% to 3.1%. A reduction of 20% in compressive strength is recorded when fiber content was reduced to 0%. After 28 days of air curing, the reduction in compressive strength is 8.0% when fiber content was reduced from 6.2% to 3.1%. A reduction of 25% in the compressive strength is recorded when fiber content was reduced to 0%. This indicates that reduction in the fiber content even by 50% has no substantial negative impact on compressive strength.

In fact, researchers disagree on whether fibers increase the compressive strength or not. Schmidt et al. (2003) remarked that compressive strength “is practically not increased by the fibers,” which occupied 2.5% of the volume of the Ductal mix in their tests. Reda et al. (1999) disagree, but note that the increase due to fibers is not as great as the increase that may be achieved through an appropriate heat treatment, although the observed increase in strength is statistically significant with a fiber content of 2.0 percent by volume (6.2% by weight).

It is important to note that the specimens prepared for compressive strength in the present study showed different modes of failure. All specimens prepared without fibers (0% fibers) exhibited very brittle explosive type failure as shown in Figure 4.4, while all specimens prepared with fibers either 6.2 percent or 3.1 percent showed ductile failure, as shown in Figure 4.5.



Figure 4.2: Failure mode of Ductal without fiber (0% fibers).



Figure 4.3: Failure mode of Ductal (6.2% fibers).

c) Effect of Exposure Conditions on Compressive Strength

Compressive strength obtained for the Ductal specimens subjected to air, heat-cool and wetting-drying cycles for a period of 180-days is presented in Table 4.2 and plotted in Figure 4.4.

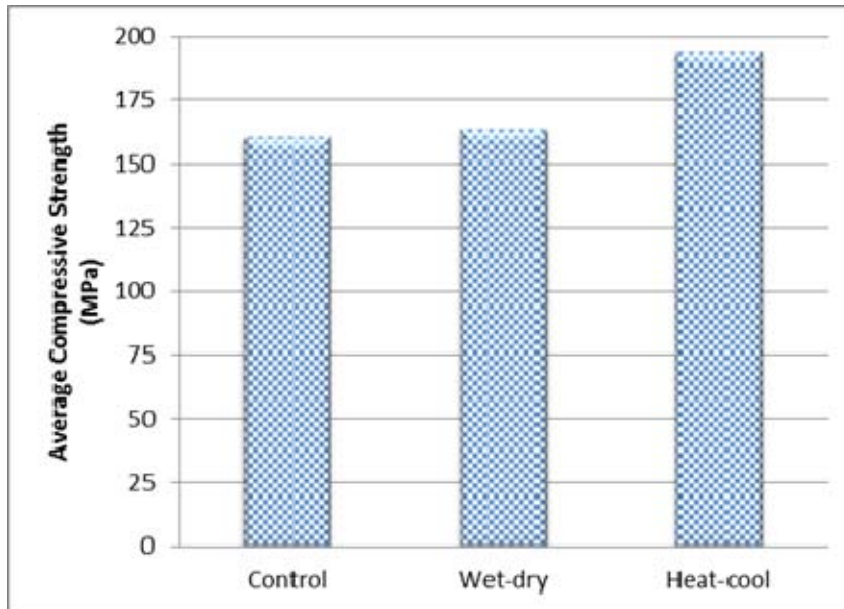


Figure 4.4: Average compressive strength after 6 months of exposure.

Like conventional concrete, Ductal also shows time-dependent gain in strength, the strength maturing at about 28 days of moist-curing, as six-month control specimens showed hardly any increase in strength. In exposure tests, the specimens did not show any adverse effect in strength. On the other hand, specimens exposed to heat-cool cycles showed an increase in strength of about 19% as compared to 28 days water-cured specimens. All researchers have reported higher strength in steam-curing. Because of the fact that a very low amount of water is used in Ductal (w/c ratio about 0.15), the hydration seems to remain partially incomplete under normal wet-curing condition due to high impermeability of mix. Repeated heat-cool cycles allow the mix to gain higher degree of hydration, achieving higher compressive strength.

4.1.2 Modulus of Elasticity

The modulus of elasticity of Ductal subjected to different curing regimes is presented in Table 4.3 and Figure 4.5.

The modulus of elasticity after 28 days of water curing shows a value of about 57 GPa, which is significantly higher than that for normal concrete and is about one-fifth the value of reinforcing steel. Like compressive strength, the modulus of elasticity also increases with heat-cool cycles.

a) Effect of Curing time and Exposure Condition on the Modulus of Elasticity of Ductal

Table 4.3: Modulus of elasticity of Ductal at different curing time and exposure conditions

Curing Time/ Exposure Conditions	Modulus of Elasticity, GPa
7 day water curing	43
28 day water curing	57
Control specimens @ 6 months	59
Wet-dry cycles @ 6 months	58
Heat-cool cycles @ 6 months	62

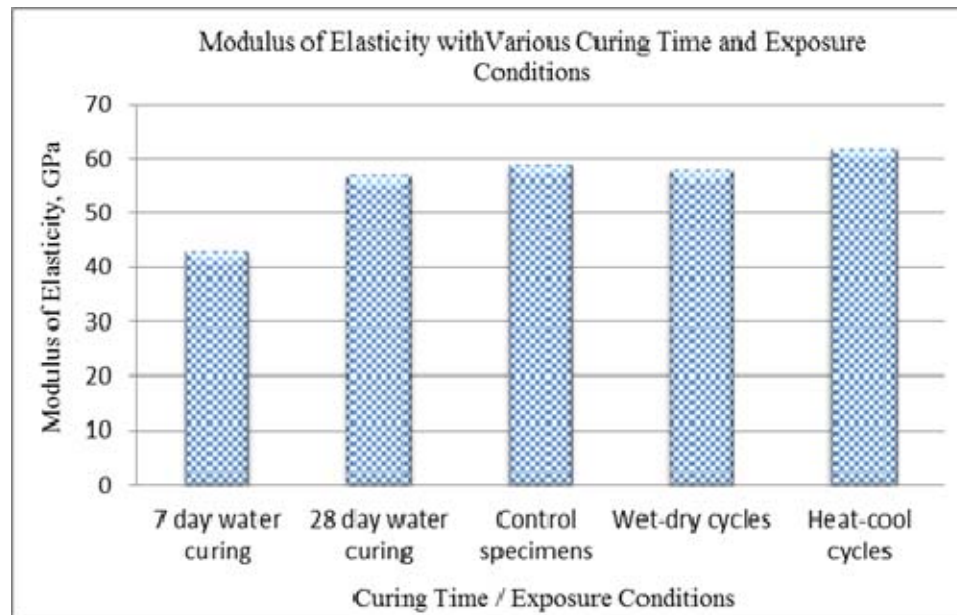


Figure 4.5: Effect of curing time and exposure conditions on the modulus of elasticity of Ductal.

Like compressive strength, the modulus of elasticity of Ductal increased with an increase in the curing period, as shown in Table 4.3 and Figure 4.5. The modulus of elasticity of specimens cured for 28 days was 32% higher than that of 7-day water-cured modulus of elasticity. The modulus of elasticity of Ductal exposed to wet-dry and heat-cool cycles did not decrease as compared to the specimens water-cured for 28 days. Instead, heat-cool cycles have significantly increased the modulus of elasticity (i.e., about 9%). Like compressive strength, the reason for the improvement in modulus of elasticity is the continuation of hydration at significant rate because of heat treatment.

b) Effect of Fiber Content on the Modulus of Elasticity

The modulus of elasticity of Ductal subjected to different curing regimes is presented in Table 4.4 and plotted in Figure 4.6.

Table 4.4: Modulus of elasticity of Ductal at different fiber content and curing methods

Fiber content (% by weight)	Modulus of Elasticity, GPa	
	28 day Water-Cured	28 day Air-cured
6.2%	57	49
3.1%	55	48
0% (without fibers)	39	36

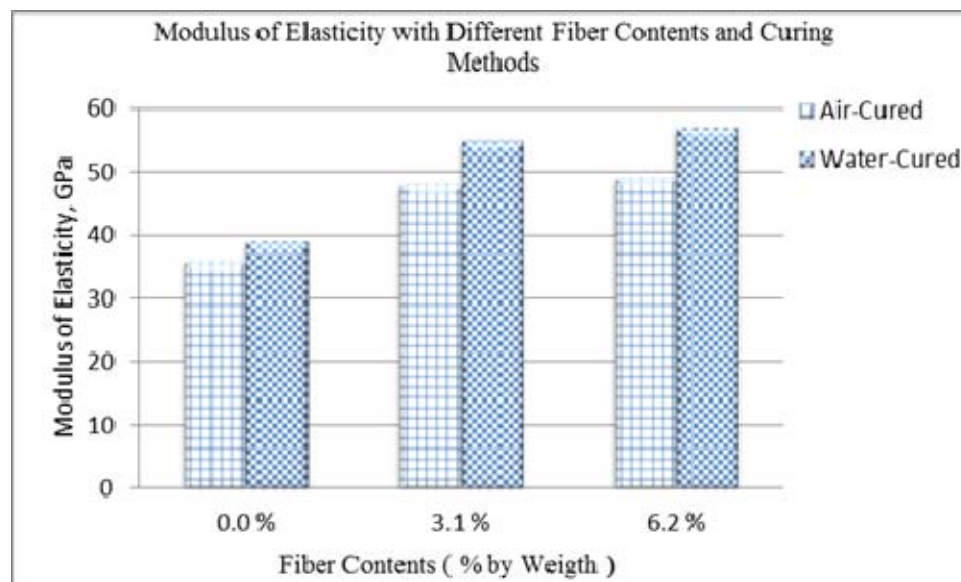


Figure 4.6: Effect of fiber contents on the modulus of elasticity of Ductal.

From the data presented in Table 4.4 and plotted in Figure 4.6, it can be noted that there is an increase in the modulus of elasticity of Ductal with an increase in the fiber

content. However, the increase in modulus of elasticity is significant only when the fiber content was increased from 0% to 3.1%. There was no significant increase in the modulus of elasticity when the fiber content was increased from 3.1 to 6.2 percent.

For the effect of curing method, the modulus of elasticity of Ductal with 6.2% fibers at 28 days water curing exhibited 14% higher than the air curing, similarly for 3.1% fibers, the modulus of elasticity of 28 days water curing was around 13% higher than the 28 day air cured specimens.

Only one selected samples of the stress strain diagram of Ductal samples tested at 28 days water curing is presented in Figure 4.7 and all the other test results for all specimens tested are shown in Appendix A.

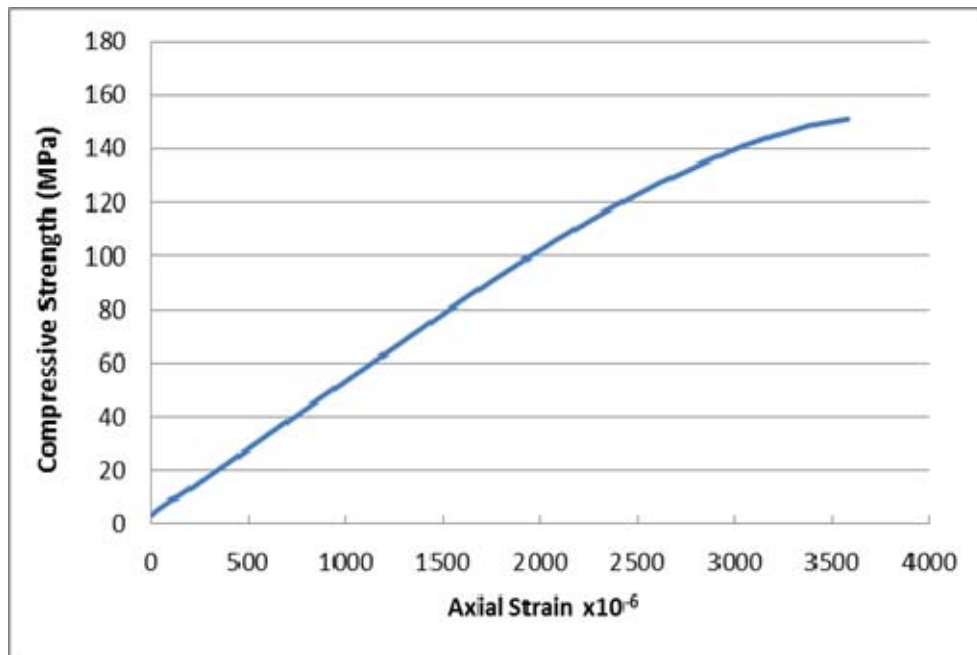


Figure 4.7: Selected stress-strain responses for 28 days water-cured Ductal (6.2% fibers) specimens.

4.2 Tensile Properties of Ductal

4.2.1 Flexural Properties

4.2.1.1 Effect of Curing

The load-deflection plots of three replicate prisms, each set water-cured for 7 and 28 days, are shown in Figures 4.8 and 4.9. The average results of the flexural strength and toughness parameters after 7 and 28 days water curing are presented in Table 4.5.

Tests have shown that after the cracking load, which is defined as the load corresponding to the development of first crack at the bottom (tension) face, the beams continue to carry more loads with an increase in the deflection until the maximum load (peak load) is reached. This increase in load is attributable to the presence of steel fibers, that become fully mobilized as crack arrestor after first cracking. Following the attainment of peak load, softening mode of collapse takes place, exhibiting gradual decrease in load with increased deflection and crack-growth as shown in Figures 4.8 and 4.9.

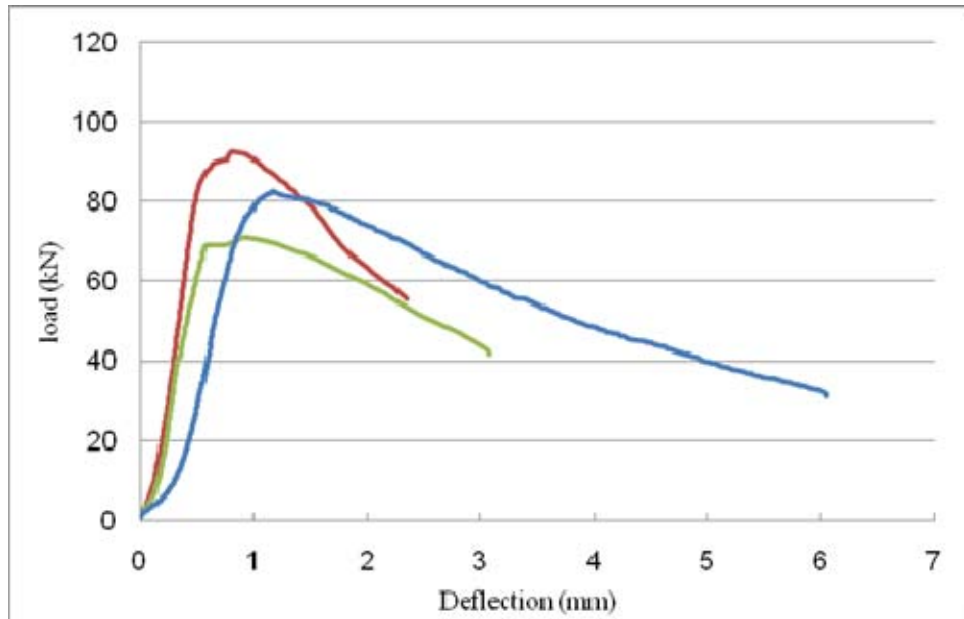


Figure 4.8: Load-deflection curves for three similar specimens tested after 7 days water curing.

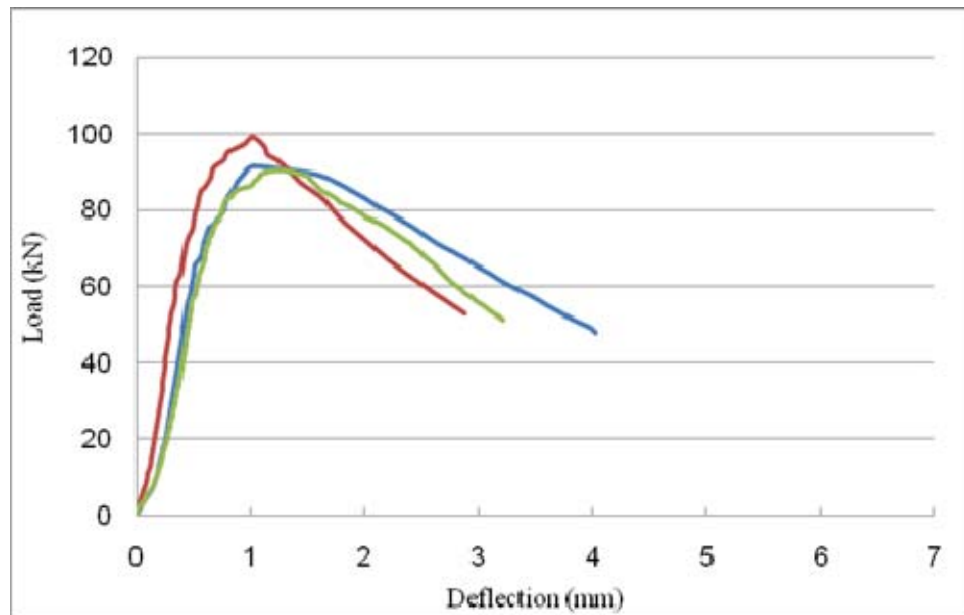


Figure 4.9: Load-deflection curves for three similar specimens tested after 28 days water curing.

Table 4.5: Average flexural toughness parameter for water-cured specimens (6.2% fibers)

Curing time in water	First-Peak Strength (MPa)	Peak Strength or MOR (MPa)	Deflection at Peak Load (mm)	$P_{100,0.5}$ (KN)	$F_{100,0.5}$ (MPa)	$P_{100,2}$ (KN)	$F_{100,2}$ (MPa)	$T_{100,2}$ (N.m)
7 days	12	27.35	1.14	65	20.2	63.6	19.51	130.0
28 days	18.9	31.4	1.1	66.31	22	80.5	26.6	157.3

The flexural behavior of fiber-reinforced Ductal can be characterized by elastic deformation up to the first cracking load, followed by a further increase in deformation due to increase in load (stiffening due to mobilization of fibers as crack arrestors) and subsequent prolonged softening after reaching the peak-load. The first cracking load corresponds approximately to the load at which specimens without fiber would fail in flexure i.e. to the tensile strength of plain Ductal in flexure. Consistent with the definition of modulus of rupture, the tensile strength at the peak-load can be taken as modulus of rupture (MOR) for fiber-reinforced Ductal.

Load-deflection plots show that for all practical purposes, a linear relationship between load and deflection can be assumed upto about 70% of the peak-load. The beam stiffness is essentially constant upto about this load level.

The presence of longer softening zone in the post peak-load deformation indicates high ductility of fiber-reinforced Ductal. As an indication of the appreciable softening, the deflection at about 60% of the post peak-load level becomes almost 3 times the value of deflection at the peak-load.

The flexural tensile strengths at the first cracking and corresponding to the peak-loads are shown in Table 4.5. The peak-load strength is calculated on the basis of elastic section modulus of the gross section of the prisms, and is taken as the value of MOR. The average value of flexural strength, MOR, is 31.4 MPa for Ductal with 6.2% fiber. The flexural toughness or the absolute toughness according to ASTM C 1609, $T_{100,2}$ after 28 days water curing was calculated as the area under load-deflection curve up to 2 mm deflection achieved 20% higher than 7 days of water curing .

As the strength increases with curing period, the 28-day water-cured specimens showed an increase in the flexural tensile strength by about 37% compared to that for 7-day water-cured samples. The cracking load strength also increased by about 50%, indicating the beneficial impact of longer curing period.

The test results pertaining to flexural performance of Ductal specimens (6.2% fibers) at different ages are plotted in Figures 4.10 and 4.11.

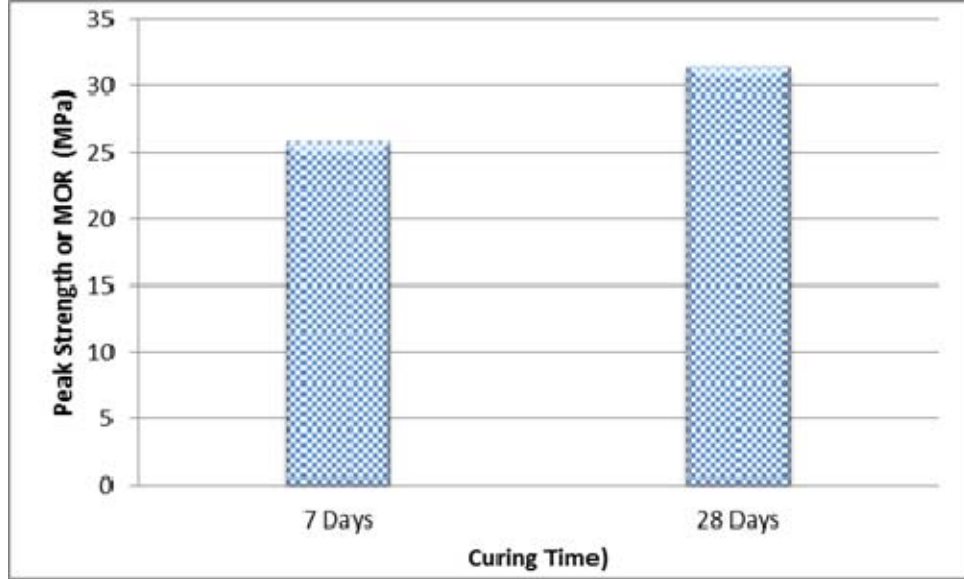


Figure 4.10: MOR of Ductal cured in water for 7 and 28 days.

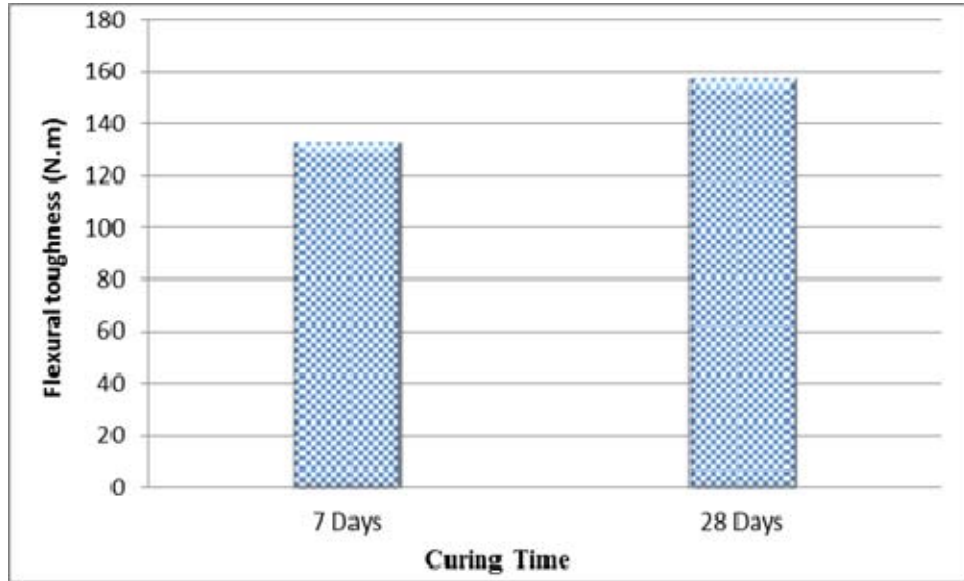


Figure 4.11: Flexural toughness of Ductal cured in water for 7 and 28 days.

4.2.1.2 Effect of Exposure Conditions

The load-deflection plots for 28-day water-cured specimens with 6.2% fiber, which were subjected to different exposure conditions for six months, are shown in Figures 4.12 through 4.14. The strength values are shown in Table 4.6. It should be noted that for exposure tests, all samples contained 6.2% fiber.

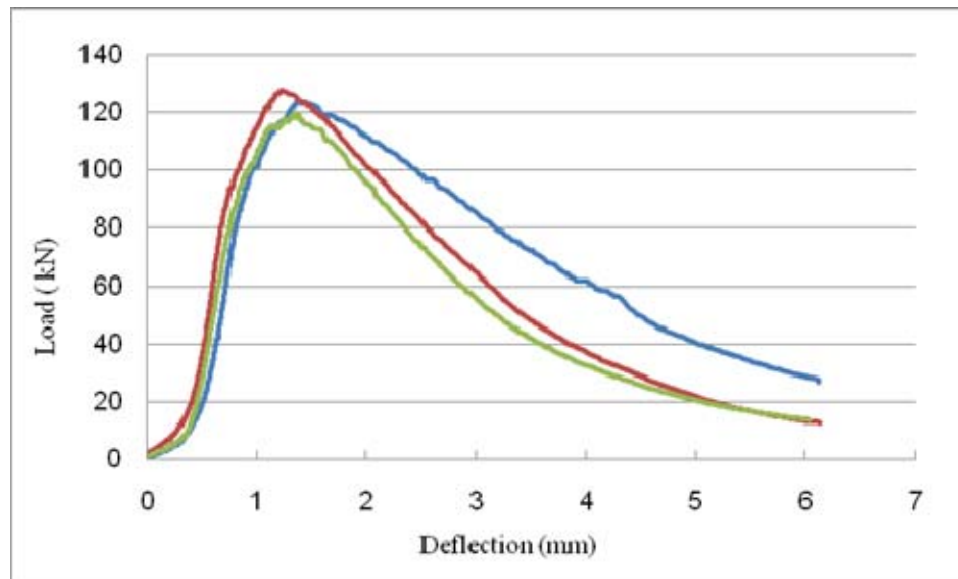


Figure 4.12: Load-deflection plots for three specimens tested after 6 months of normal exposure (control).

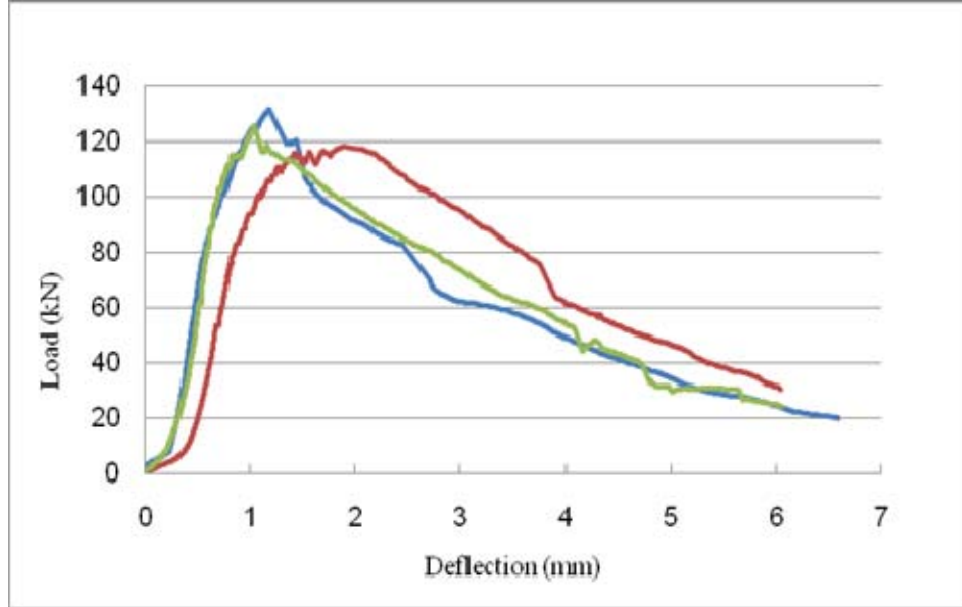


Figure 4.13: Load-deflection plots for three specimens tested after 6 months of wet-dry cycles.

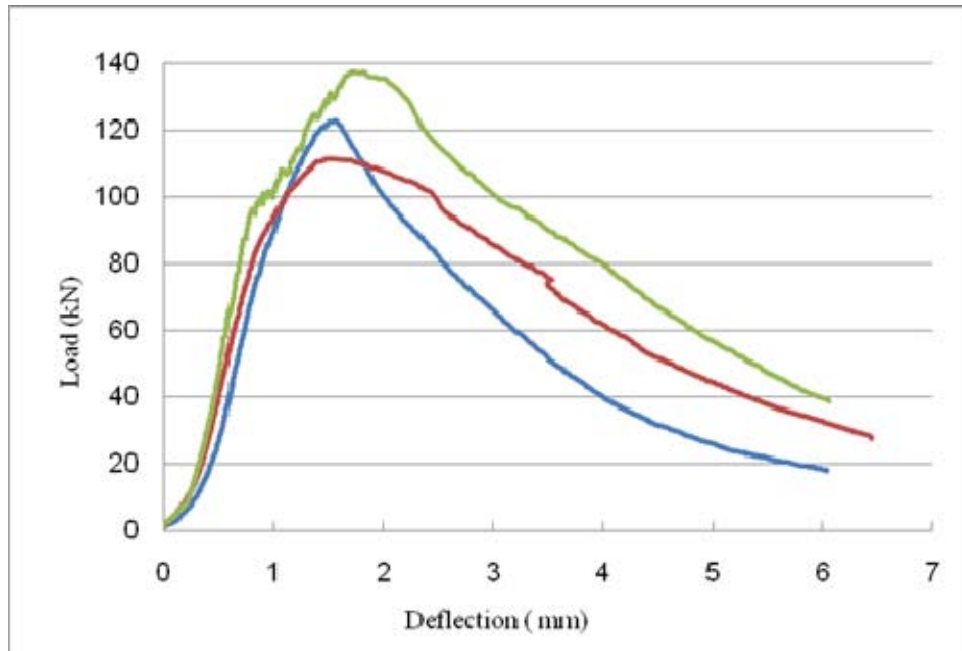


Figure 4.14: Load-deflection plots for three specimens tested after 6 months of heat-cool cycles.

Table 4.6: Average flexural toughness parameter for exposure specimens (6.2% fibers)

Exposure Condition	First-Peak Strength (MPa)	Peak Strength or MOR (MPa)	Deflection at Peak Load (mm)	$P_{100,0.5}$ (KN)	$F_{100,0.5}$ (MPa)	$P_{100,2}$ (KN)	$F_{100,2}$ (MPa)	$T_{100,2}$ (N.m)
Control	20.6	37.11	1.3	31.3	9.4	103	31	157
Wet-dry	17.4	37.5	1.3	63.3	19	101.4	30.5	170
Heat-cool	22.24	37.9	1.6	43.1	13	114.4	34.3	173.5

The test data indicate that the average tensile strength corresponding to first cracking is the highest for heat-cool cycled specimens as expected. However, the average flexural tensile strength (MOR) corresponding to peak-load is essentially the same with no significant variation due to different exposure conditions.

The test results pertaining to flexural performance of Ductal subjected to different exposure conditions for 6 months after 28 days curing are plotted in Figures 4.15 and 4.16. It can be seen from these plots that the wet-dry and heat-cool conditions have virtually no negative impact on the flexural properties of Ductal. Contrarily, heat-cool cycles have shown to improve the all properties. While the values of MOR seem to be the same for all three exposure conditions, the flexural toughness and residual flexural strength values increases in heat-cool cycles.

4.2.1.3 Effect of Fiber

The load-deflection plots of three replicate prisms each set water-cured for 28 days with 3.1% and 0% steel fibers are shown in Figures 4.17 and 4.18. The average

results of the flexural strength and toughness parameters after 28 days water curing for different fiber contents are presented in Tables 4.7.

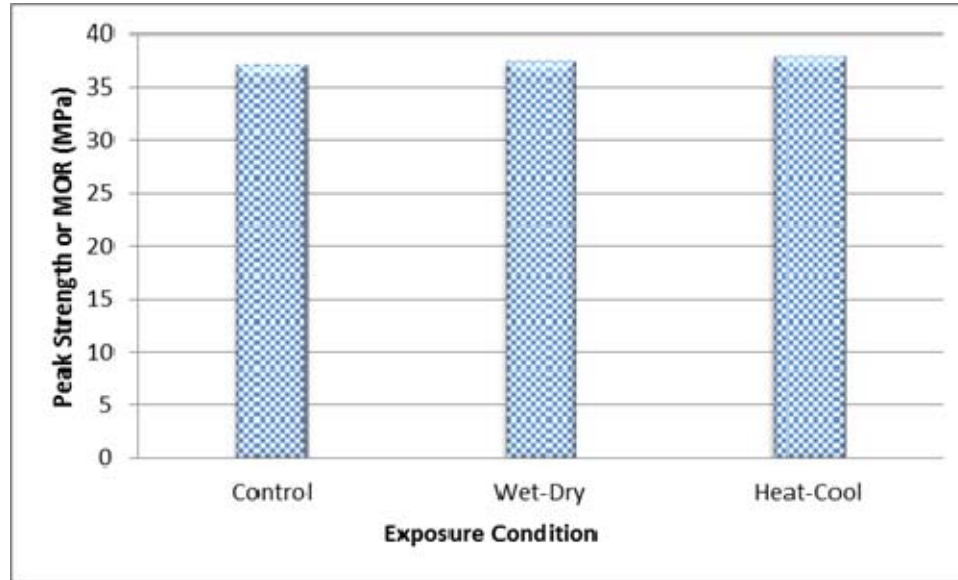


Figure 4.15: MOR of Ductal subjected to different exposure conditions for 6 months after 28 days of water-curing.

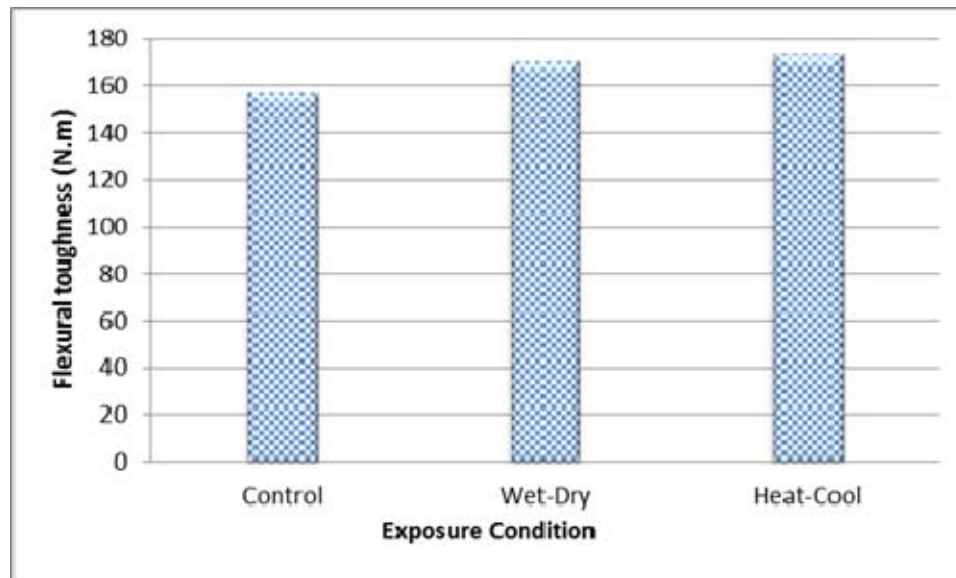


Figure 4.16: Flexural toughness of Ductal subjected to different exposure conditions for 6 months after 28 days of water-curing.

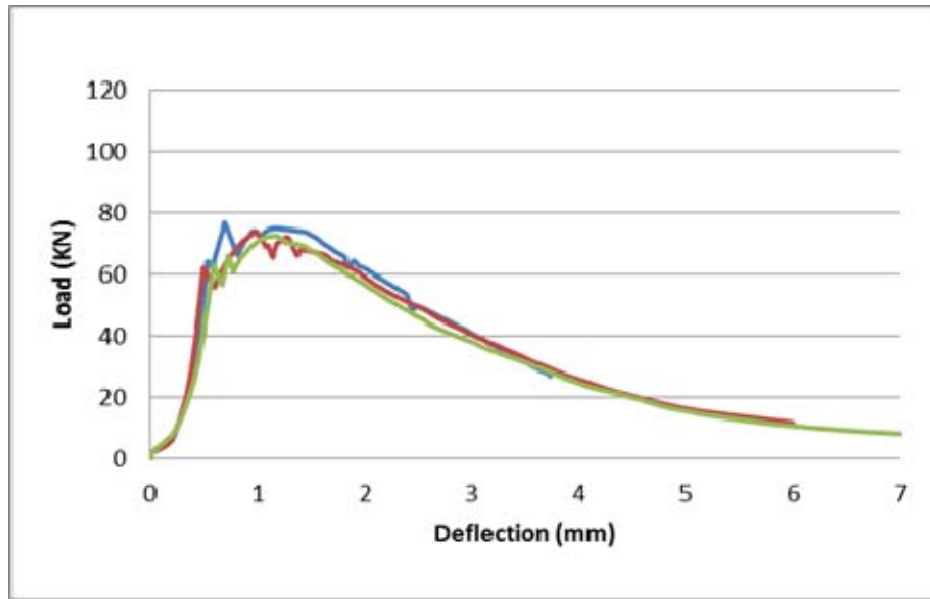


Figure 4.17: Load-deflection curves for three similar specimens of Ductal (with 3.1% fiber) tested after 28 days water curing.

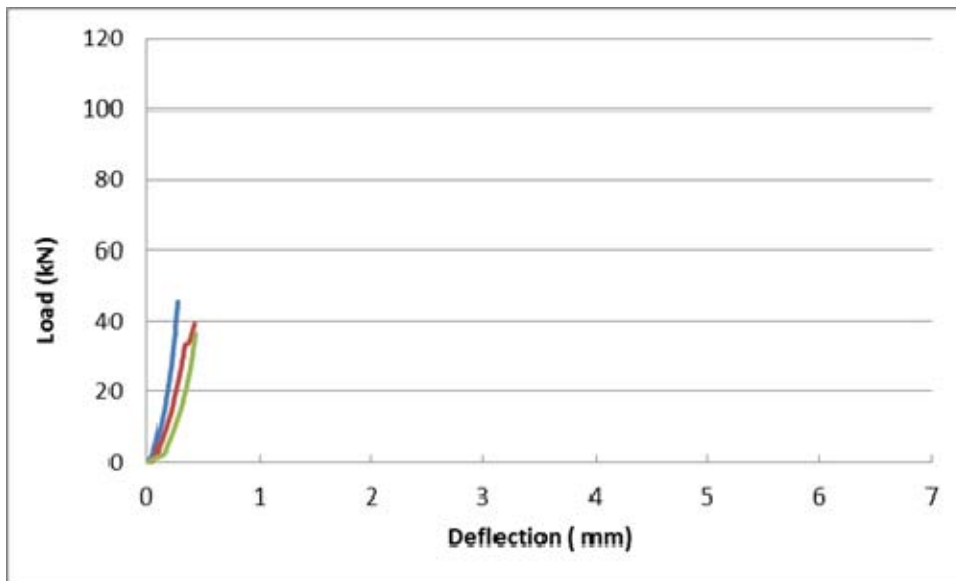


Figure 4.18: Load-deflection curves for three similar specimens of Ductal (with 0% fiber) tested after 28 days water curing.

Table 4.7: Average flexural toughness parameter for 28 days water- cured specimens with different percentage of fibers

Percentage of fibers (% by weight)	First-Peak Strength (MPa)	Peak Strength or MOR (MPa)	Deflection at Peak Load (mm)	$P_{100,0.5}$ (KN)	$F_{100,0.5}$ (MPa)	$P_{100,2}$ (KN)	$F_{100,2}$ (MPa)	$T_{100,2}$ (N.m)
6.2	18.9	31.4	1.1	66.31	22	80.5	26.6	157.3
3.1	20.4	24.4	1.11	59.1	19.5	54.7	18.1	120.1
0.0	15.2	15.2	0.55	43.6	14.5	-	-	8.8 [#]

[#] Toughness calculated here with 0% fibers based on the area under load-deflection curve up to the max deflection on each samples before failure.

Three cases of fiber reinforcement were considered: 0% (no fiber), 3.1% and 6.2%. Results shown in Table 4.7 highlight the significance of fiber content in the enhancement of flexural tensile strength. The tensile strength at the peak-load increases from 15.2 MPa with no fiber to 24.4 MPa with 3.1% fiber and 31.4 MPa with 6.2% fiber. The tensile strength almost doubles with 6.2% fiber. However, the tensile strength at the first cracking load is marginally enhanced by the addition of fiber. This is expected as the resistance to first crack is mostly provided by the concrete.

The test results pertaining to flexural performance after 28 days water curing with different percentage of fibers are plotted in Figures 4.19 and 4.20.

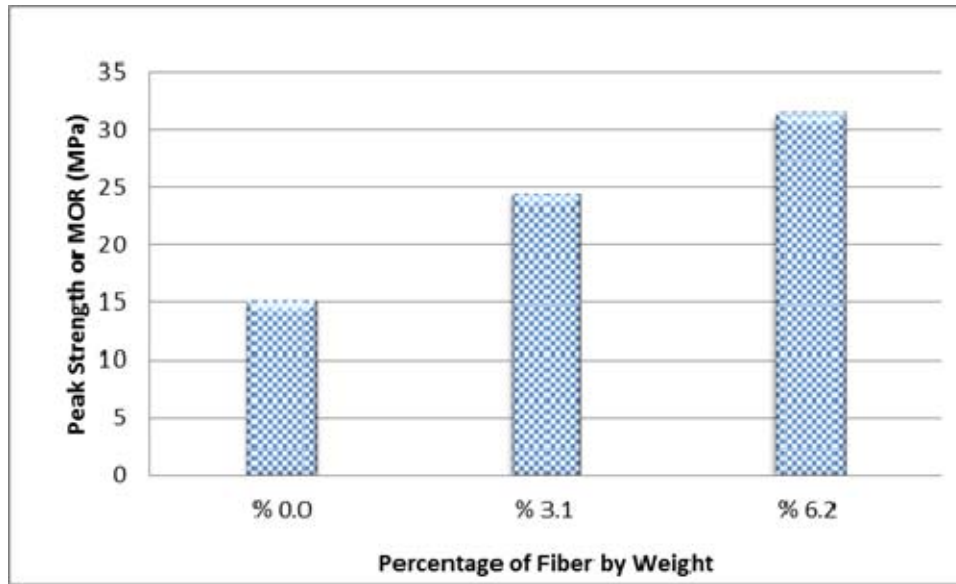


Figure 4.19: MOR of specimens with different fiber contents and cured in water for 28 days.

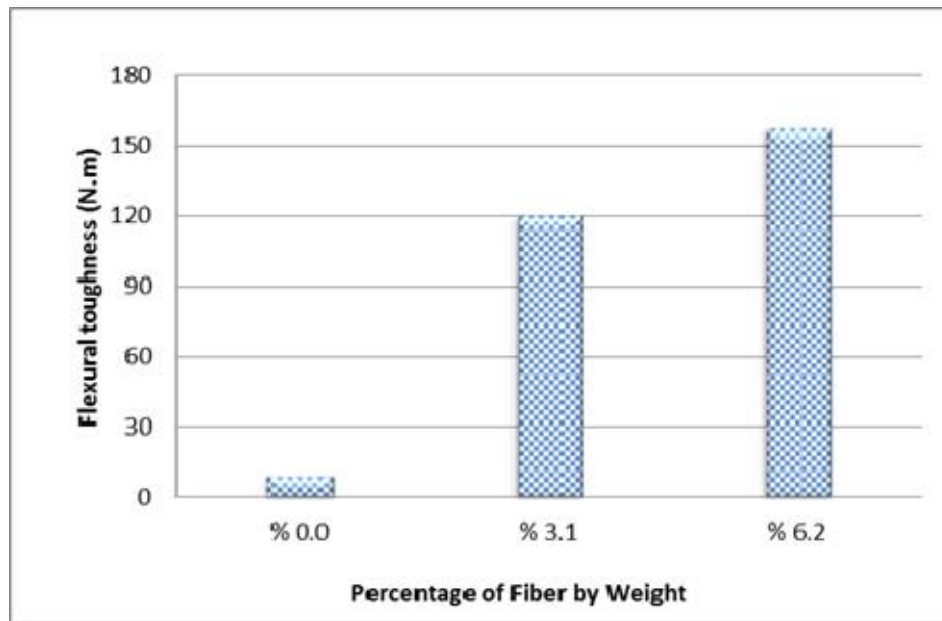


Figure 4.20: Flexural toughness of specimens with different fiber contents and cured in water for 28 days.

For a better perspective of the key experimental data, all test results are shown collectively in Table 4.8, which also includes results for specimens with no fiber and 3.1% fiber. It is observed that heat-cool cycled specimens and control specimens had higher peak-load tensile strength than those for 28-day water-cured specimens.

Table 4.8: Comparison of the average first peak strength of different ages and different fiber contents and different exposure conditions

Curing Time/Exposure Conditions/Fiber Content	First Cracking Strength (MPa)	Peak Strength (MPa)	Ratio of Peak/First Cracking Strength
7 days water curing (Ductal, 6.2% fibers)	12.0	27.3	2.28
28 days water curing (Ductal, 6.2% fibers)	18.9	31.4	1.66
28 days water curing (Ductal, 3.1% fibers)	20.4	24.4	1.20
28 days water curing (Ductal, 0% fibers)	15.2	15.2	1.00
6 months exposure (Control specimens)	20.6	37.1	1.80
6 months exposure (Wet-dry cycles)	17.4	37.5	2.16
6 months exposure (Heat-cool cycles)	22.2	38.0	1.71

It is important to note that the first-peak strength is defined as the value at the first appearance of flexural-induced crack in a test specimen. This strength is essentially that of the Ductal concrete alone. It increases somewhat with addition of fibers, as some fibers will appear at the tension face of the test specimens. While the load-deflection plots with 3.1% of steel fibers clearly shows the first peak values (Figure 4.17), the specimens with 6.2% have less clarity with regard to the clear visibility in the plots.

Calculation of Residual Flexural Strength (Post-Cracking Flexural Strength)

As explained in section 3.6.1 for evaluation of the residual flexural strength by using three techniques named, ASTM C 1609, JSCE SF-4 and PCS methods, the values of residual flexural strength determined using all three methods, together with MOR and flexural toughness values, for Ductal with different curing lengths, fiber contents, and exposure conditions are presented in Tables 4.9 through 4.11.

Table 4.9: Average flexural properties of Ductal cured in water for 7 and 28 days

Curing Time (days)	Peak Strength MOR (MPa)	Flexural Toughness $T_{100,2}$ (N-m)	Residual flexural strength ASTM C 1609	Residual flexural strength PCS	Residual flexural strength JSCE SF-4
			$f_{100,2}$ (MPa)	PCS (MPa)	$f_{e,2}$ (MPa)
7 days	27.35	130.0	21.2	23.7	19.7
28 days	31.4	157.3	27.5	27.4	23.6

Table 4.10: Average flexural properties of specimens contained different fiber contents and cured in water for 28 days

Fiber content (% by weight)	Peak Strength or MOR (MPa)	Flexural Toughness $T_{100,2}$ (N-m)	Residual flexural strength ASTM C 1609	Residual flexural strength PCS	Residual flexural strength JSCE SF-4
			$f_{100,2}$ (MPa)	PCS (MPa)	$f_{e,2}$ (MPa)
6.2	31.4	157.3	27.5	27.4	23.6
3.1	24.4	120.1	18.1	21.5	18
0	15.2	-	-	-	-

Table 4.11: Average flexural properties of Ductal subjected to different curing conditions for 6 months after curing in water for 28 days

Exposure Condition	Peak Strength or MOR (MPa)	Flexural Toughness $T_{100,2}$ (N-m)	Residual flexural strength ASTM C 1609	Residual flexural strength PCS	Residual flexural strength and ratio JSCE SF-4
			$f_{100,2}$ (MPa)	PCS (MPa)	$f_{e,2}$ (MPa)
Control	37.1	157.0	32.0	34.5	23.5
Wet-dry	37.5	170.0	32.0	32.8	24.5
Heat-cool	37.9	173.5	34.3	36.0	26.0

From Tables 4.9 through 4.11, it can be observed that the values of residual flexural strength determined using ASTM C 1609 and PCS methods are somewhat close to each other, while the values of residual flexural strength determined using JSCE SF-4 are less in all the cases. The values determined using ASTM C 1609 method was considered for discussing the effects of curing, fiber contents, and exposure conditions.

The results of the residual flexural strength determined using ASTM C 1609 for different ages, different fiber content and exposure conditions are plotted in Figures 4.21 through 4.23, respectively.

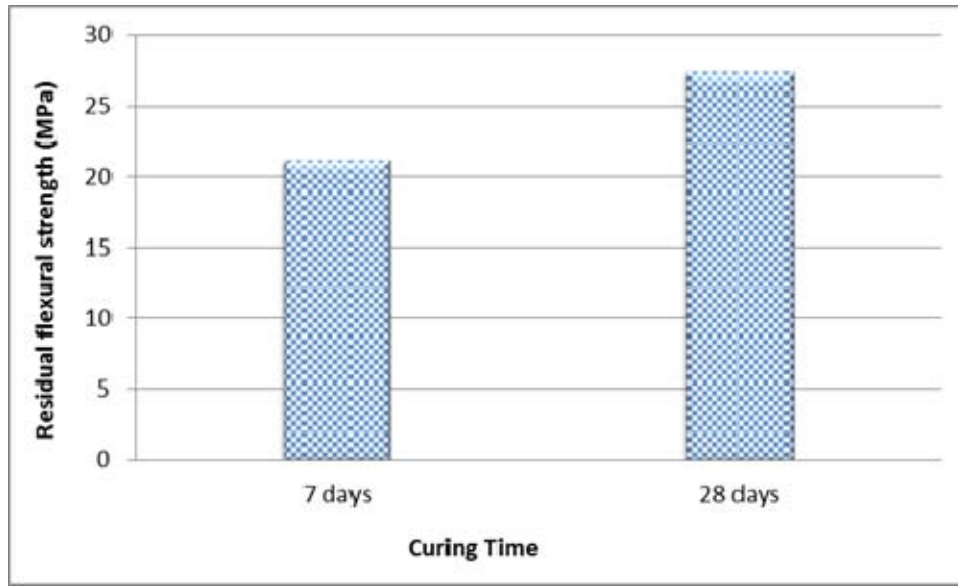


Figure 4.21: Residual flexural strength (ASTM C 1609) of Ductal (6.2% fibers) cured in water for 7 and 28 days.

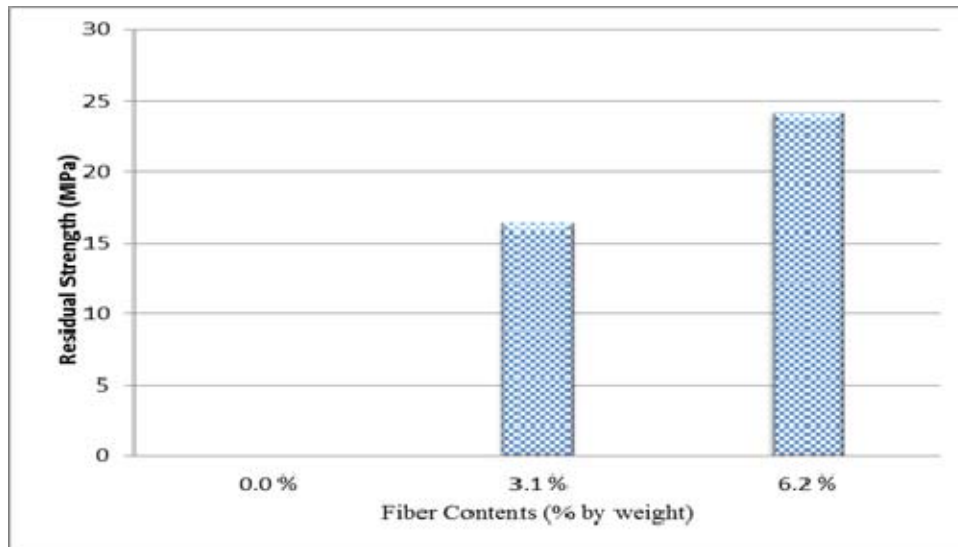


Figure 4.22: Residual flexural strength (ASTM C 1609) of specimens with different fiber contents and cured in water for 28 days.

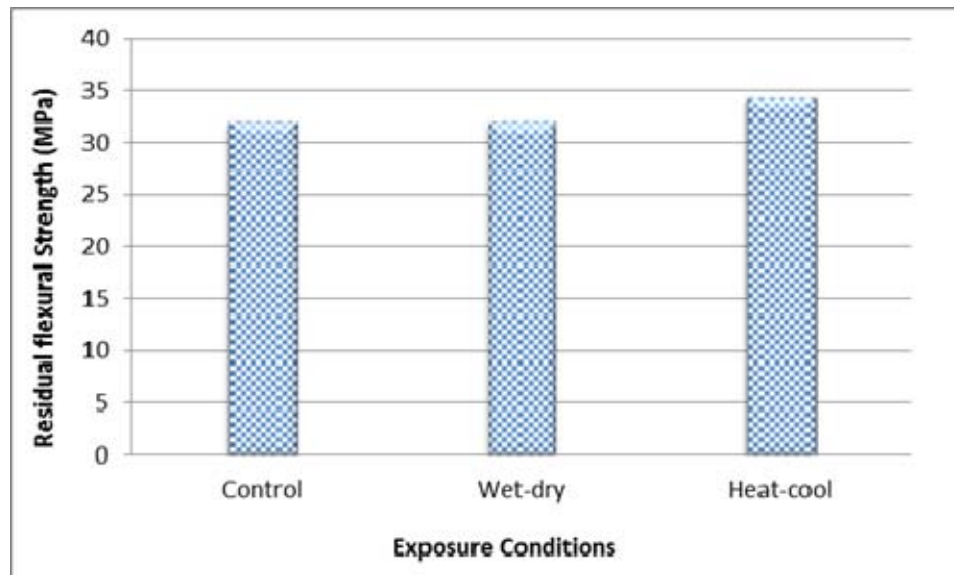


Figure 4.23: Residual flexural strength (ASTM C 1609) of Ductal subjected to different exposure conditions for 6 months after 28 days of water-curing.

4.2.2 Mortar Briquette Test (Direct Tension Test)

The tensile strength results for 28 days water and air cured specimens are presented in Table 4.12. The results from five specimens in each group have been averaged, and the average value is shown in Table 4.12. Plots of load versus cross-head displacement are shown in Figures 4.24 and 4.25.

Table 4.12: Average mortar briquette test for Ductal at 28 days water curing

Curing Method	Average Max.Load (KN)	Max Cross-Head Displacement (mm)	Tensile Strength (MPa)
Water-cured	8.25	3.25	12.8
Air-cured	5.7	2.62	8.8

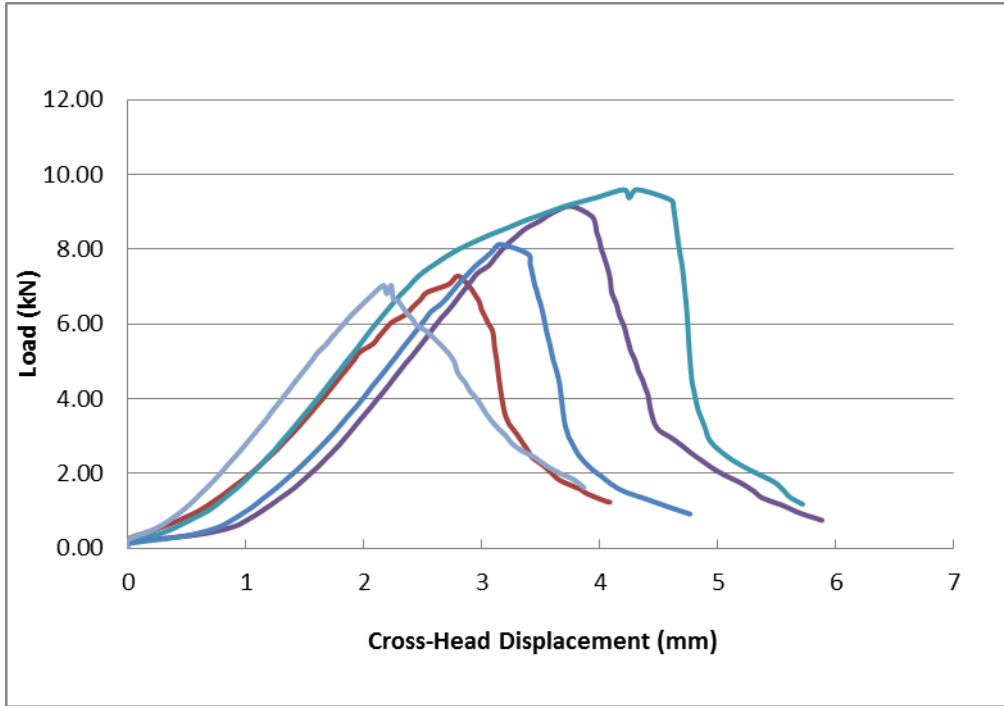


Figure 4.24: Load-cross head displacement plots for 28 days water-cured (6.2% steel fibers).

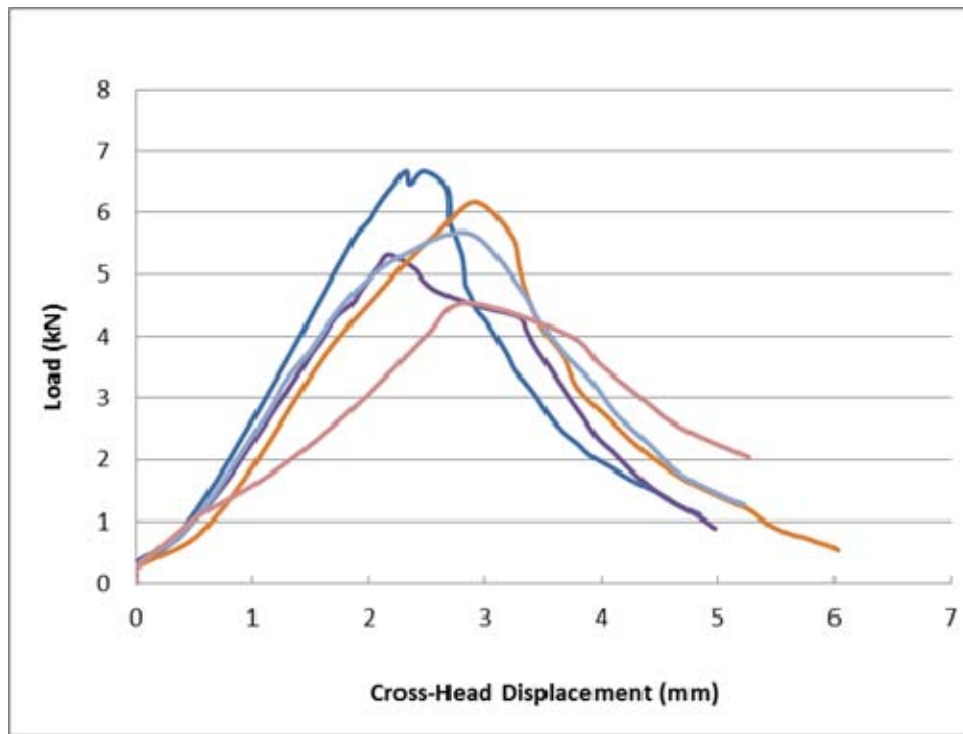


Figure 4.25: Load-cross head displacement plots for 28 days air-cured (6.2% steel fibers).

The tensile cracking strength of the 28 day water cured specimens is 12.82 MPa, while the air cured shows lower value of 8.84 MPa which is around 31% lower.

It is important to note here that after the peak load reached (Figures 4.24 and 4.25) there is a softening decline in the load due to the effect of steel fibers. Fibers also prevent brittle failure and imports ductility.

4.2.3 Split Tensile Strength

The results of the average peak split cylinder load and strength values of Ductal (6.2% fibers) are presented in Table 4.21. Also the plot of the average splitting tensile strength against exposure conditions presented in Figure 4.26.

Table 4.13: Average splitting tensile strength of Ductal

Curing Regimes	Average Max.Load (kN)	Average Splitting Tensile Strength (MPa)
28 days water curing	208.2	12.6
Control	246.7	15
Wet-dry	202	12.3
Heat-cool	284.1	17.2

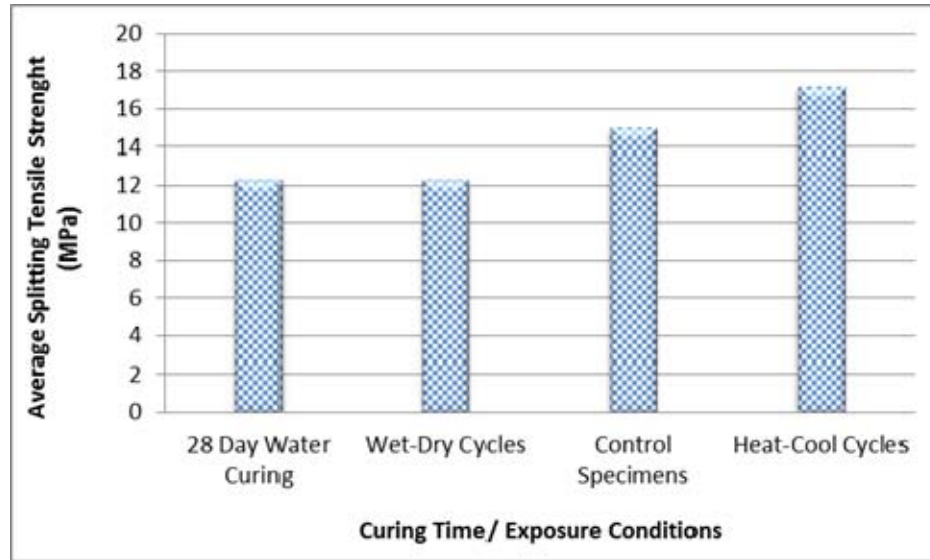


Figure 4.26: Average splitting strength against exposure conditions.

The splitting tensile strength of Ductal specimens after 28 days water curing is 12.6 MPa. After 6 months of wet-dry cycles, no adverse effect was observed, but after 6 months of exposure to laboratory condition (control) this value increased by 19% to 15 MPa, and after 6 months of heat-cool cycles the splitting tensile strength increased by 36% to 17.2. Heat-cool cycles increased the splitting tensile strength, as expected due to the effect of heat treatment.

At failure, the cylinders are split into two halves as normally seen in plain concrete cylinders. Because of binding fibers, the cylinders show longitudinal cracks without being completely split into two halves as shown in Figure 4.27.



Figure 4.27: Mode of failure after splitting tensile test.

4.3 Drying Shrinkage

The drying shrinkage was measured on prism specimens after 28 days of water curing over a period of about 4 months. Plot of average shrinkage strains versus time data is shown in Figure 4.28. As can be observed from Figure 4.28, the maximum shrinkage was 300×10^{-6} , which occurred within the first one month of the post-curing exposure. It then reduced to about 250×10^{-6} within the next month and then remained almost constant thereafter.

The drying shrinkage, after 28-day wet curing period, precludes any shrinkage that may have occurred during the curing period. Past research (VandeVoort et al., 2008; Spasojević, 2008; Yanni, 2010) has drawn attention to autogenous shrinkage during steam curing or heat treatment, a factor attributable to the presence of high amount of cement and reduced amount of water in concrete mix.

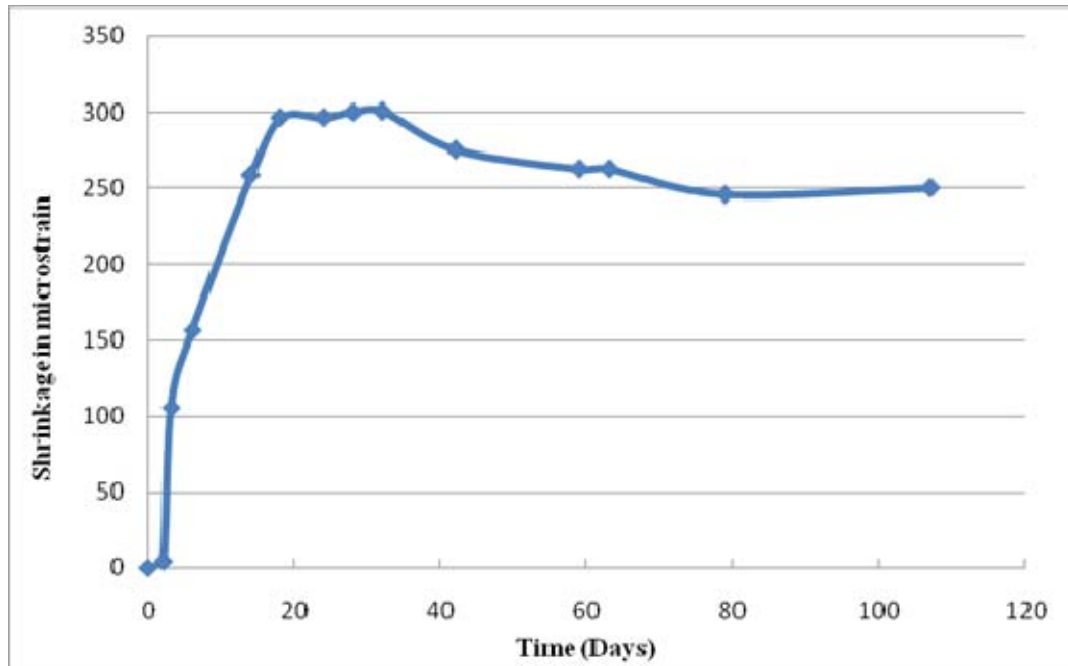


Figure 4.28: Drying shrinkage in micro strain with time after 28-day water curing.

4.4 Water Absorption

The test results on 9 of 3×6 in. cylinders under different exposure conditions are presented in Table 4.22. Three specimens were performed for each exposure condition.

Table 4.14: Average water absorption of Ductal specimens

Exposure Conditions	Average Absorption (%)
Wet-dry cycles	0.0235
Heat-cool cycles	0.054
Control specimen	0.0982

The above results show that for all the exposure conditions, the water absorption is much lower compared to that of conventional concrete and high strength concrete. Wet-dry cycled specimens showed even smaller amount of water absorption.

4.5 Water Permeability (DIN Test)

The tests were conducted on 150 mm cubes, three specimens being used for each exposure condition. Results reveal that all the tested specimens exhibited virtually zero depth of water penetration into the samples.

4.6 Rapid Chloride Ion Penetrability Testing

Results from these tests are presented in Table 4.23. Three samples were used for each exposure condition.

Table 4.15: Average rapid chloride ion penetrability results

Average Rapid Chloride Ion Penetrability (Coulombs)		
Control Samples	Wet-Dry Cycles	Heat-Cool Cycles
300	225	48
Very Low	Very Low	Negligible

The above results suggest that Ductal specimens have very low permeability of chloride ion for both control specimens (300 Coulombs) and wet dry cycles (225 Coulombs), and negligible value for heat-cool cycles (48 Coulombs) as expected

because of the effect of heat treatment which helped densify the microstructure of Ductal as explained earlier.

4.7 Chloride Diffusion

The results of average water-soluble chloride contents of specimens exposed to chloride for 4 and 6 months are presented in Table 4.24 for various depths from the exposed surface. The plots of the chloride concentration as percentage of mass versus depth from the exposed surface are shown in Figures 4.29 and 4.30 for four and six months, respectively.

Table 4.16: Average water soluble chloride contents of Ductal

Average Depth (cm)	Average Chloride Content as Percentage Weight of Ductal	
	Time = 4 Months	Time = 6 Months
0.25	0.051	0.055
1.25	0.01777	0.019
2.25	0.00402	0.011
3.25	0.00191	0.0041
4.25	0.00011	0.002
5.25	0.0001	0.001

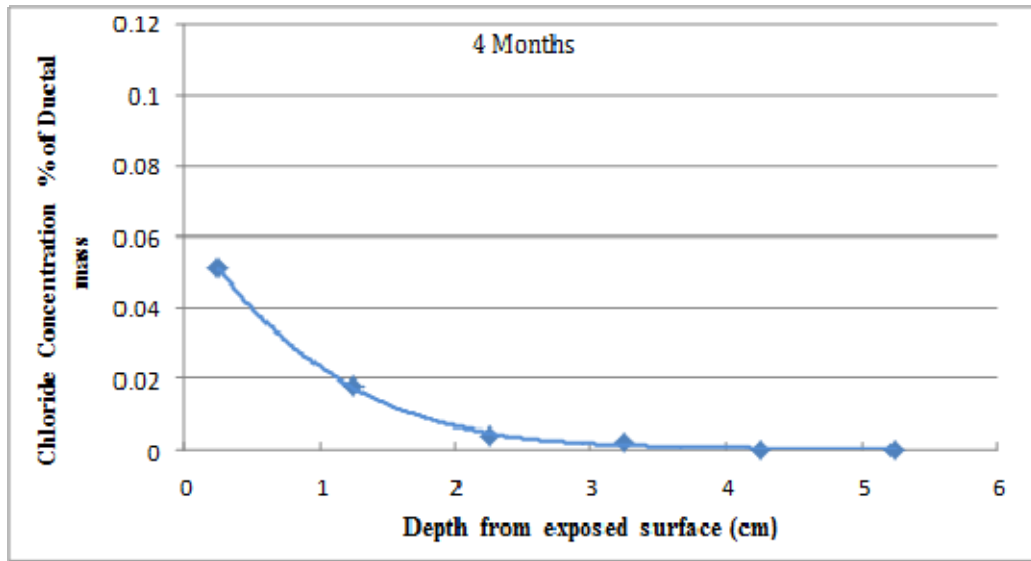


Figure 4.29: Chloride concentrations Cl% of Ductal mass versus depth from the exposed face after 4 months.

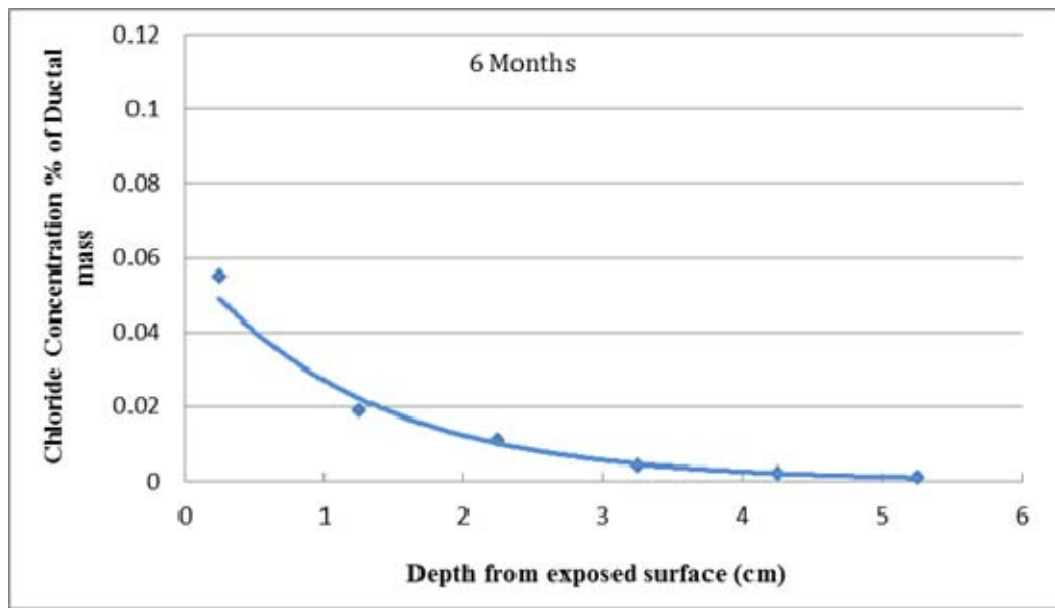


Figure 4.30: Chloride concentrations Cl% of Ductal mass versus depth from the exposed face after 6 months.

The values of average apparent diffusion coefficient, D_e , of Ductal were computed from data as: at four months, $D_e = 7.8 \times 10^{-9}$ cm²/sec and at six months, $D_e = 5.8 \times 10^{-9}$ cm²/sec. An average value of D_e can be established as 7.0×10^{-9} cm²/sec for moist-cured specimens. Lafarge website and other researchers reported that the diffusion coefficient of Ductal is 2×10^{-10} cm²/sec after heat treatment at 90°C. Heat treatment is normally recommended for Ductal. A comparison of D_e for heat-treated and water-cured Ductal shows that the value for the latter samples is almost forty times the value for heat-treated specimens. This clearly highlights the importance of heat treatment.

4.8 Fracture Toughness Test Results

The results of loading and unloading tests for one elected specimen on notched specimens are presented in Figures 4.31 and 4.32 for water-cured specimens. The calculated values of critical stress intensity factor (K_{ic}) and the critical crack tip opening displacement ($CTOD_c$) are shown in Tables 4.25 and 4.26 for 28-day water-cured for different percentage of fibers and for six months of exposure: control specimens and heat-cool cycled specimens, respectively.

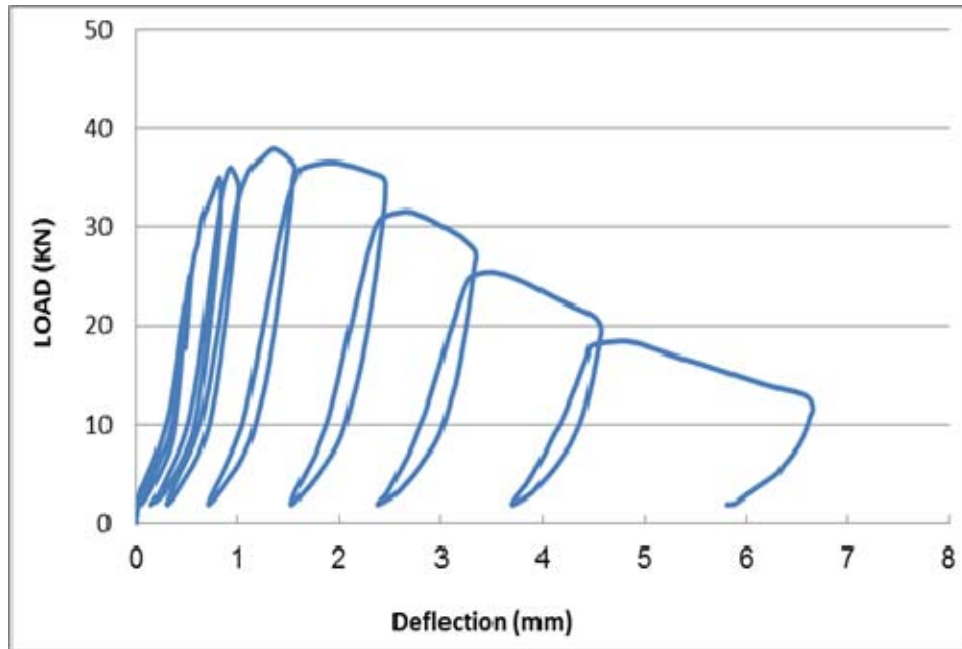


Figure 4.31: Selected loading and unloading deflections for 28-day water-cured (6.2% fibers).

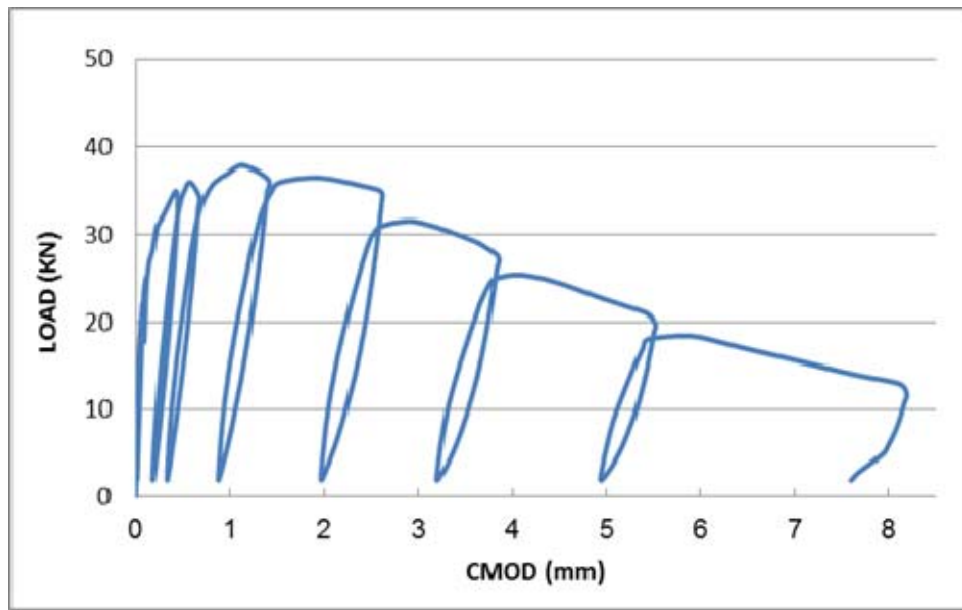


Figure 4.32: Selected loading and unloading deflections for 28-day water-cured (6.2% fibers).

From a comparison of results presented in Tables 4.25 and 4.26, it is observed that the heat-cool cycled specimens showed an increase in K_{ic} values, by about 15%, compared with those calculated for water-cured specimens. However, there is no meaningful change in $CTOD_c$ values.

Table 4.17: Average fracture toughness test results for 28-day water-cured specimens

Fiber content (% by weight)	P_{\max} (kN)	C_i (mm/kN)	C_u (mm/kN)	a_c (mm)	K_{ic} MPa \sqrt{m}	$CTOD_c$ (mm)	δ_{\max} (mm)	$CMOD_c$ (mm)
6.2 %	38.9	0.0024	0.0149	62.32	16.8	0.3113	1.364	1.135
3.1 %	24.2	0.00335	0.0135	58.9	8.3	0.151	1.146	0.921
0 %	8.46	0.0024	0.003	34.17	1.334	0.0053	0.227	0.0165

Table 4.18: Average fracture toughness test results for heat-cool cycled and control specimens of Ductal (6.2% fibers)

Exposure Conditions	P_{\max} (kN)	C_i (mm/kN)	C_u (mm/kN)	a_c (mm)	K_{ic} MPa \sqrt{m}	$CTOD_c$ (mm)	δ_{\max} (mm)	$CMOD_c$ (mm)
Heat-Cool	45.73	0.0022	0.0132	62.1	19.32	0.2766	1.02	1.132
Control	41.3	0.00215	0.01471	63.41	18.66	0.4531	1.656	1.439

The results of the critical stress intensity factor for different percentage of fibers after 28 days water curing and both exposure conditions of Ductal (6.2% fibers) are shown in Figures 4.33 and 4.34, respectively. These results demonstrated that Ductal with 6.2% fibers exhibited around 50% higher K_{ic} than specimens prepared with 3.1% fibers at 28 days water curing.

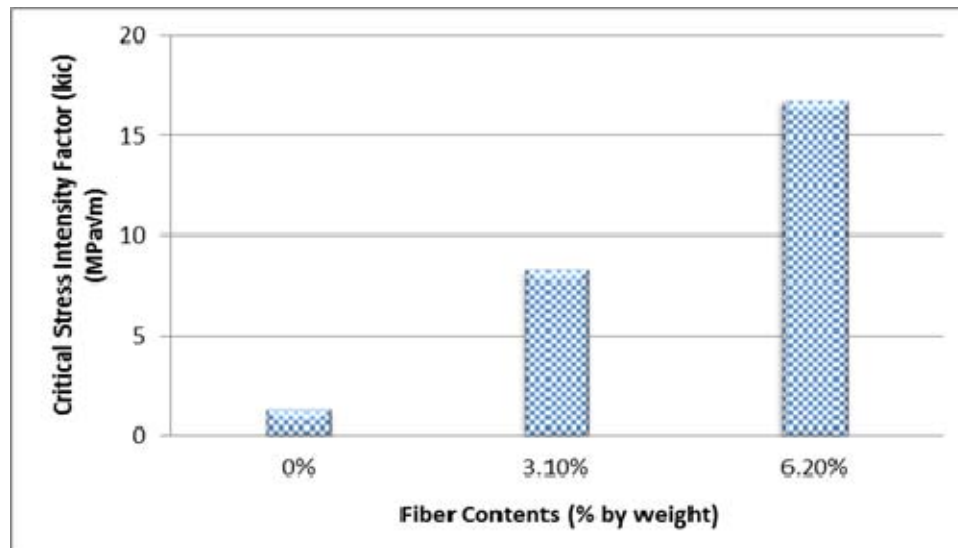


Figure 4.33: Critical stress intensity factor (K_{ic}) vs. fiber content after 28 days water curing.

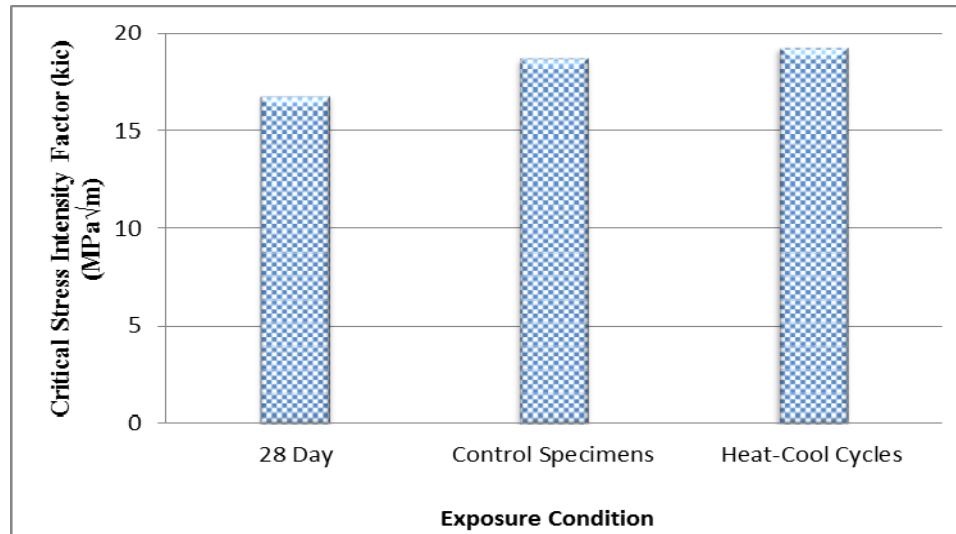


Figure 4.34: Critical stress intensity factor (K_{ic}) vs. exposure condition of Ductal (6.2% fibers).

4.8.1 Fracture Energy

From the experimental beam fracture data, the following average critical energy release rate (G_f) and total fracture energy (GF) for Mode I for 28-day water-cured of Ductal with different percentage of fibers were calculated and are summarized in Table 4.27.

Table 4.19: Average critical energy release rate (G_f) and total fracture energy (GF) for Mode I at 28 days water curing

Fiber Content (% by weight) (%)	Critical Energy Release Rate (G_f) (N/m)	Total Fracture Energy, GF (N/m)
6.2	5786	31600
3.1	1755	21825
0	48*	-

*For 0% steel fibers, this value is almost like that of ordinary concrete.

Table 4.28 also presents the average critical energy release rate (G_f) and total fracture energy (GF) for Mode I for 28 days water curing, six months control specimens and heat-cool cycles, respectively.

Table 4.20: Average critical energy release rate (G_f) and total fracture energy (GF) for Mode I of Ductal (6.2% fibers)

Curing Time/Exposure	Critical Energy Release Rate (G_f) (N/m)	Total Fracture Energy, GF (N.m)
28-day water-cured	5786	31,600
Control Specimens	7003	33450
Heat-cool cycled	8188	36,633

Results show that the heat-cool cycled specimens achieved around 41% higher G_f values and approximately 16% higher total fracture energy than those for water-cured specimens. The plots of the total fracture energy against exposure conditions and different fiber contents are presented in Figures 4.35 and 4.36, respectively.

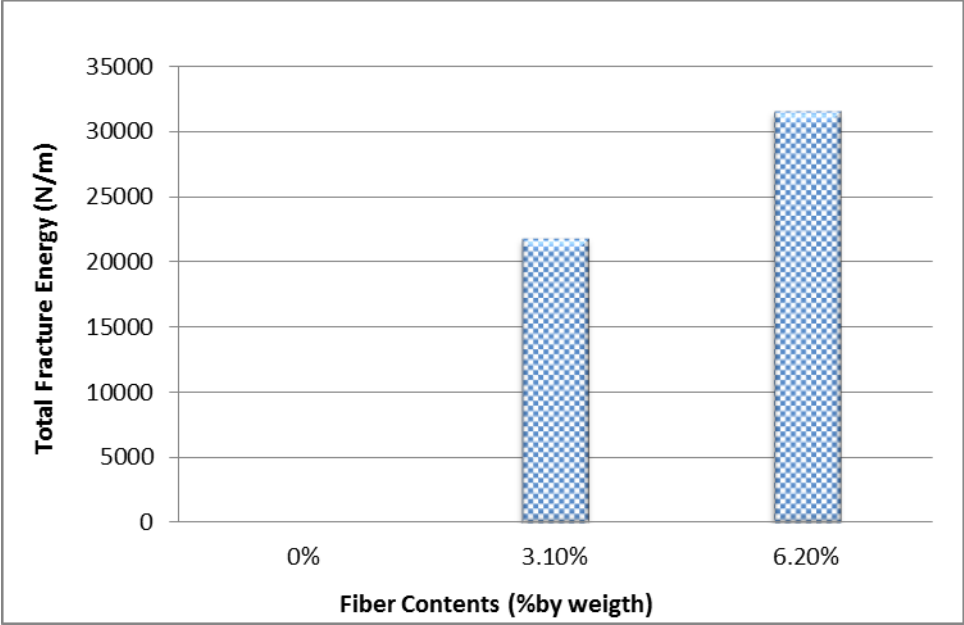


Figure 4.35: Total fracture energy vs. percentage of fibers.

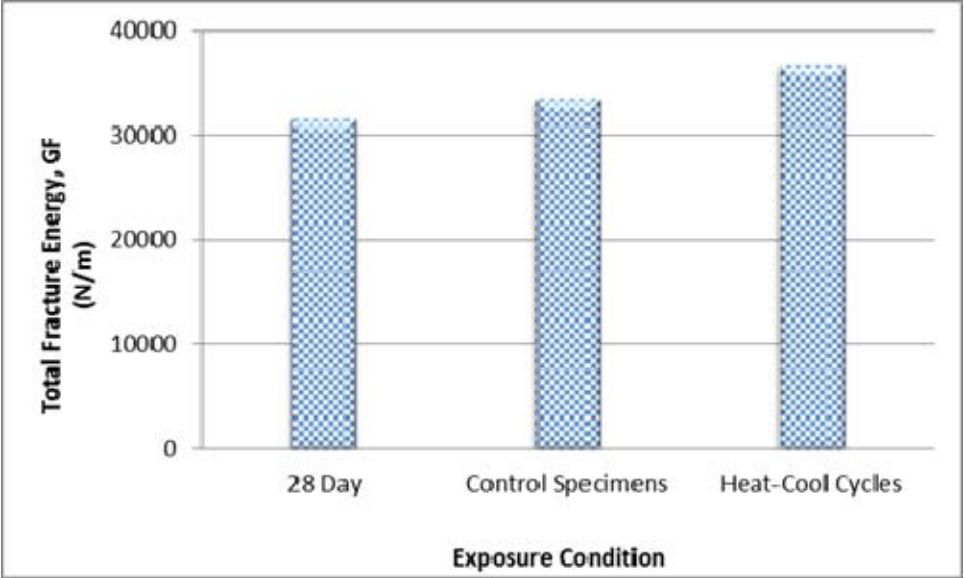


Figure 4.36: Total fracture energy vs. exposure condition of Ductal (6.2% fibers).

CHAPTER 5

MICROSTRUCTURAL INVESTIGATION OF DUCTAL

5.1 General

Microstructural investigation of Ductal mix is intended to help understand how to enhance further the performance of this type of concrete. Specimens of Ductal (6.2% fibers) were prepared after 28 days of water curing and after 6 months of heat-cool cycles.

Two techniques were used to examine the microstructure of the mixes. The first is direct observation with scanning electron microscope (SEM) and the second is qualitative mineralogical analysis by X-ray diffraction (XRD). Combined use of the two techniques facilitates an understanding of the link between engineering behavior and composition and microstructure. Each technique is described in detail below.

5.2 Scanning Electron Microscope (SEM)

Specimens were taken from the inner part of the test sample then fractured into six small pieces and coated with gold prior to examination for heat-cool cycled specimens and non-heat treated specimens(after 28 days water curing) to study the effect of heat treatment on the microstructure of Ductal. JEOL-5800LV Scanning Microscope machine was used to conduct the test.

All the Ductal specimens tested showed a very dense microstructure. There was well-developed bond between the cement paste and the silica sand and also between the steel fibers and Ductal matrix for both heat-cool cycled specimens and non-heat treated specimens as can be seen from Figures 5.1 and 5.2. The dense and homogeneous microstructure in the fiber vicinity provides good bond between the fibers and the cement paste. The excellent bond developed allows good shear transfer throughout the composite system.

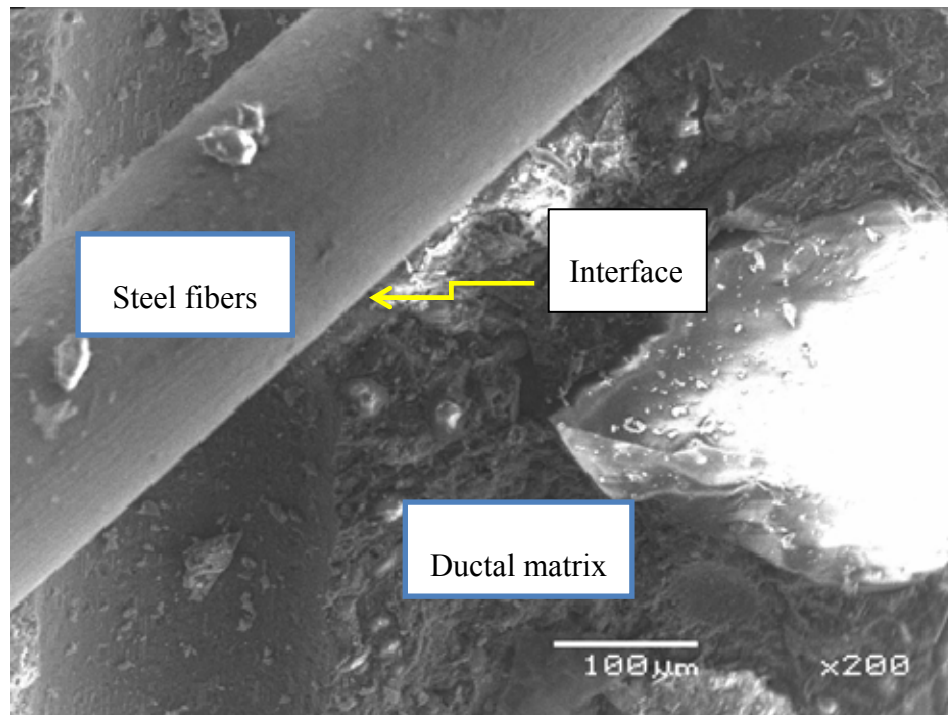


Figure 5.1: SEM image for heat-cool cycled specimen around the fiber.

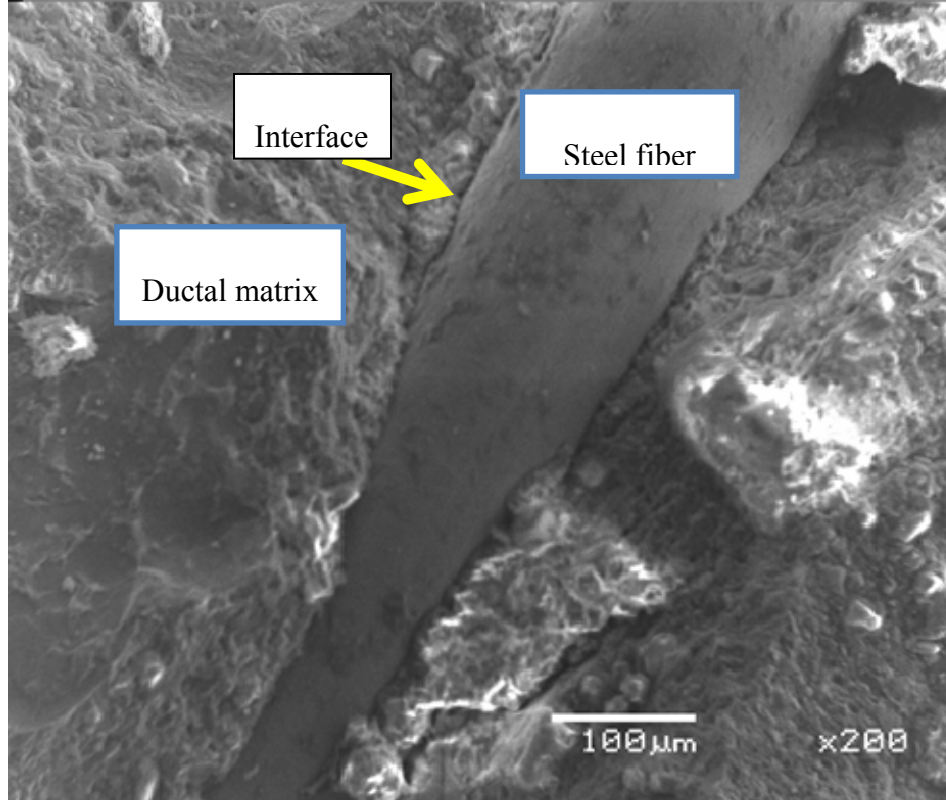


Figure 5.2: SEM image for non-heat treated specimen around the fiber.

It was evident from Figure 5.1 that the specimens exposed to heat-cool cycles have resulted in an improvement in the fiber-matrix interface. This interfacial zone appears to be dense with no apparent interfacial voids or cracks, such as those observed with non-heat treatment (Figure 5.2). This increase in the densification in the paste and lack of voids or cracking may be attributed to the thermal treatment.

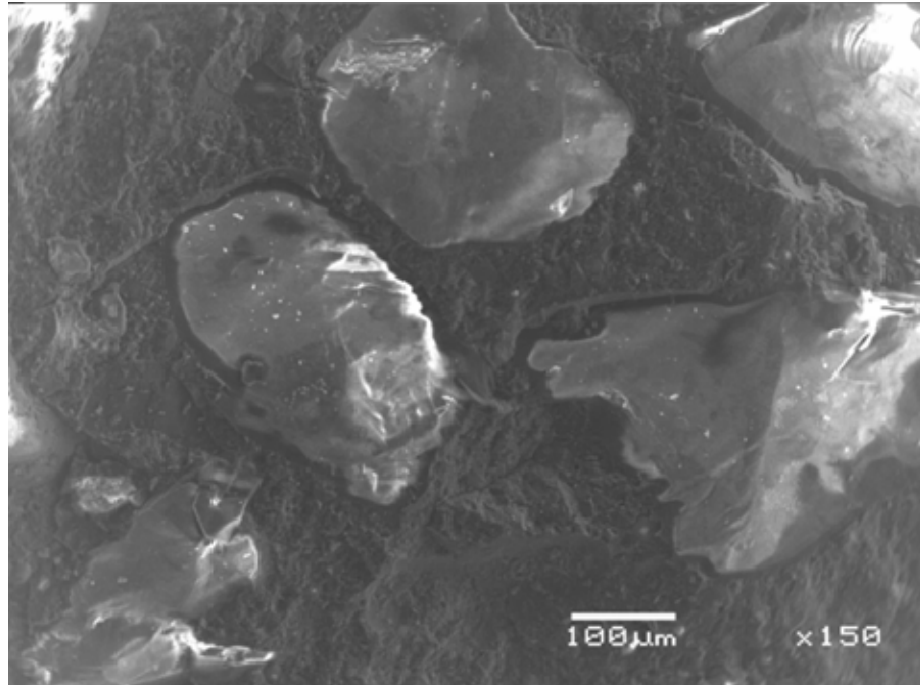


Figure 5.3: SEM image for cementitious matrix of heat-cool treated specimen (100 μm \times 150).

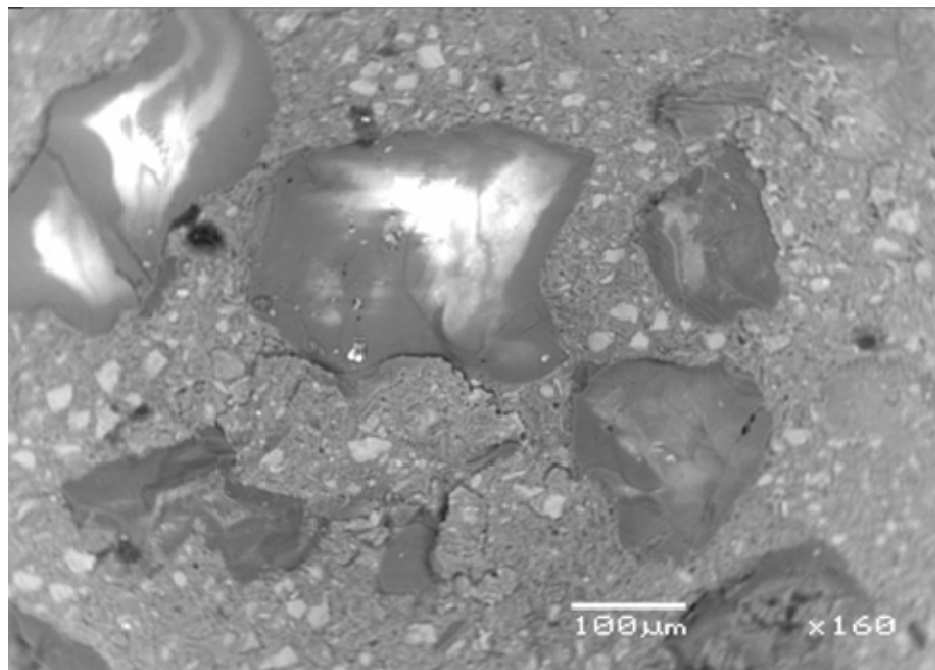


Figure 5.4: SEM image for cementitious matrix of non-heat-treated specimen (100 μm \times 160).

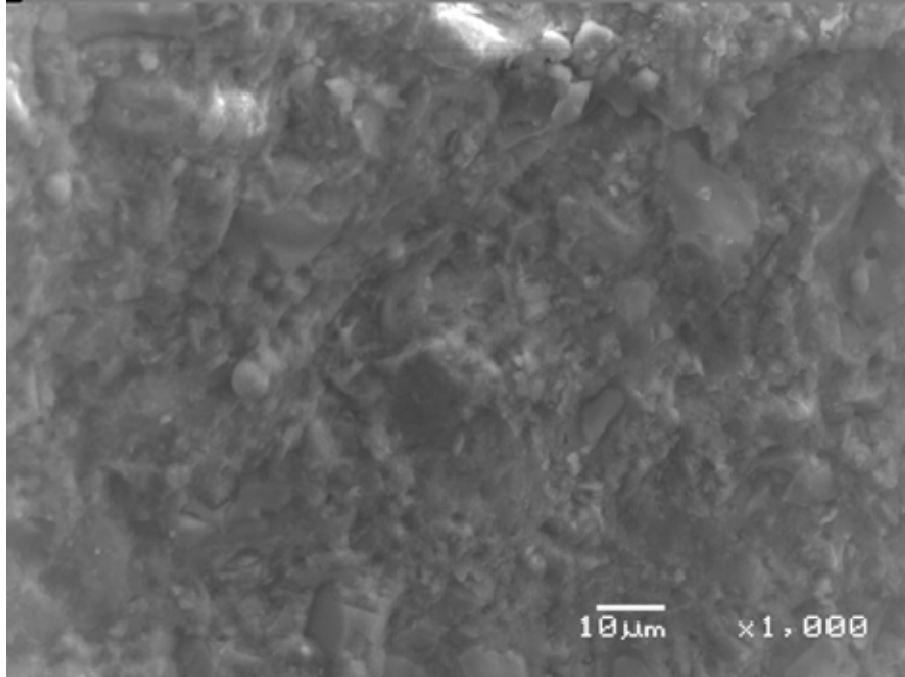


Figure 5.5: SEM image for cementitious matrix of heat-cool treated specimen (10µm×1000).

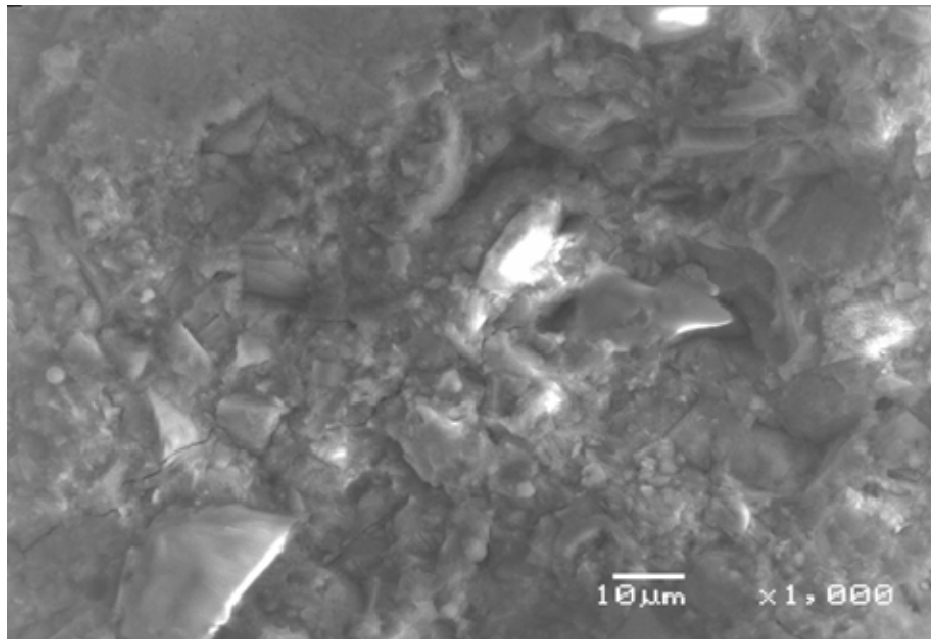


Figure 5.6: SEM image for cementitious matrix of non-heat treated specimen (10µm×1000).

Figures 5.3 through 5.6 show the enlarged SEM image of the matrix with up to 10 μm size and 1000 times magnification. These images clearly show a dense, compacted microstructure having no micro cracks, segregation or voids for all heat-cool cycled specimens. Non heat treated showed difference in the micro structure with small voids found and also very fine microcrack. The heat-cool specimens could promote further reaction of the cementitious paste, leading to reduction in the porosity around the fibers and thus decreasing the overall relative weakness in the interfacial region.

5.3 X-Ray Diffraction (XRD)

X-ray diffractograms were recorded from samples of Ductal powdered concrete (plain samples) taken from the same samples used for SEM after 28 days water curing.

The X-RD analysis revealed that the majority of the Ductal matrix is composed of Quartz (SiO_2) and Calcium carbonate (CaCO_3) (Figure 5.7).

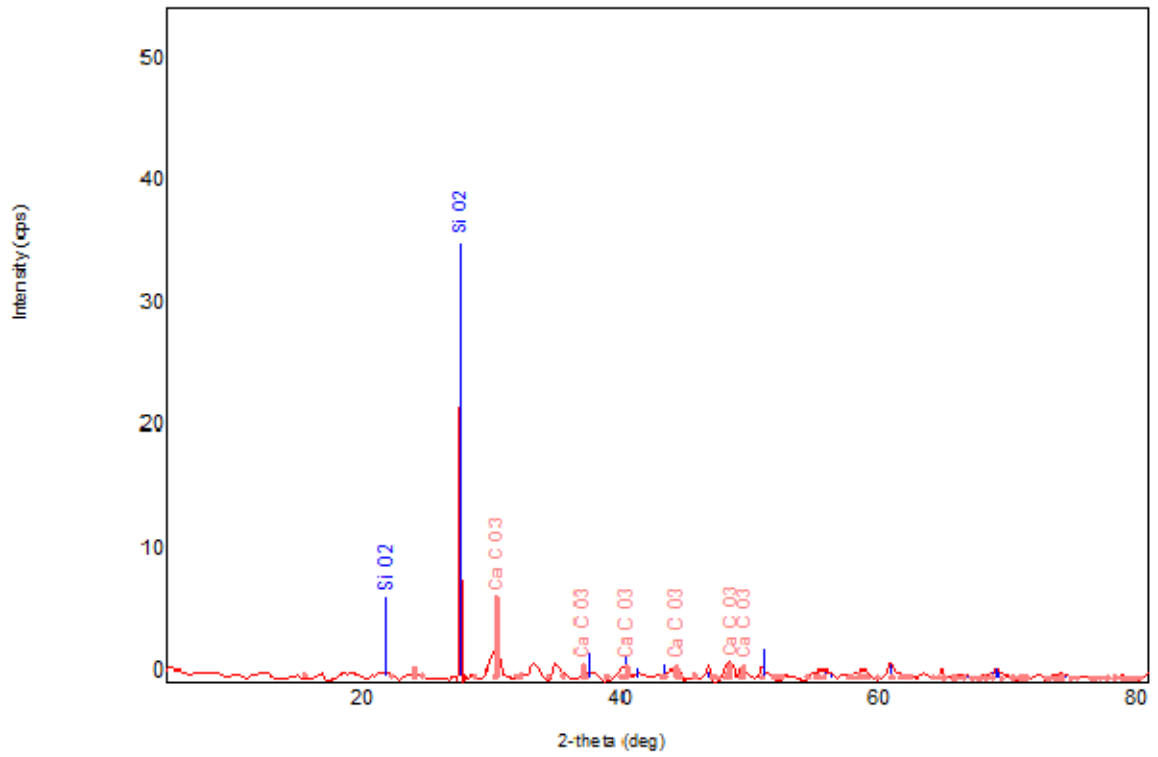


Figure 5.7: X-RD results of Ductal matrix.

CHAPTER 6

UTILIZATION OF DUCTAL CONCRETE

This study has found Ductal concrete (a proprietary product imported from Bouygues-TP and Lafarge Company, Switzerland) to have excellent mechanical and durable properties, almost similar to that claimed by the supplier. Very high mechanical properties combined with prestressing technology offer engineers and architects opportunities to design elegant structures by avoiding heavy steel reinforcement. Ductal technology gives access to very thin slender and elegant structures like footbridges. The very dense microstructure of Ductal matrix offers a material which resists to a very aggressive media and opens therefore a wide range of applications. A very wide range of texture and colors effects are accessible to Ductal. Such properties provide architects with very high potential of innovative design in all elements that build up new architecture.

This product with high performance may have wide applications which include: structural members (beams, columns, roofs, floors, bridge decks, pier cores, and anchor plates for bridges and seawalls); security appliances (explosion protection, military protection, prisons, and safe deposit boxes); containers and material storage bins.

Despite the advantages of Ductal concrete as mentioned above, its application on a large scale would have two limitations: (i) a high cost because this is an imported item and (ii) its preparation needs specialized skills and mixing tool. However, Ductal concrete can be used in special cases, such as precast concrete members having long

spans, large diameter concrete pipes, high capacity water storage tanks, concrete members subjected to high impact, important concrete installations subjected to highly aggressive exposure conditions, etc.

In the coastal areas of Saudi Arabia, where durability is a major concern with conventional reinforced concrete construction due to corrosion, Ductal offers some advantages despite its higher cost. Apart from the possible applications mentioned above, its advantage as noncorrosive material can be exploited. A new type of hybrid construction can be developed utilizing Ductal concrete in the tension face of a member, eliminating passive reinforcement.

CHAPTER 7

CONCLUSIONS AND RECOMMENDATIONS

7.1 Conclusions

Based on this exploratory study of Ductal with regard to its physical and mechanical properties and durability characteristics, the following conclusions are drawn. The past studies by several investigators have affirmed that heat treatment improves the material properties of Ductal significantly and as such, it should be the preferred method of curing. In this study, however, 28 days of water curing has been used to examine the effect of this curing on properties. The rationale behind this choice is that the heat treatment in field applications is difficult to engage, and water curing is commonly used in concrete construction.

1. Ductal, a proprietary ultra high strength concrete material, is found to be an excellent cementitious material capable of achieving high compressive strength of about 163 MPa with modulus of elasticity of 57 GPa with addition of 6.2% fiber. Compressive strength increases with the curing period, reaching about the maximum value in 28 days of water curing. Tests have shown that heat-cool cycles increase also the compressive strength.
2. The flexural tensile strength of fiber-reinforced Ductal (with fiber content of 6.2%) is approximately 31.0 MPa, with a ratio of the peak strength to the first

cracking strength of about 1.66. The prolonged softening mode of collapse of fiber-reinforced Ductal provides significant amount of ductility.

3. Because of the dense microstructural matrix, Ductal exhibits low water absorption and low water permeability and chloride permeability. Chloride diffusion coefficient for water-cured samples is found to be smaller than that of conventional concrete.
4. The fracture toughness tests show that critical stress intensity factor (Mode I), K_{Ic} , is about $16.0 \text{ MPa}\sqrt{\text{m}}$ for 28-day water-cured samples.
5. For the two cyclic exposure conditions that were used in this experiment, it was found that specimens showed improved properties in 6-month heat-cool cycles. The enhancement in material properties, including strength, for heat-cool cycles, is due to the more completed hydration of cement within the specimens.
6. Cyclic wet-dry exposure conditions show marginal loss in strength and durability properties compared with 28-day water-cured specimens. But this slight impairment is of no real concern in view of the excellent residual properties.
7. Heat treatment at curing stage has been signaled by others as the most effective form of curing of Ductal. The improvement of material properties of Ductal in heat-cool cycles as seen in this study fully supports the beneficial impact of heat treatment. Properties of heat-treated Ductal specimens reported by others are higher than those found for 28-day water-cured samples used in this study. It can therefore be concluded that heat treatment yields improved properties, compared to those achieved in 28-day water curing.

8. Excellent material and durability characteristics make Ductal as an attractive concrete construction material which can be utilized beneficially in many applications. However, the limitations in the form of high cost, proprietary product and mixing conditions may prove to be deterrent factors for a wider application of this product.

7.2 Recommendations for Future Studies

1. In view of superior material properties, attempt should be made to develop UHPC using local materials. If development succeeds, this will encourage use of UHPC in construction.
2. Attempt should be made to make use of this material in special applications.
3. Hybrid construction using UHPC in the tension face of members looks also promising and can be explored for further development.

CHAPTER 8

REFERENCES

- Acker, P. (2001), “Micromechanical Analysis of Creep and Shrinkage Mechanisms”, Creep, Shrinkage and Durability Mechanics of Concrete and Other Quasi-Brittle Materials, F.J. Ulm, Z.P. Bažant, and F.H. Wittmann, Editors, Elsevier, pp. 15-25.
- Acker, P. and Behloul, M. (2004), “Ductal® Technology: A Large Spectrum of Properties, A Wide Range of Applications”, Proceedings of the International Symposium on Ultra High Performance Concrete, Kassel University Press, Kassel, Germany, pp. 11-24.
- ASTM C 1609 (2005), “Standard Test Method for Flexural Performance of Fiber-reinforced Concrete (Using Beam with Third-point Loading)”.
- Banitha, N. and Trottier, J.F. (1995), “Test Methods for Flexural Toughness Characterization of Fiber Reinforced Concrete: Some Concerns and a Proposition”, ACI Material Journal, Vol. 92, No. 1, pp. 48-57.
- Bonneau, O., Lachemi, M., Dallaire, E., Dugat, J., and Aïtcin, P.-C. (1997), “Mechanical Properties and Durability of Two Industrial Reactive Powder Concretes”, ACI Materials Journal, Vol. 94, No. 4, July-Aug., pp. 286-290.
- Bordelon, A.C. (2007), “Fracture Behavior of Concrete Materials for Rigid Pavement Systems”, Master Thesis, University of Illinois at Urbana-Champaign.

- Cavill, B. (2005), “Ductal, An Ultra-high Performance Material for Resistance to Blasts, Safeguarding Australia”, Canberra, 12-14 July, 2005.
- Cheyrezy, M. and Behloul, M. (2001), “Creep and Shrinkage of Ultra-High Performance Concrete. Creep, Shrinkage and Durability Mechanisms of Concrete and Other Quasi-Brittle Materials”, Proceedings of the Sixth International Conference CONCREEP-6@MIT, Cambridge, MA, USA, 20-22 August, 2001, F.-J. Ulm, Z.P. Bažant and F.H. Wittmann, Editors, Elsevier, pp. 527-538.
- Cheyrezy, M., Maret, V., and Frouin (1995), “Microstructural Analysis of RPC (Reactive Powder Concrete)”, Cement and Concrete Research, Vol. 25, No. 7, Oct., pp. 1491-1500.
- Cwirzen, A. (2007), “The Effect of the Heat-treatment Regime on the Properties of Reactive Powder Concrete”, Advances in Cement Research, Vol. 19, No. 1, Jan., pp. 25-33.
- Dugat, J., Roux, N., and Bernier, G. (1996), “Mechanical Properties of Reactive Powder Concretes”, Materials and Structures, Vol. 29, May, pp. 233-240.
- Gilliland, S.K. (1996), “Reactive Powder Concrete (RPC), A New Material for Prestressed Concrete Bridge Girders”, Structures Congress – Proceedings, Vol. 1, Building an International Community of Structural Engineers, pp. 125-132.
- Gowripalan, N. and Gilbert, R.I. (2000), “Design Guidelines for RPC Prestressed Concrete Beams”, The University of New South Wales.

- Graybeal, B.A. (2005), "Characterization of the Behavior of Ultra-High Performance Concrete", PhD Dissertation submitted to the Faculty of the Graduate School of the University of Maryland.
- Graybeal, B.A. (2006a), "Structural Behavior of Ultra-High Performance Concrete Prestressed I Girders", FHWA-HRT-06-115, Federal Highway Administration, Washington, D.C.
- Graybeal, B.A. (2006b), "Material Property Characterization of Ultra-High Performance Concrete", FHWA-HRT-06-103, Federal Highway Administration, Washington, D.C.
- Graybeal, B.A. and Hartmann, J.L. (2003), "Strength and Durability of Ultra-High Performance Concrete", Paper presented at the Concrete Bridge Conference, Portland Cement Association.
- Habel, K., Charron, J.-R., Denarié, E., and Brühwiler, E. (2006), "Autogenous Deformations and Viscoelasticity of UHPFRC in Structures", Magazine of Concrete Research, Vol. 58, No. 3, April, pp. 135-145.
- Heinz, D. and Ludwig, H.-M. (2004), "Heat Treatment and the Risk of DEF Delayed Ettringite Formation in UHPC", Proceedings of the International Symposium on Ultra-High Performance Concrete, Kassel, Germany, Sept. 13-15, pp. 717-730.
- Herold, G. and Müller, H.S. (2004), "Measurement of Porosity of Ultra High Strength Fibre Reinforced Concrete", Proceedings of the International Symposium on Ultra-High Performance Concrete, Kassel, Germany, Sept. 13-15, pp. 685-694.

- Hillerborg, A. (1985), "The Theoretical Basis of a Method to Determine the Fracture Energy GF of Concrete", *Materials and Structures*, Vol. 16, pp. 291-296.
- Jenq, Y. and Shah, S.P. (1985), "Two Parameter Model for Concrete", *Journal of Engineering Mechanics*, Vol. 111, No. 10, pp. 1227-1241.
- JCI Standard SF-4 (1984), "Method of Tests for Flexural Strength and Flexural Toughness of Fiber-reinforced Concrete" Japan Concrete Institute Standards for Test Methods of Fiber Reinforced Concrete, Japan Society of Civil Engineers, Tokyo, pp. 58-66.
- Loukili, A., Khelidj, A., and Richard, P. (1999), "Hydration Kinetics, Change of Relative Humidity, and Autogenous Shrinkage of Ultra-High-Strength Concrete", *Cement and Concrete Research*, Vol. 29, No. 4, April, pp. 577-584.
- Lukasik, J. (2005), "Concrete: A High-Techmaterial of the 21st Century", 8th Hitachi EU Science and Technology Forum, Athens, May 20-22, 2005.
- Lubbers, A.R. (2003), "Bond Performance of Ultra-High Performance Concrete and Prestressing Strands", MS Thesis, Ohio University, August.
- Majdzadeh F., (2003), "Fracture Toughness of Hybrid Fiber Reinforced Self-compacted Concrete", MS Thesis, University of British Columbia.
- Moallem, M.R. (2010), "Flexural Redistribution in Ultra-High Performance Concrete Lab Specimens", M.S. Thesis, Ohio University.

- Perry, V. and Zakariassen, D. (2004), "First Use of Ultra-High Performance Concrete for an Innovative Train Station Canopy", *Concrete Technology Today*, Vol. 25, No. 2, Aug., pp. 1-2.
- Reda, M.M., Shrive, N.G., and J.E. Gillott. (1999) "Microstructural Investigation of Innovative UHPC", *Cement and Concrete Research*, Vol. 29, No. 3, March, pp. 323-329.
- Reineck, K.-H. and Greiner, S. (2004), "Tests on Ultra-High Performance Fibre Reinforced Concrete Designing Hot-Water Tanks and UHPFRC-Shells", *Proceedings of the International Symposium on Ultra High Performance Concrete*, Kassel, Germany, Sept. 13-15, pp. 361-374.
- Richard, P. and Cheyrezy, M. (1994), "Reactive Powder Concretes with High Ductility and 200-800 MPa Compressive Strength", *ACI SP-144-24*, pp. 507-518.
- Richard, P. and Cheyrezy, M. (1995), "Composition of Reactive Powder Concretes", *Cement and Concrete Research*, Vol. 25, No. 7, pp. 1501-1511.
- RILEM Committee on Fracture Mechanics of Concrete-Test Methods (1990), "Determination of the Fracture Parameters (KICS and CTODC) of Plain Concrete Using Three-Point Bend Tests on Notched Beams," *Materials and Structures*, Vol. 23, No. 138, pp. 457-460.
- Rossi, P., (2001), "Ultra-High-Performance Fiber-Reinforced Concretes – A French Perspective on Approaches Used to Produce High-strength, Ductile Fiber-reinforced Concrete," *Concrete International*, Dec., pp. 46-52.

- Roux, N., Andrade, C., and Sanjuan, M.A. (1996), "Experimental Study of Durability of Reactive Powder Concretes", *Journal of Materials in Civil Engineering*, Vol. 8, No. 1, Feb., pp. 1-6.
- Schmidt, M., Fehling, E., Teichmann, T., Bunje, K., and Bornemann, R. (2003), "Ultra-High Performance Concrete: Perspective for the Precast Concrete Industry", *Concrete Precasting Plant and Technology*, Vol. 69, No. 3, pp. 16-29.
- Shah, S.P., Stuart E.S., and Ouyang, C. (1995), *Fracture Mechanics of Concrete: Applications of Fracture Mechanics of Concrete, Rock and Other Quasi-Brittle Materials*, Wiley-Interscience, New York, NY.
- Skazlic', M. and Bjegovic', D. (2009), "Toughness Testing of Ultra-high Performance Fibre Reinforced Concrete", *Materials and Structures*, Vol. 42, pp. 1025-1038. DOI 10.1617/s11527-008-9441-3.
- Soutsos, M.N., Millar, S.G., and Karaiskos, K. (2005), "Mix Design, Mechanical Properties, and Impact Resistance of Reactive Powder Concrete (RPC)", *International RILEM Workshop on High Performance Fiber Reinforced Cementitious Composites in Structural Applications*, Honolulu, HI, May. <http://www.hpfrcc-workshop.org/>
HPFRCCworkshop/Papers/F/Soutsos_ReactivePowderConcrete.pdf.
- Spasojević A. (2008), "Structural Implications of Ultra-High Performance Fibre-Reinforced Concrete in Bridge Design", *Ingénieur Civil Diplômée de l'Université de Niš, Serbie et de Nationalité serbe*.

- Stanish, K.D., Hooton, R.D., and Thomas, M.D.A. (2000), “Testing the Chloride Penetration Resistance of Concrete: A Literature Review”, FHWA Contract DTFH61-97-R-00022, University of Toronto, Toronto, Ontario, Canada.
- Tanaka, Y. et al. (2002), “Design and Construction of Sakata-mirai Footbridge Using Reactive Powder Concrete,” Proceedings of the First Fib Congress, Vol. 3, 2002, pp. 417-424.
- Theresa M. et al. (2008), “Ultra-High-Performance-Concrete for Michigan Bridges Material Performance – Phase I”, Final Report, Center for Structural Durability Michigan Technological University.
- VandeVoort, T., Suleiman, M., and Sritharan, S. (2008), “Design and Performance Verification of UHPC Piles for Deep Foundations”, Final Report of Project entitled ‘Use of Ultra-High Performance Concrete in Geotechnical and Substructure Applications’.
- Walraven, J.C. (2007), “Aplicaciones e Structurales de Hormigon con Fibras”, Seminar, Barcelona, 9th Oct. 2007, Delft University of Technology.
- Woodworth, M.A. (2008), “Optimization of Highway Bridge for Use with Ultra High Performance Concrete (UHPC)”, MS Thesis, Blacksburg, Virginia.
- Yanni, V.Y.G. (2009), “Multi-scale Investigation of Tensile Creep of Ultra High Performance Concrete for Bridge Applications”, Doctoral Thesis Dissertation, Georgia Institute of Technology, December.

APPENDICES

APPENDIX A

COMPRESSIVE STRENGTH AND MODULUS OF ELASTICITY RESULTS

A-1) 7 DAYS WATER CURING OF DUCTAL (6.2% STEEL FIBERS)

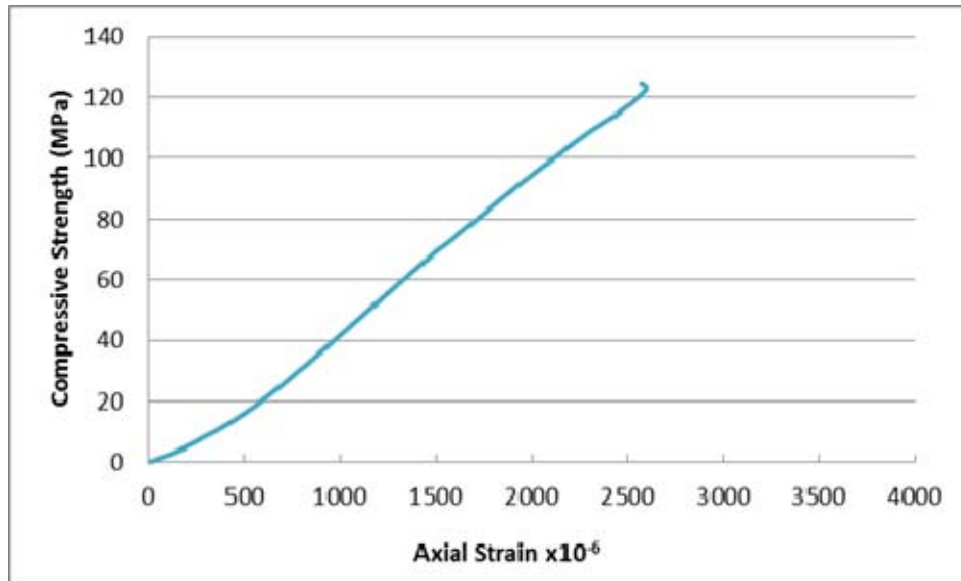


Figure A1: Stress-strain responses for 7 days water curing of Ductal (6.2% steel fibers)

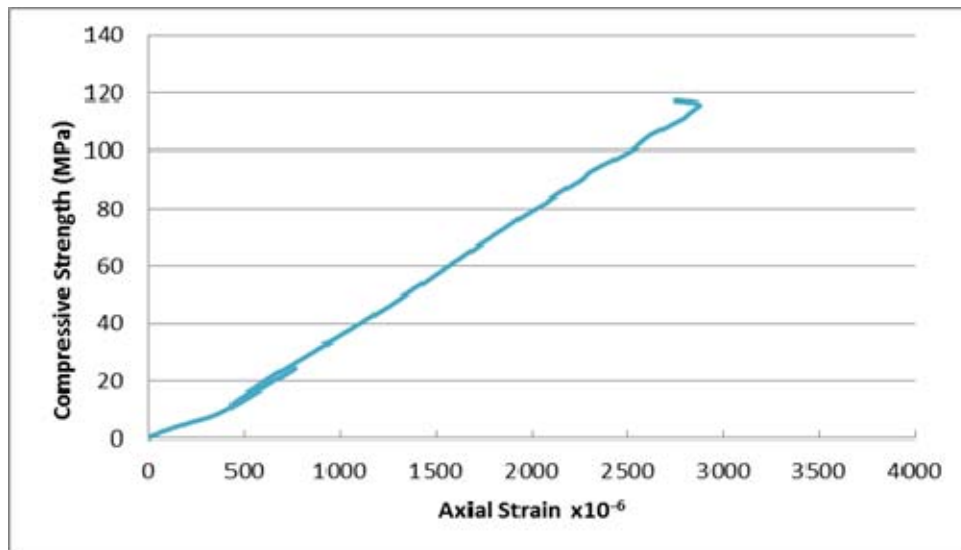


Figure A2: Stress-strain response for 7 days water curing of Ductal (6.2% steel fibers)

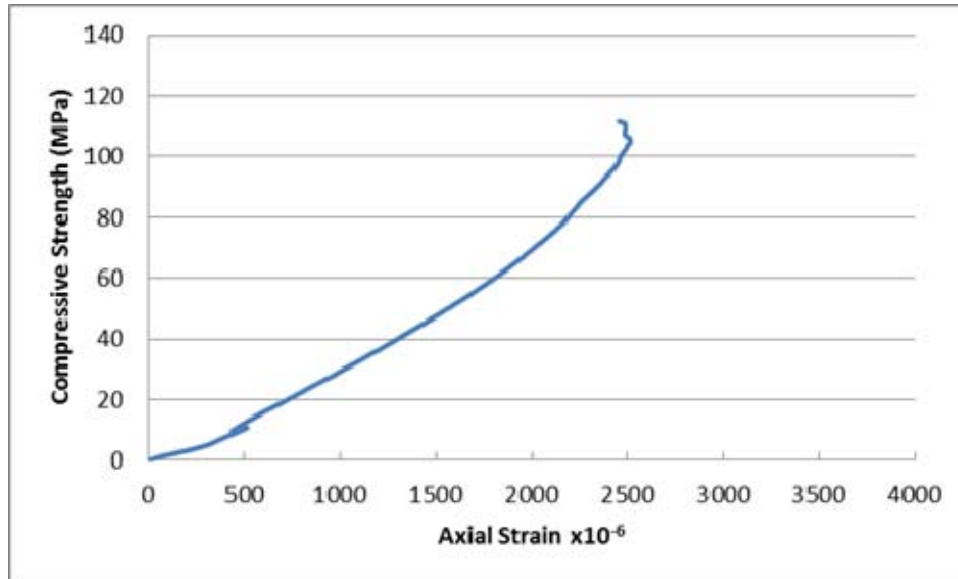


Figure A3: Stress-strain responses for 7 days water curing of Ductal (6.2% steel fibers)

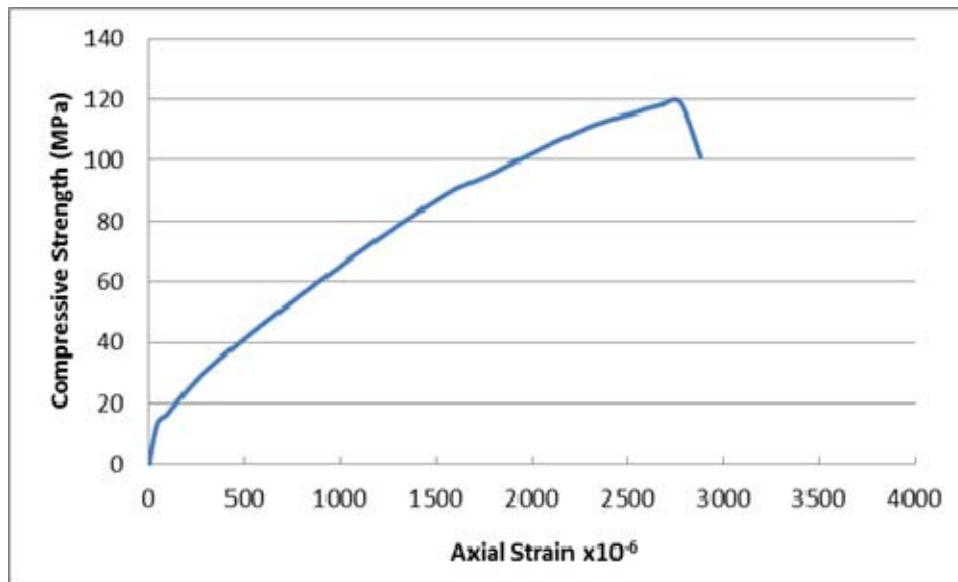


Figure A4: Stress-strain responses for 7 days water curing of Ductal (6.2% steel fibers)

A-II) 28 DAYS WATER CURING OF DUCTAL (6.2% STEEL FIBERS)

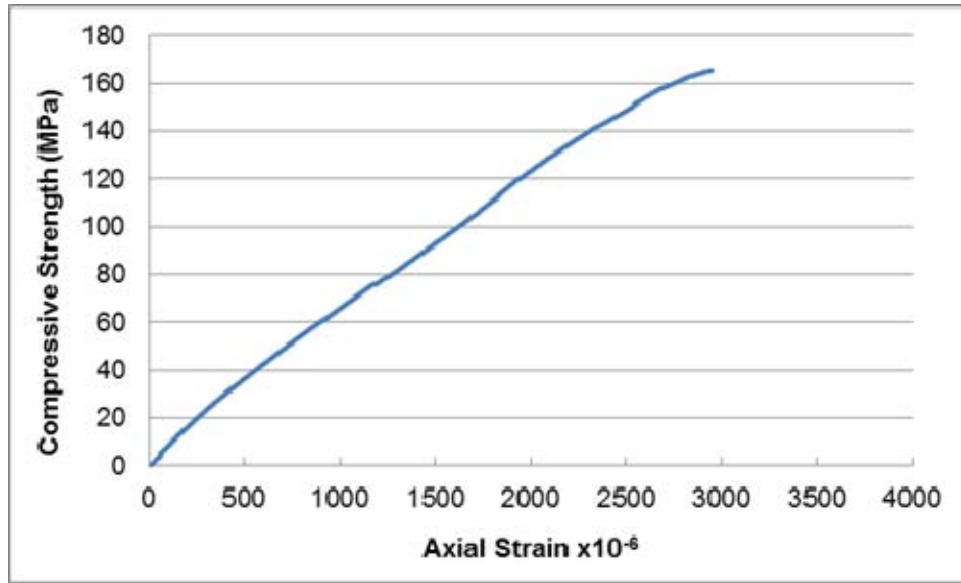


Figure A5: Stress-Strain responses for 28 days water curing of Ductal (6.2% steel fibers)

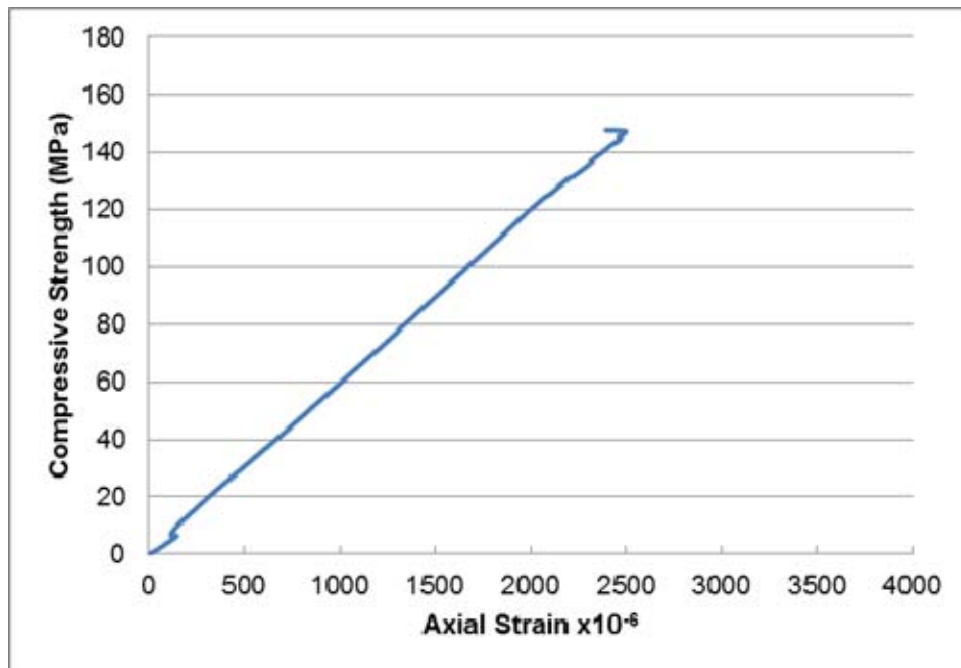


Figure A6: Stress-strain responses for 28 days water curing of Ductal (6.2% steel fibers)

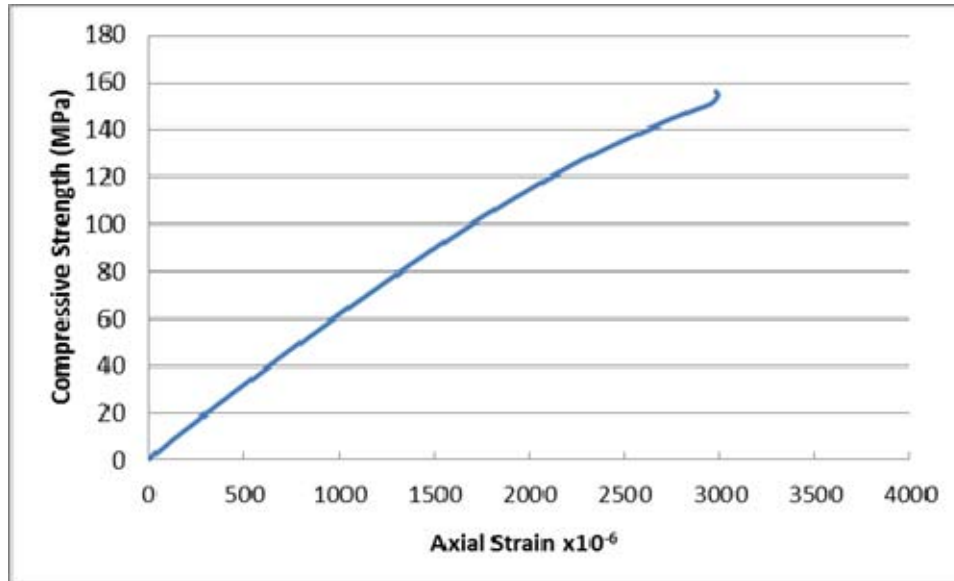


Figure A7: Stress-strain responses for 28 days water curing of Ductal (6.2% steel fibers)

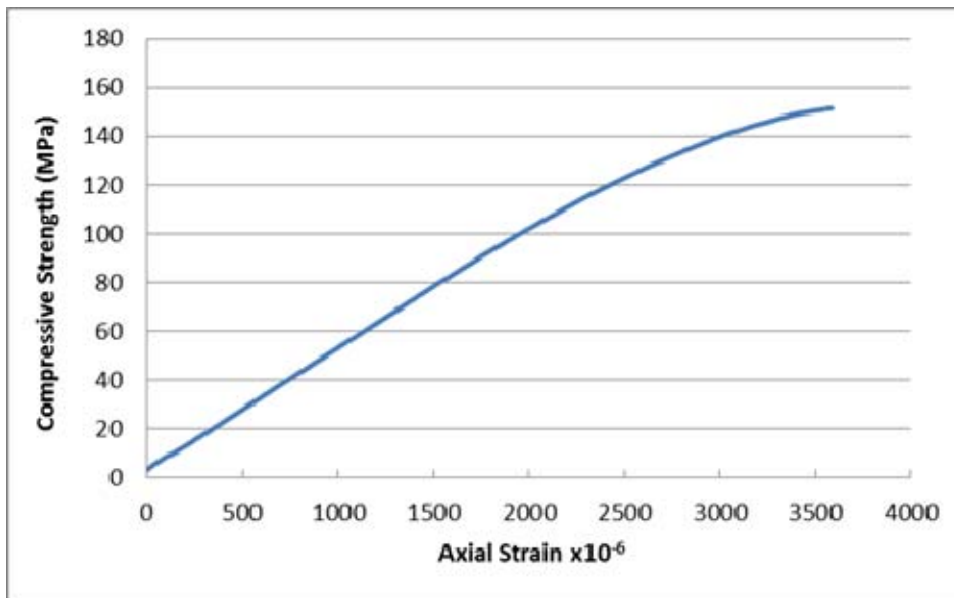


Figure A8 : Stress-Strain Responses for 28 days water curing of Ductal (6.2% steel fibers)

APPENDIX B

FRACTURE TOUGHNESS TEST RESULTS

B-I) 28 DAYS WATER CURING OF DUCTAL (6.2% STEEL FIBERS)

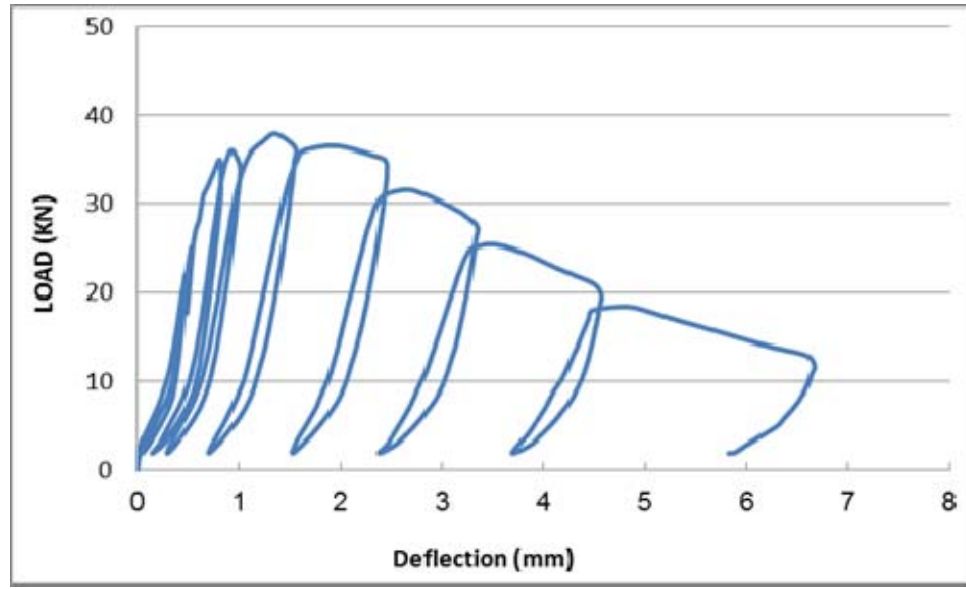


Figure B1: Loading and unloading cycles for 28 days water curing (6.2% fibers) Load vs. Deflection

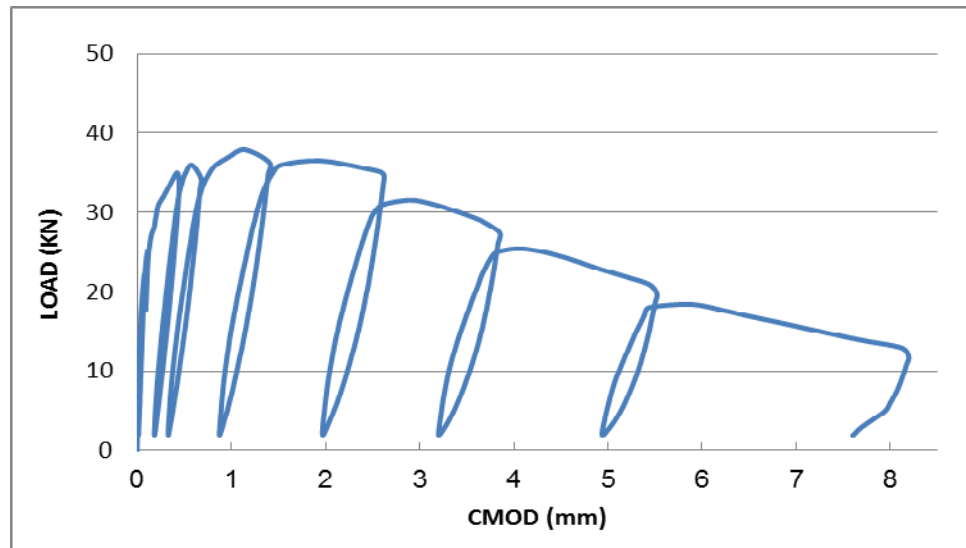


Figure B2: Loading and unloading cycles for 28 days water curing (6.2% fibers) Load vs. CMOD

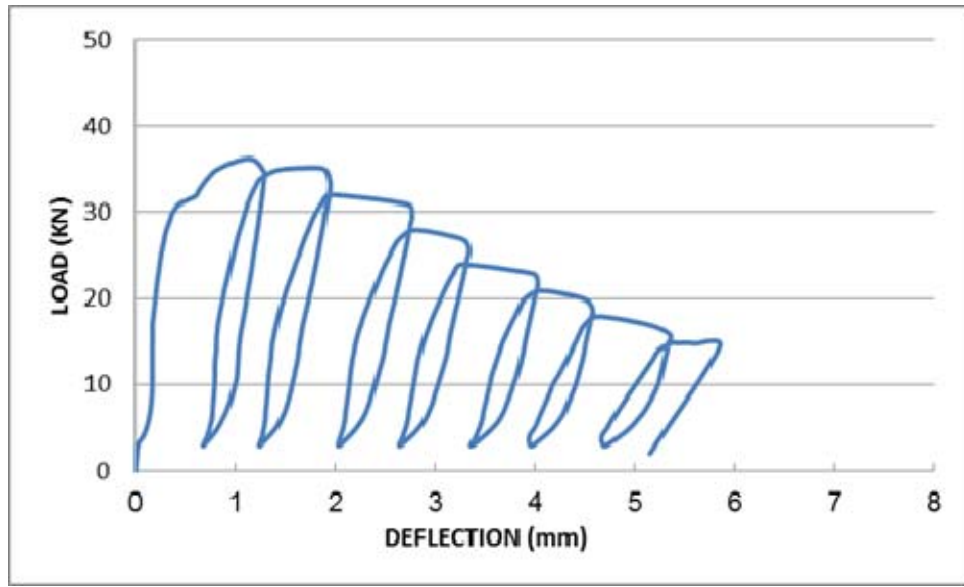


Figure B3: Loading and unloading cycles for 28 days curing (6.2% fibers)
Load vs. Deflection

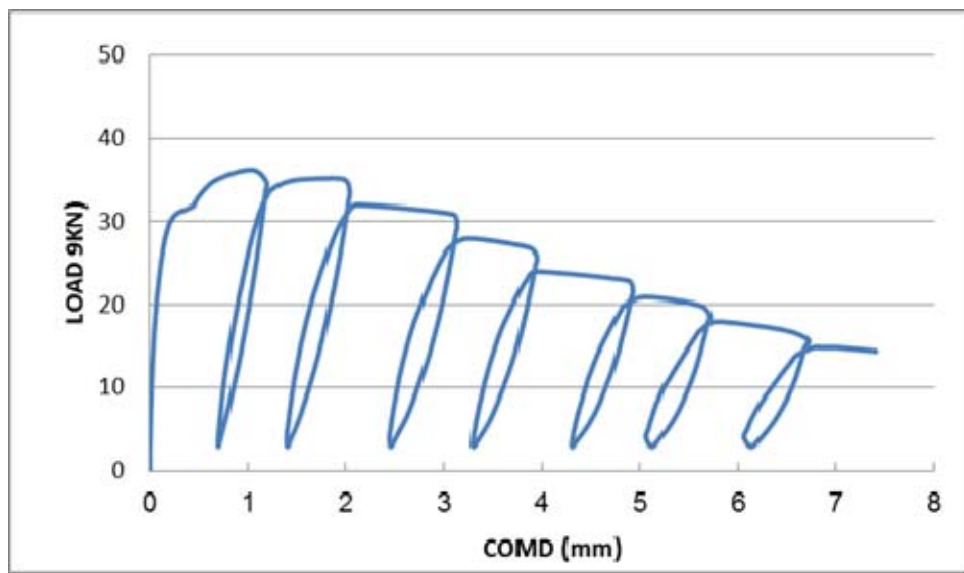


Figure B4: Loading and unloading cycles for 28 days curing (6.2% fibers)
Load vs. CMOD

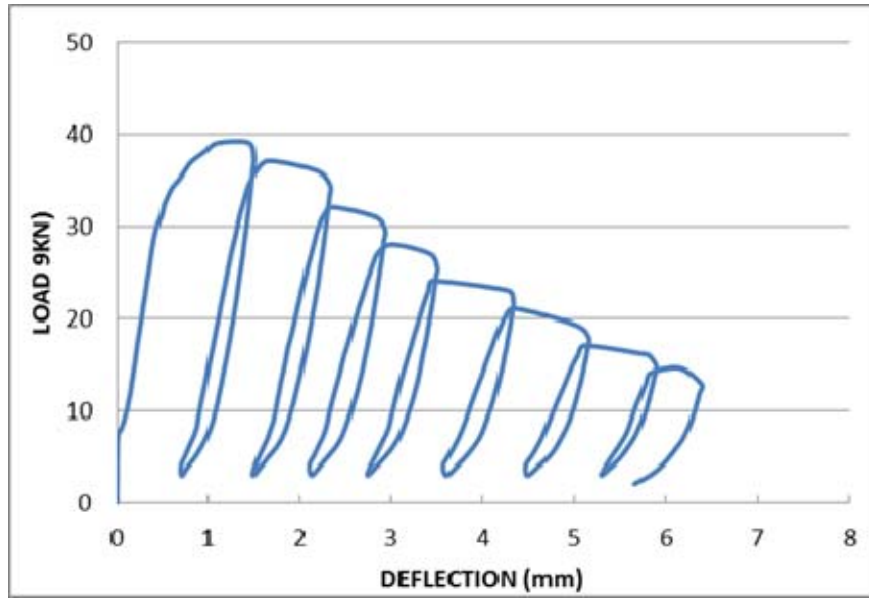


Figure B5: Loading and unloading cycles for 28 days curing (6.2% fibers)
Load vs. Deflection

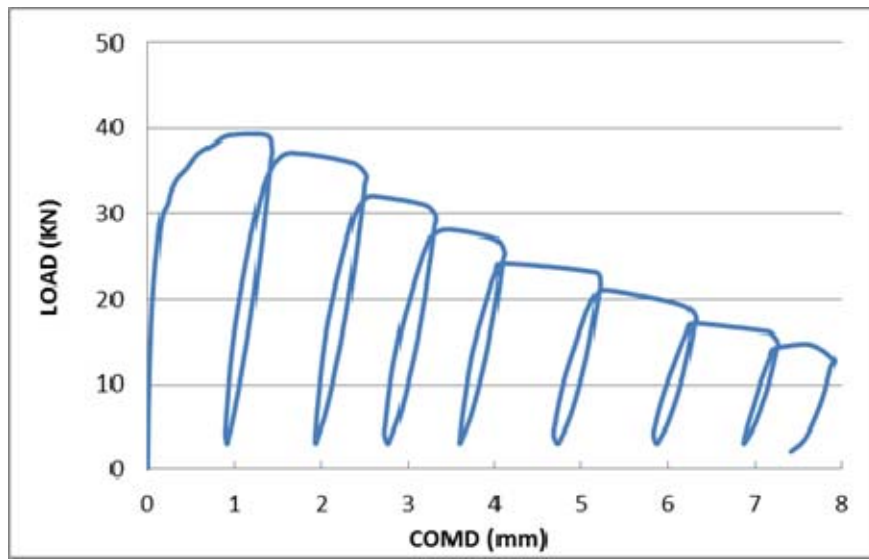


Figure B6: Loading and unloading cycles for 28 days curing (6.2% fibers)
Load vs. COMD

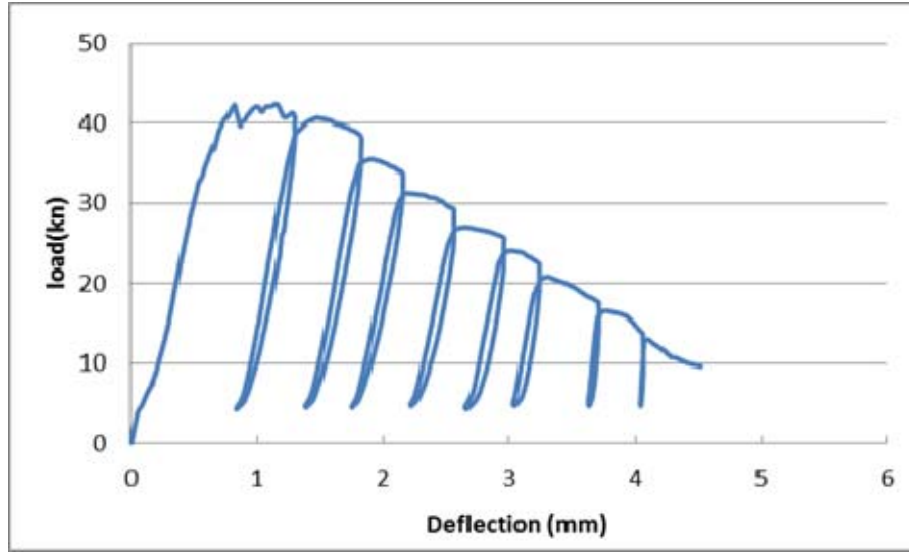


Figure B7: Loading and unloading cycles for 28 days curing (6.2% fibers)
Load vs. Deflection

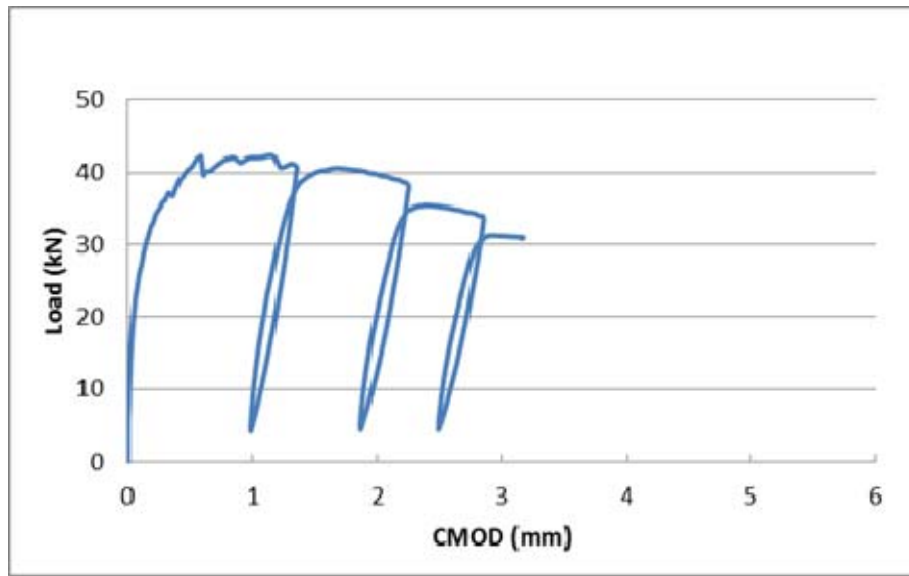


Figure B8: Loading and unloading cycles for 28 days curing (6.2% fibers)
Load vs. CMOD

B-II) CONTROL SPECIMENS OF DUCTAL (6.2% STEEL FIBERS)

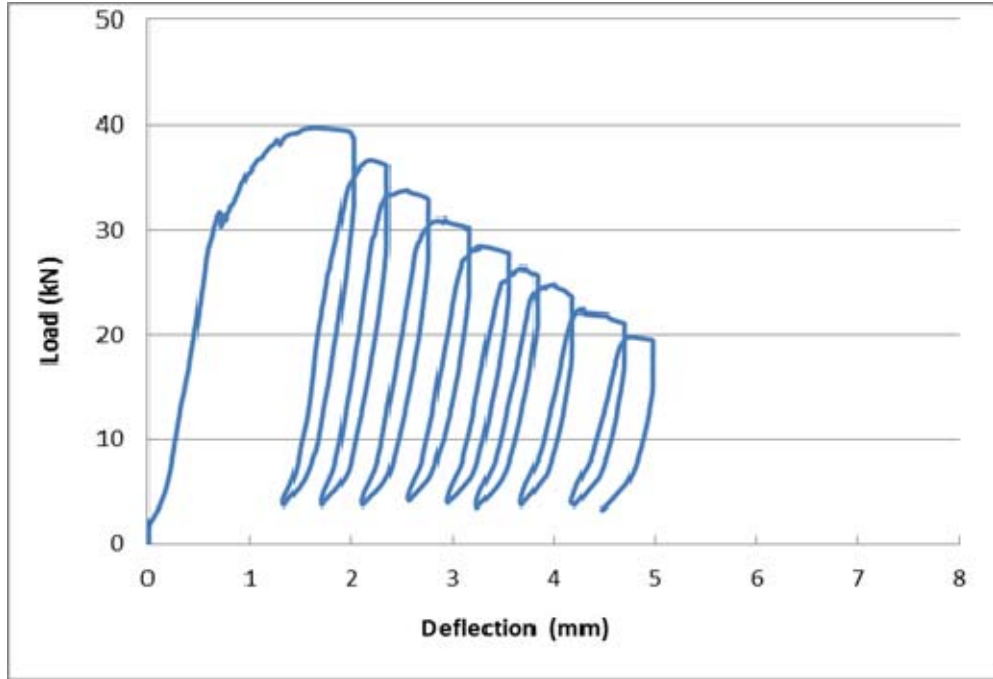


Figure B9: Loading and unloading cycles for control samples (6.2% steel fibers)
Load vs. Deflection

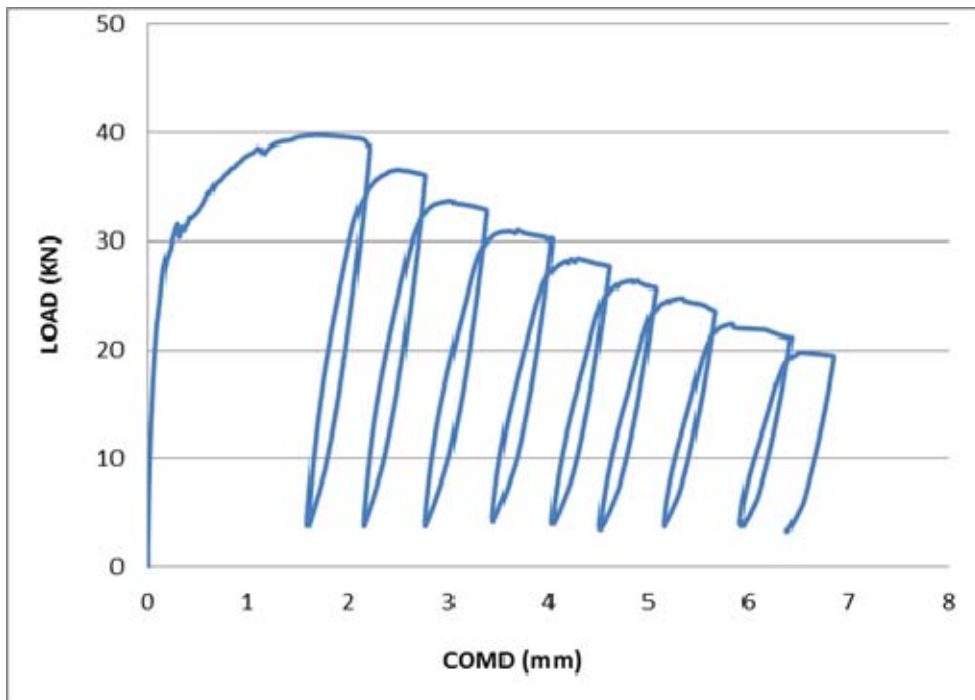


Figure B10: Loading and unloading cycles for control samples (6.2% steel fibers)
Load vs. COMD

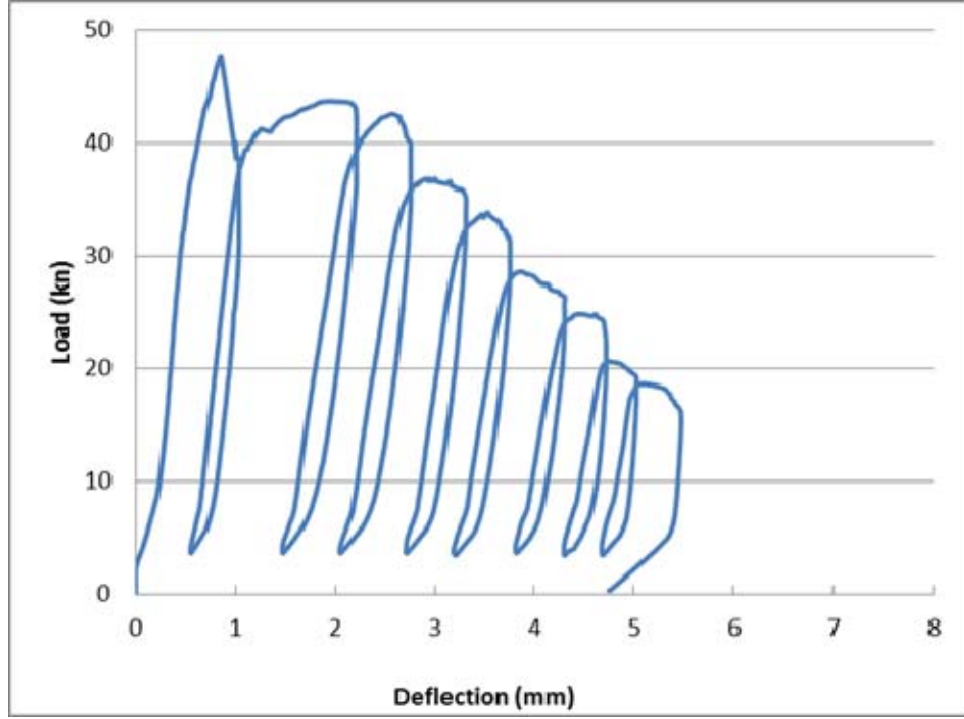


Figure B11: Loading and unloading cycles for control samples (6.2% steel fibers)
Load vs. Deflection

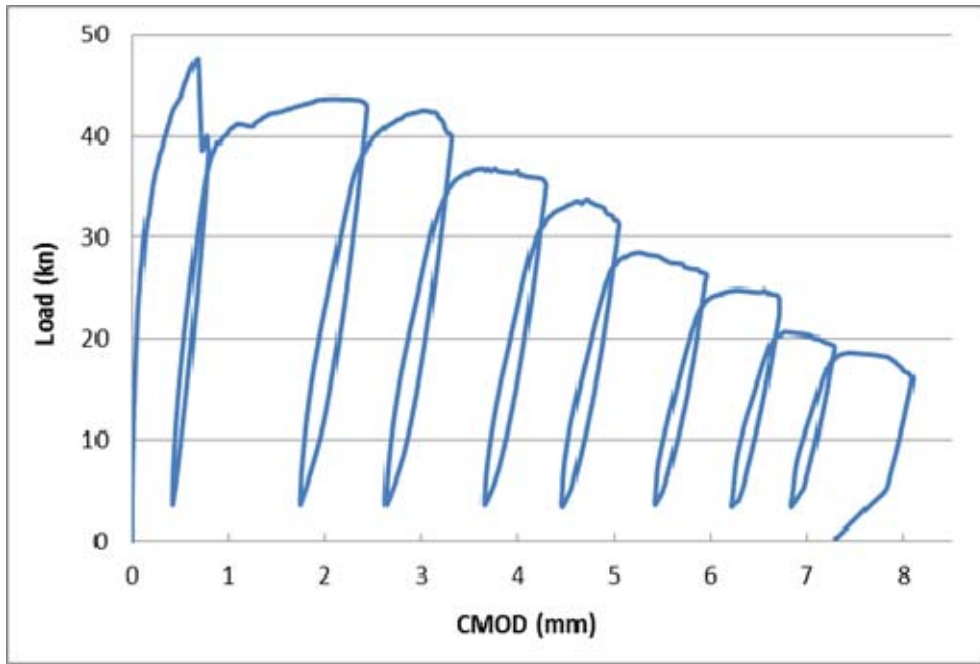


Figure B12: Loading and unloading cycles for control samples (6.2% steel fibers)
Load vs. CMOD

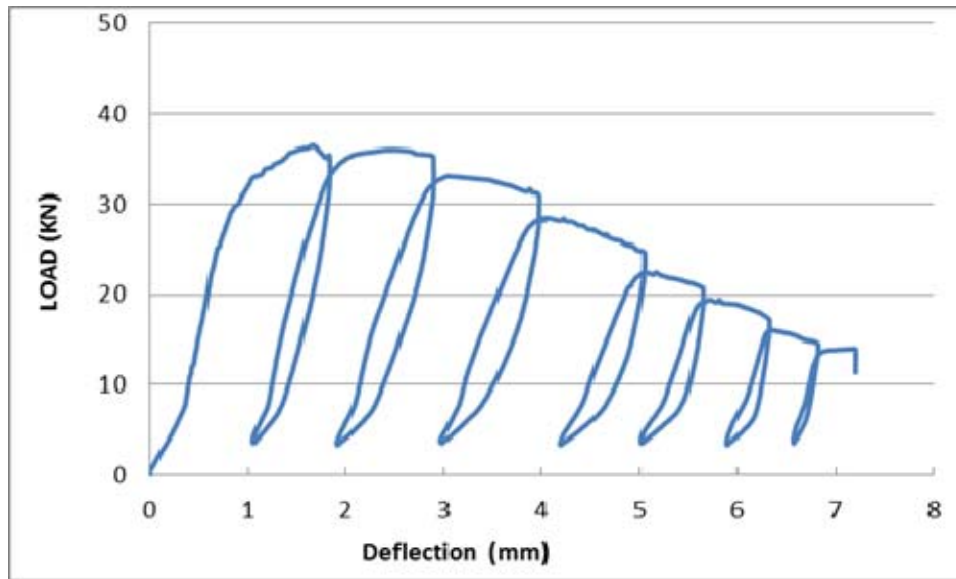


Figure B13: Loading and unloading cycles for control samples (6.2% steel fibers)
Load vs. Deflection

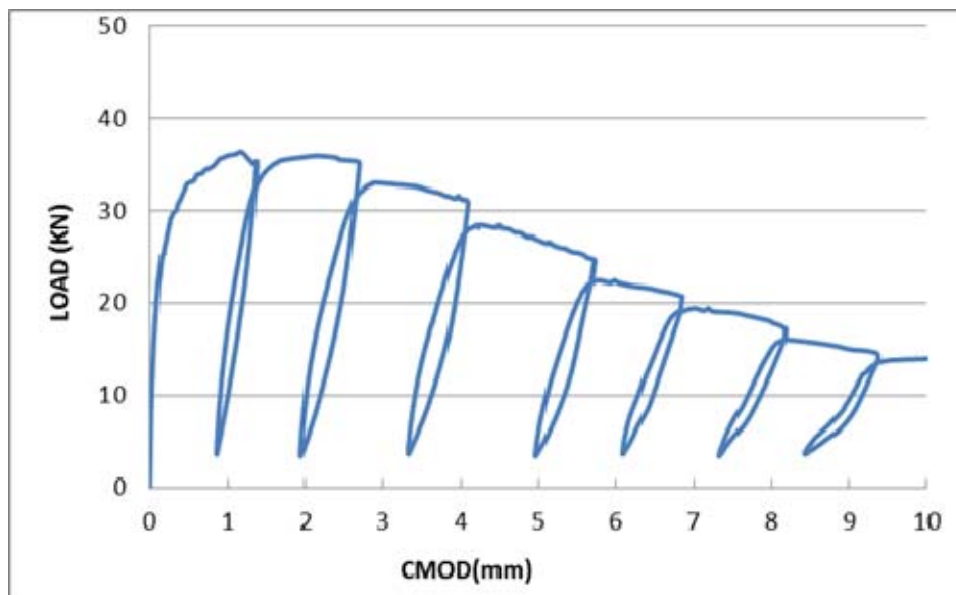


Figure B14: Loading and unloading cycles for control samples (6.2% steel fibers)
Load vs. Deflection

B- III) HEAT-COOL CYCLES OF DUCTAL (6.2% STEEL FIBERS)

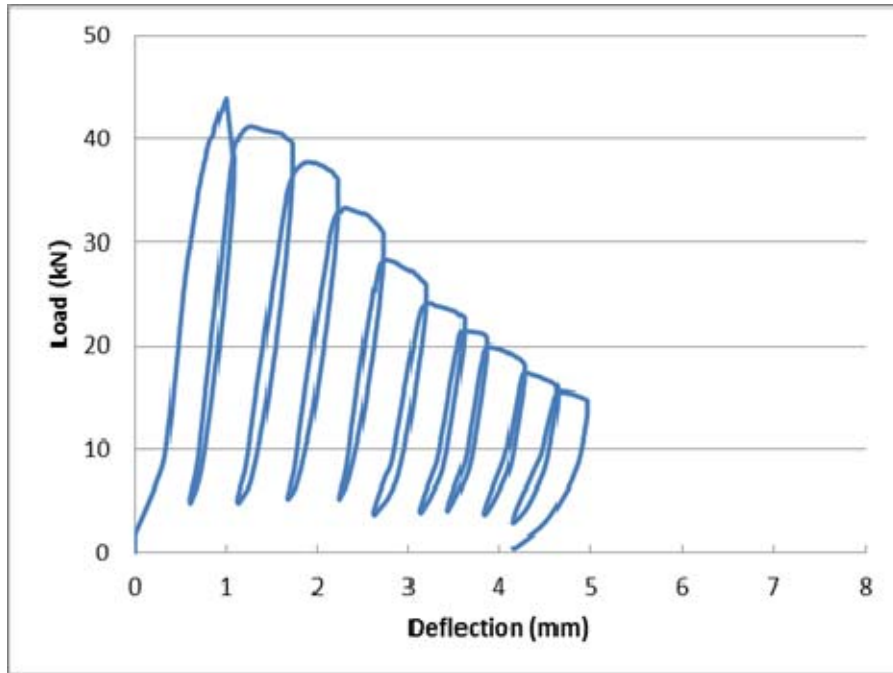


Figure B15: Loading and unloading cycles for heat-cool cycles (6.2% steel fibers) Load vs. Deflection

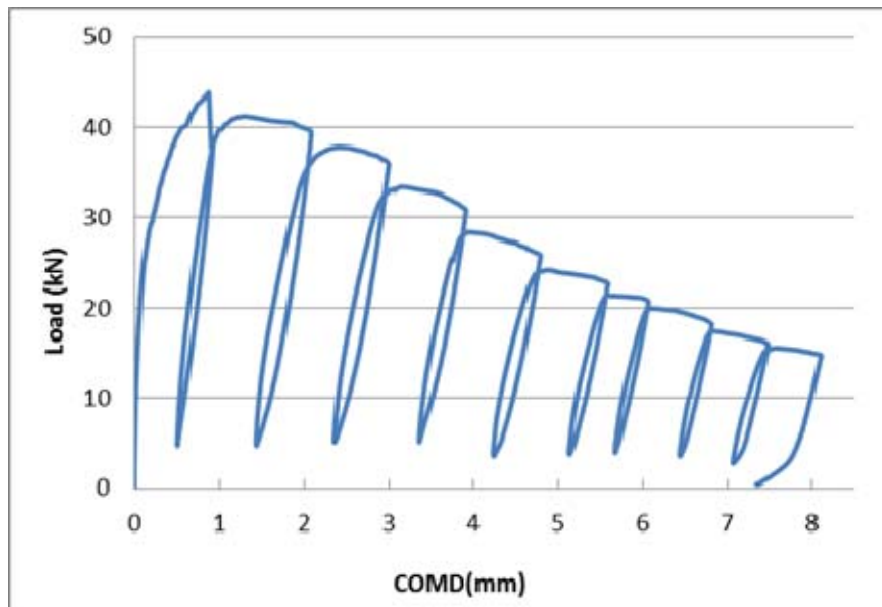


Figure B16: Loading and unloading cycles for heat-cool cycles (6.2% steel fibers) Load vs. COMD

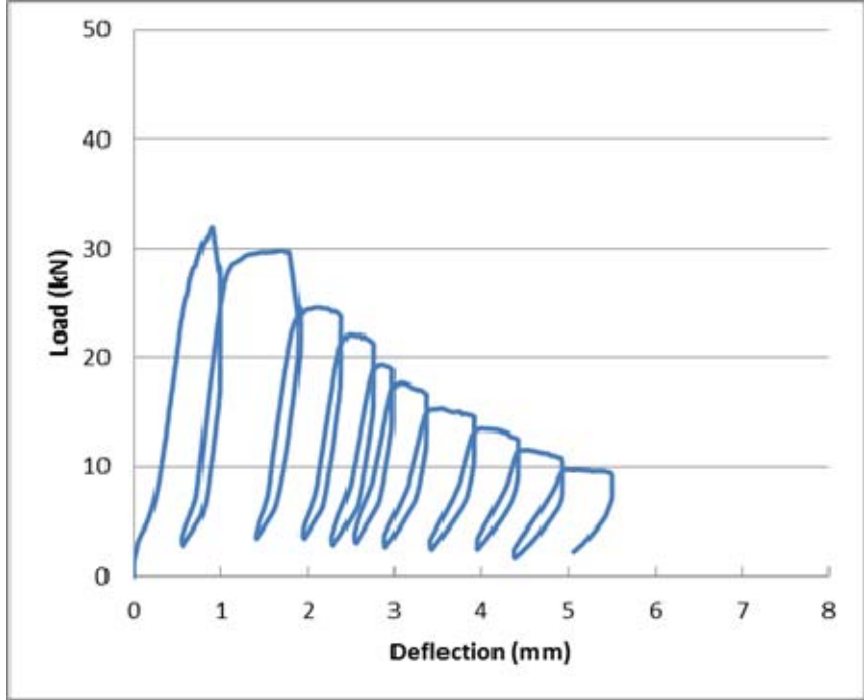


Figure B17: Loading and unloading cycles for heat-cool cycles (6.2% steel fibers) Load vs. Deflection

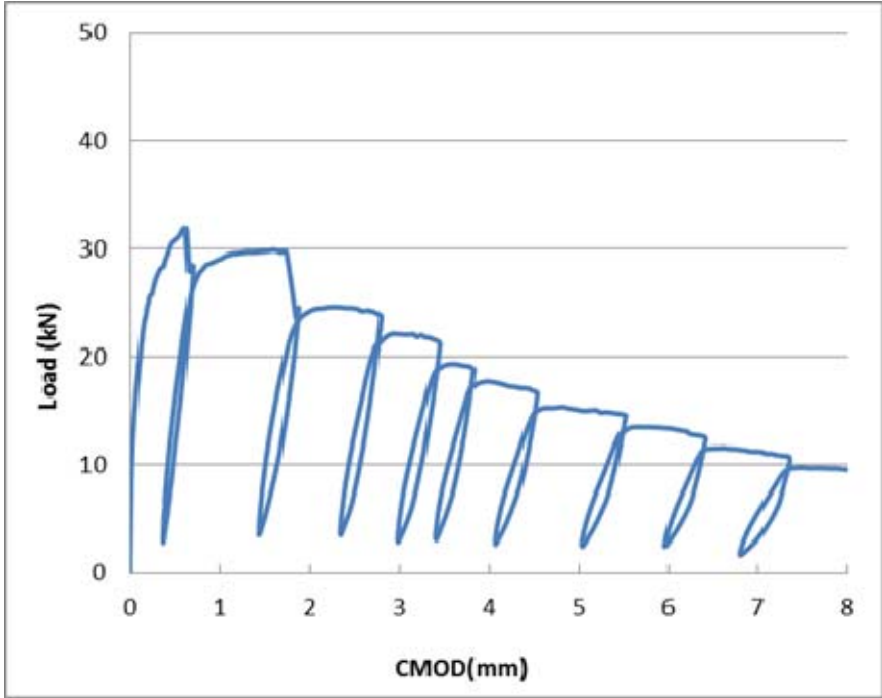


Figure B18: Loading and unloading cycles for heat-cool cycles (6.2% steel fibers) Load vs. CMOD

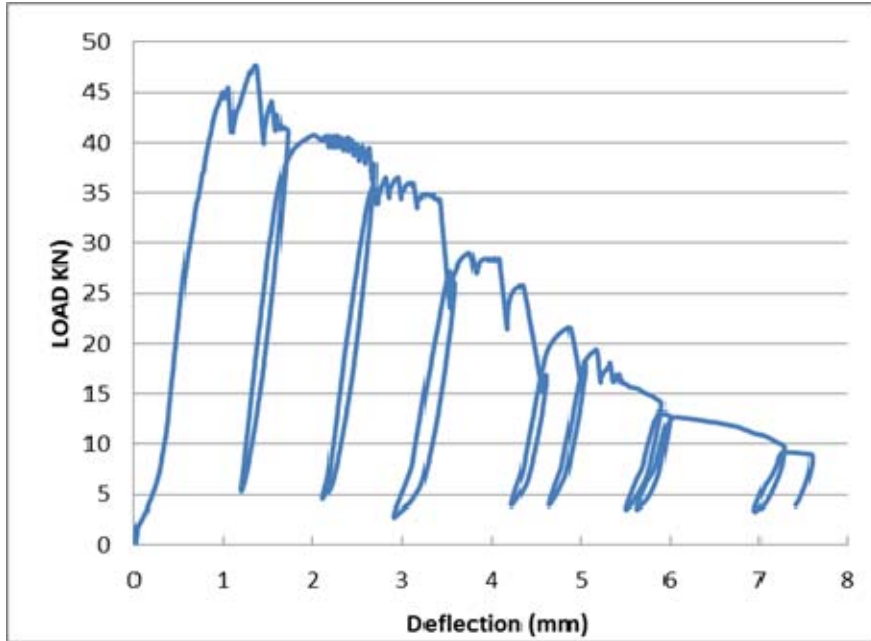


Figure B19: Loading and unloading cycles for heat-cool cycles (6.2% steel fibers) Load vs. Deflection

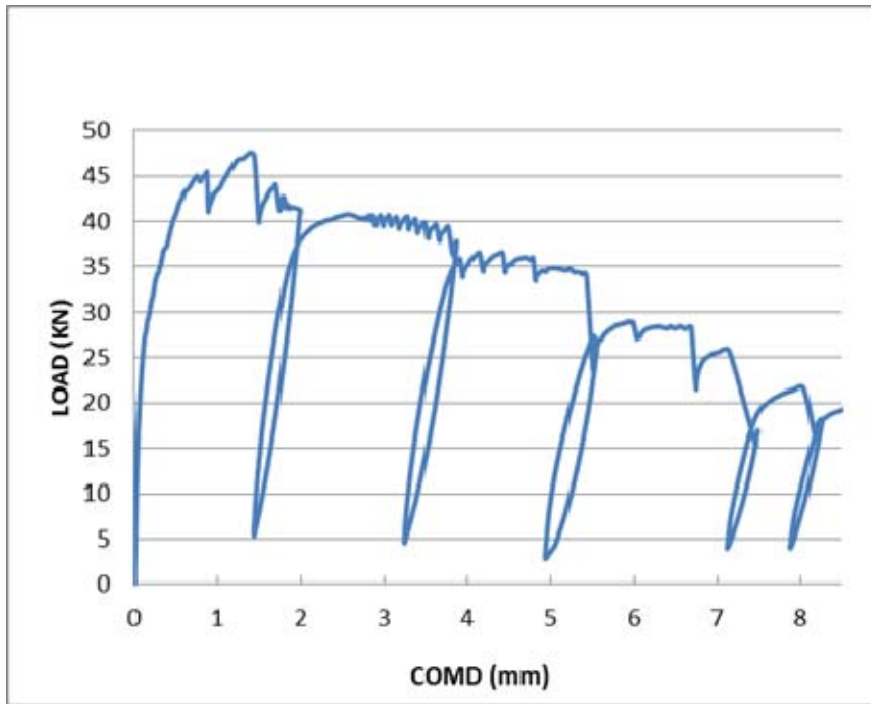


Figure B20: Loading and unloading cycles for heat-cool cycles (6.2% steel fibers) Load vs. COMD

B-IV) 28 DAYS WATER CURING OF DUCTAL (3.1% STEEL FIBERS)

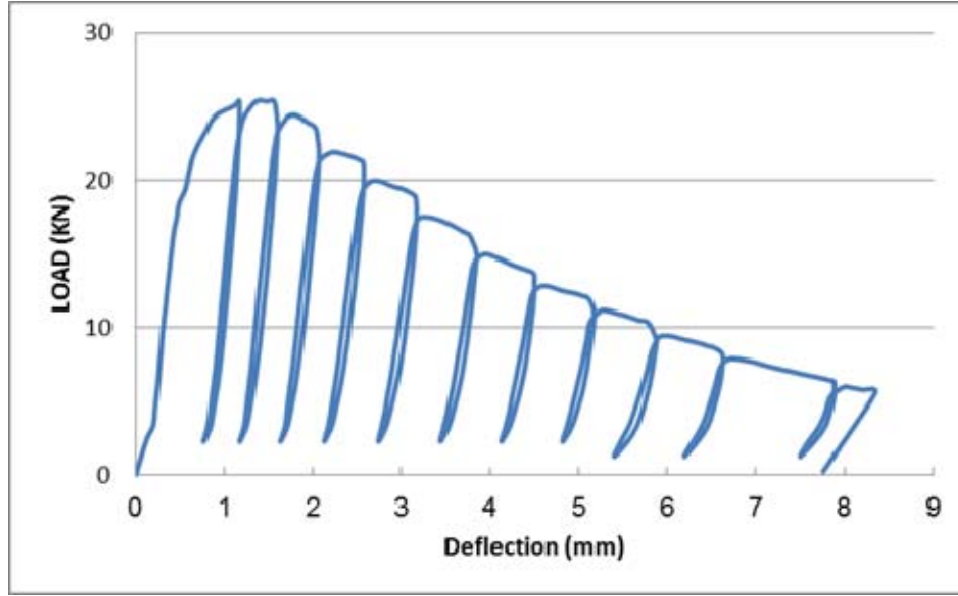


Figure B 21: Loading and unloading cycles for 28 days curing (3.1% fibers) Load vs. Deflection

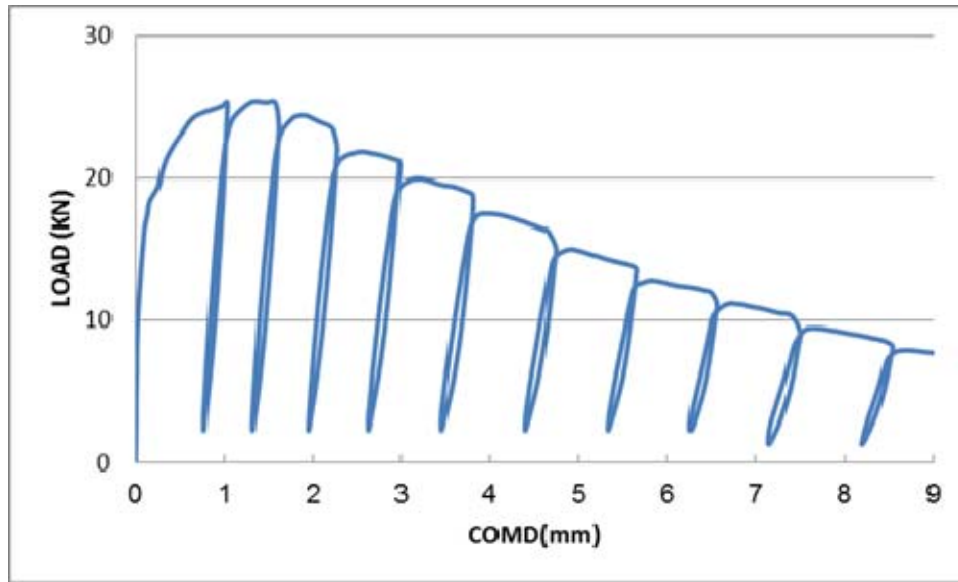


Figure B22: Loading and unloading cycles for 28 days curing (3.1% fibers) Load vs. CMOD

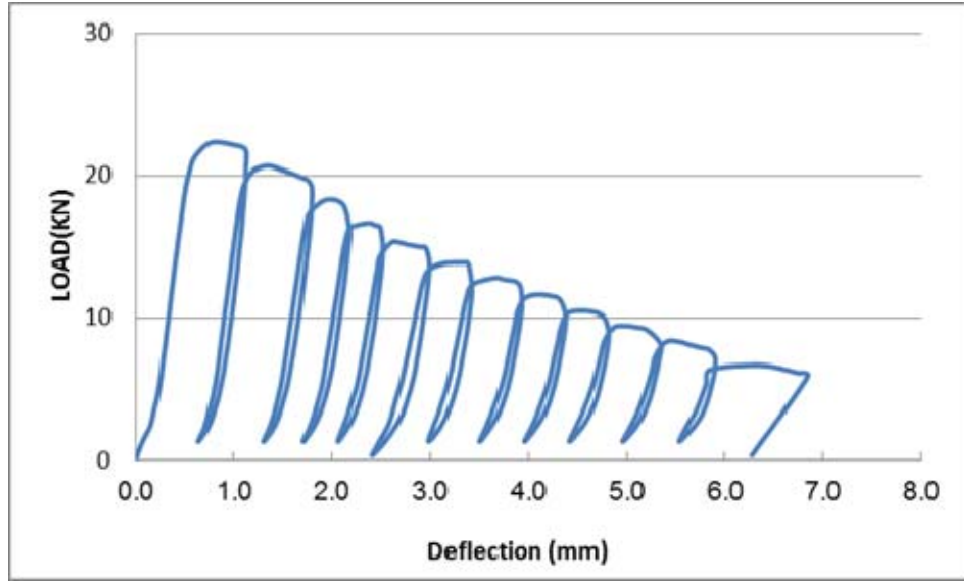


Figure B23: Loading and unloading cycles for 28 days curing (3.1% fibers) Load vs. Deflection

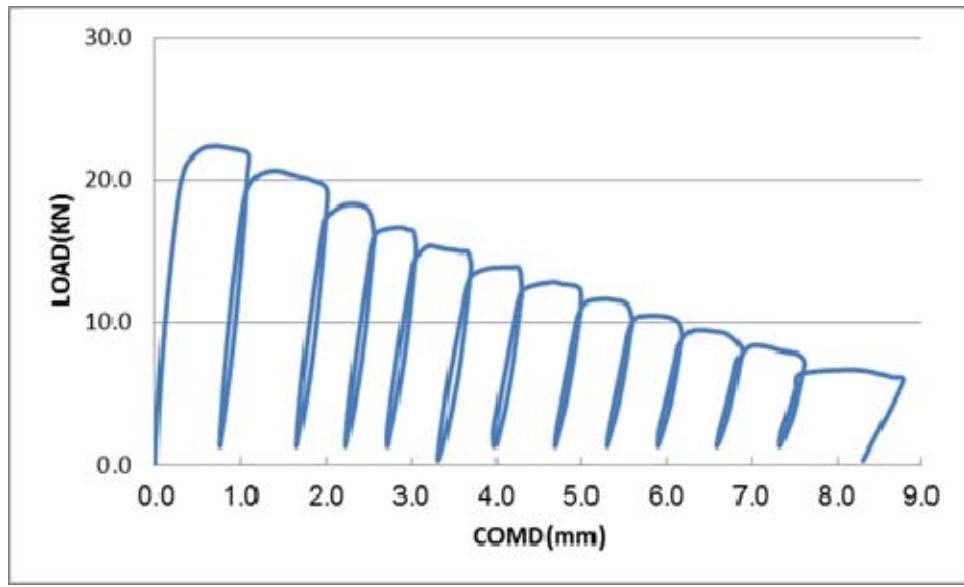


Figure B24: Loading and unloading cycles for 28 days curing (3.1% fibers) Load vs. CMOD

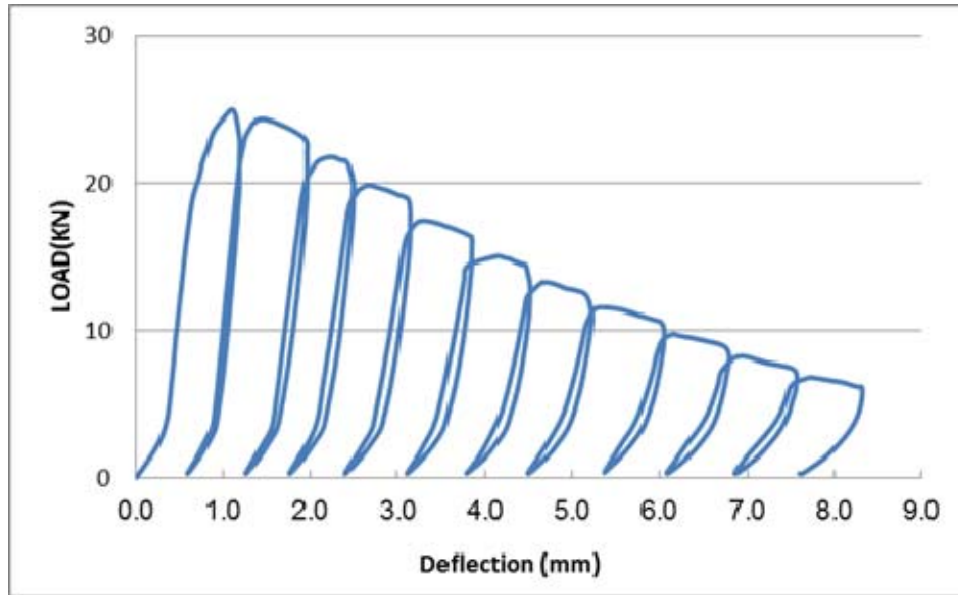


Figure B25: Loading and unloading cycles for 28 days curing (3.1% fibers) Load vs. Deflection

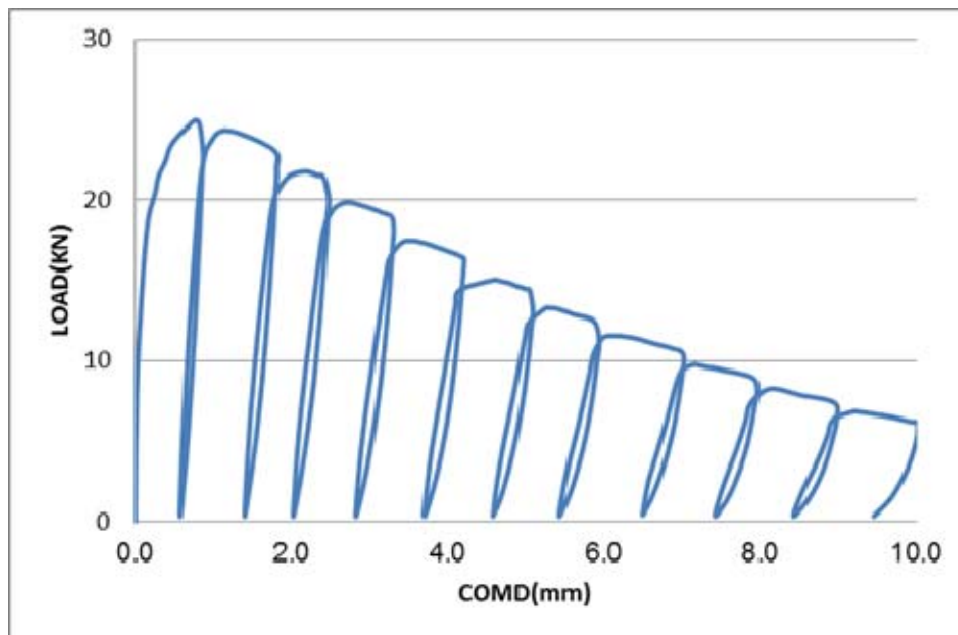


Figure B26: Loading and Unloading Cycles for 28 days curing (3.1% fibers) Load vs. CMOD

B-V) 28 DAYS WATER CURING OF DUCTAL (0% STEEL FIBERS)

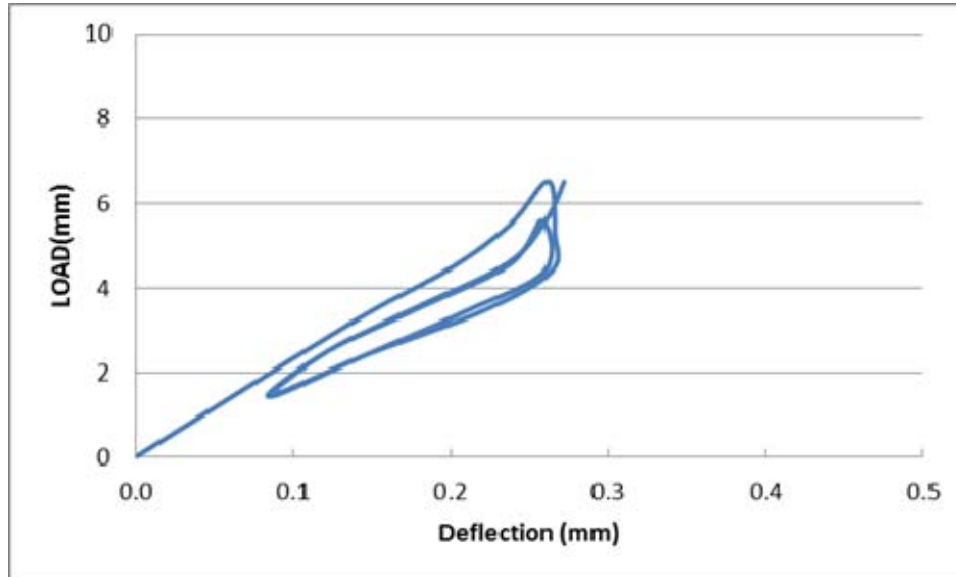


Figure B27: Loading and unloading cycles for 28 days curing (0% fibers) Load vs. Deflection

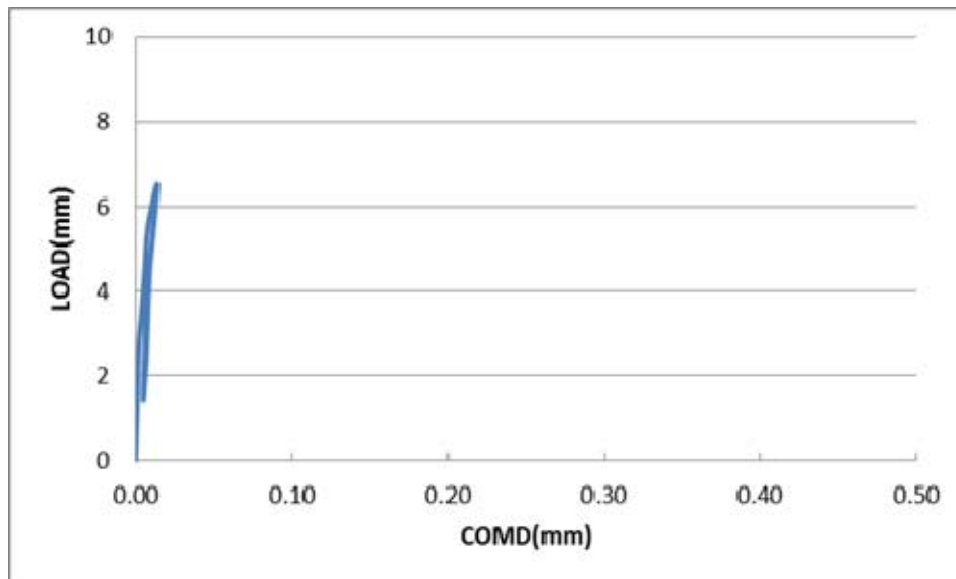


Figure B28: Loading and unloading cycles for 28 days curing (0% fibers) Load vs. COMD

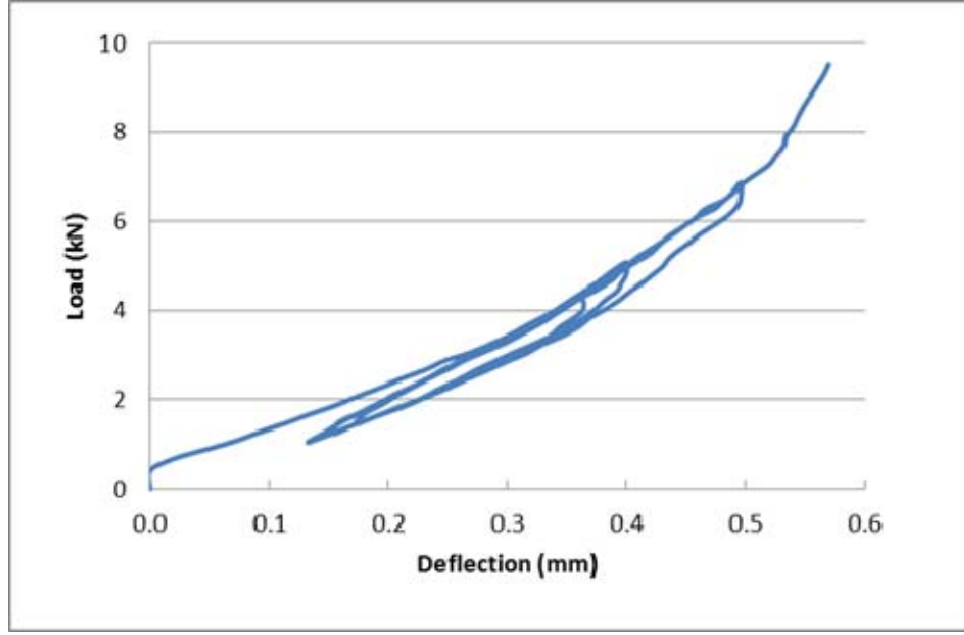


Figure B29: Loading and unloading cycles for 28 days curing (0% fibers) Load vs. Deflection

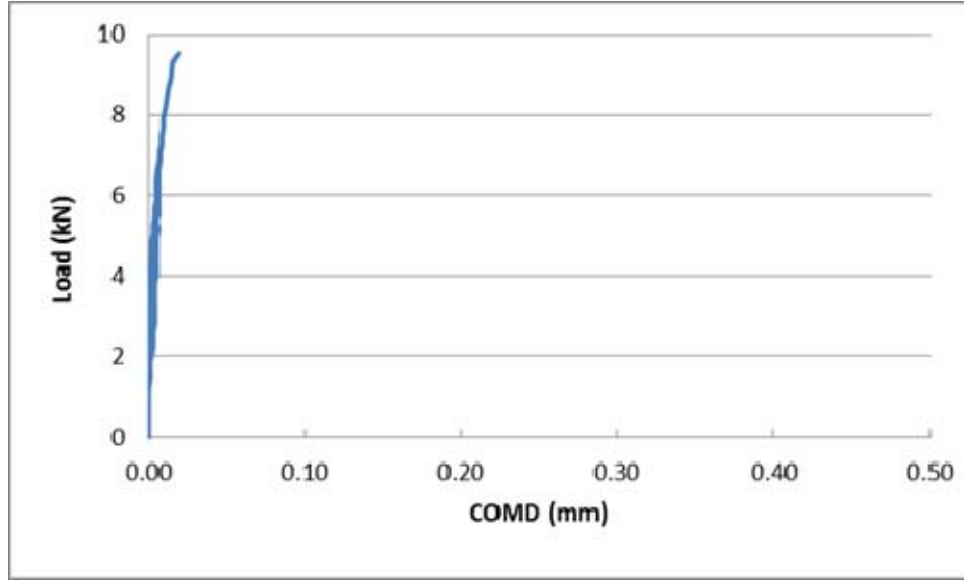


Figure B30: Loading and unloading cycles for 28 days curing (0% fibers) Load vs. CMOD

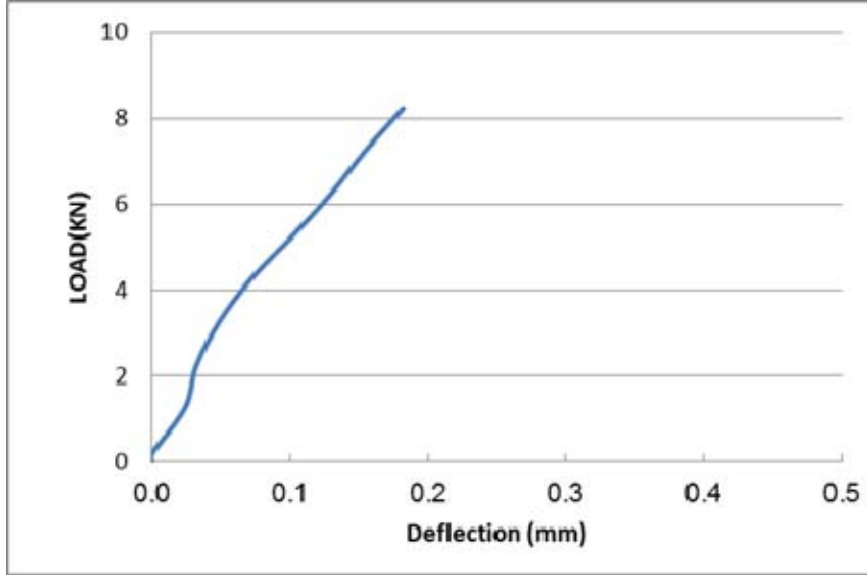


Figure B31: Loading and unloading cycles for 28 days curing (0% fibers) Load vs. Deflection

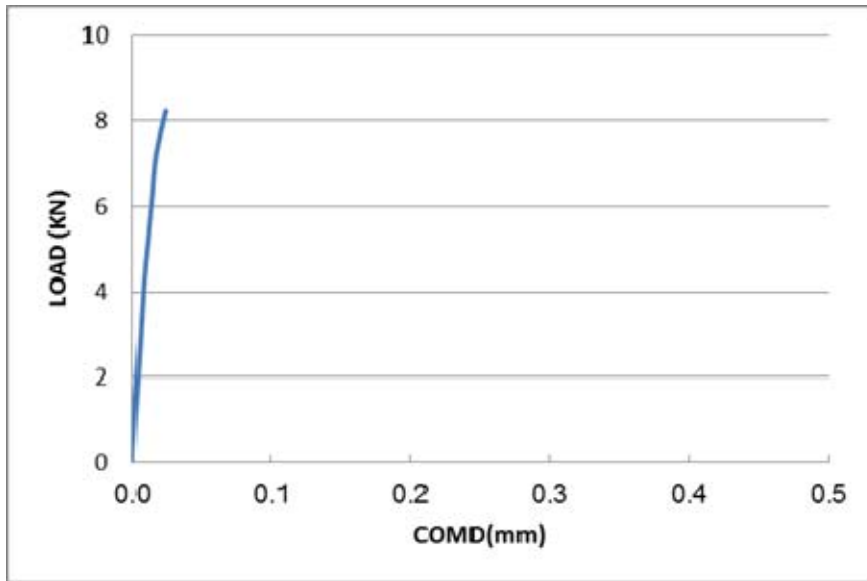


Figure B32: Loading and unloading cycles for 28 days curing (0% fibers) Load vs. CMOD

APPENDIX C

FLEXURAL STRENGTH TEST RESULTS

C-I) 7 DAYS WATER CURING OF DUCTAL (6.2% FIBERS)

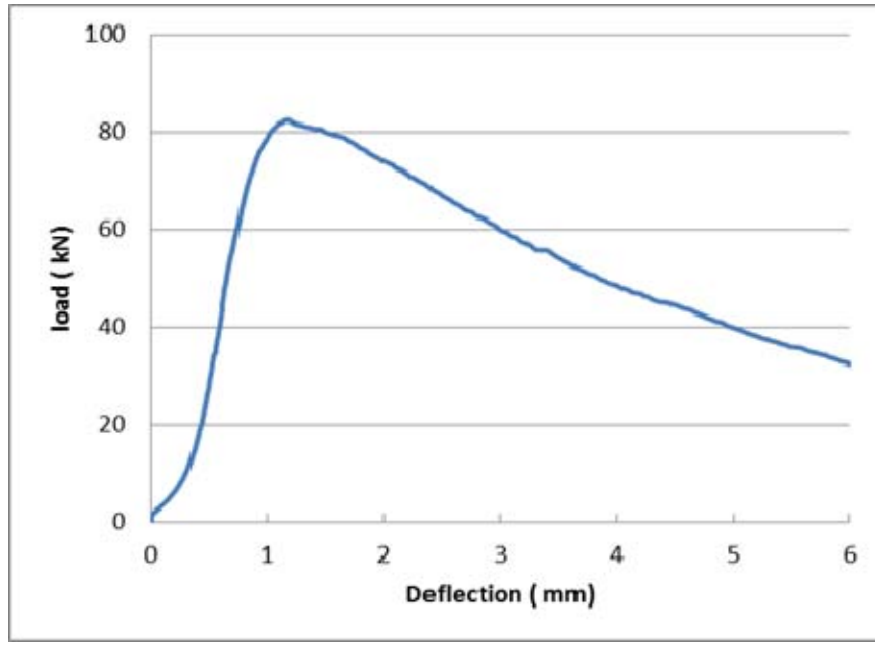


Figure C1: Load-deflection curves for Ductal specimen tested after 7 days water curing (6.2% fibers)

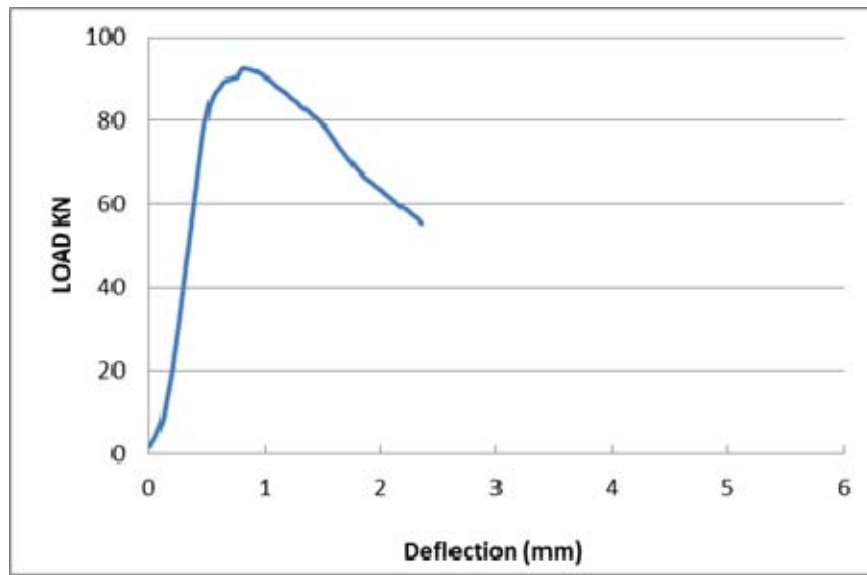


Figure C2: Load-deflection curves for Ductal specimen tested after 7 days water curing (6.2% fibers)

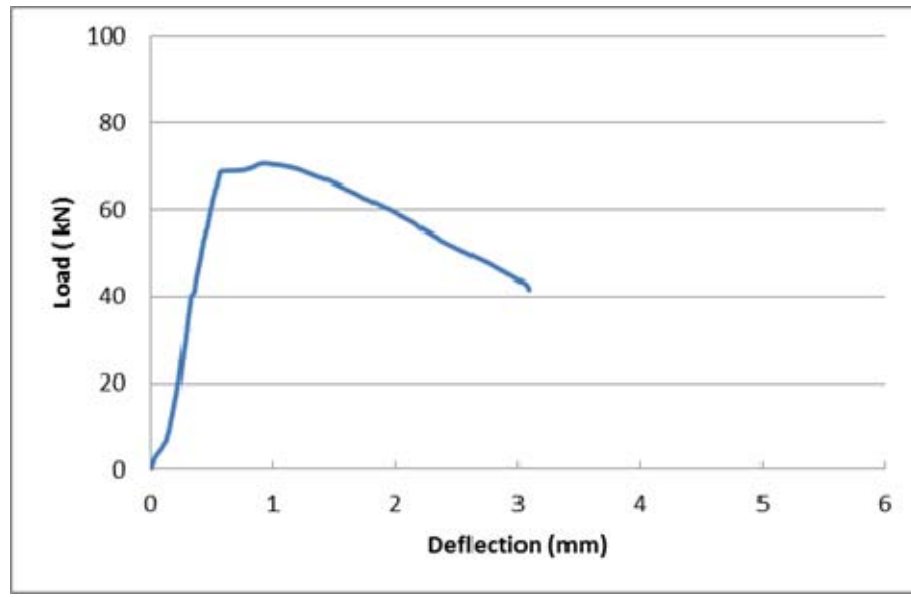


Figure C3: Load-deflection curves for Ductal specimen tested after 7 days water curing (6.2% fibers)

C-II) 28 DAYS WATER CURING OF DUCTAL (6.2% FIBERS)

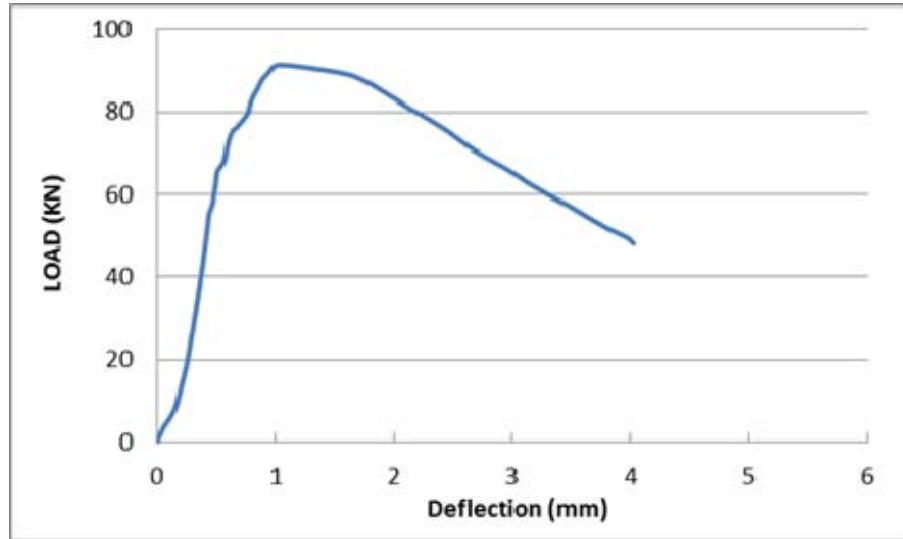


Figure C4: Load-deflection curves for Ductal specimen tested after 28 days water curing (6.2% fibers)

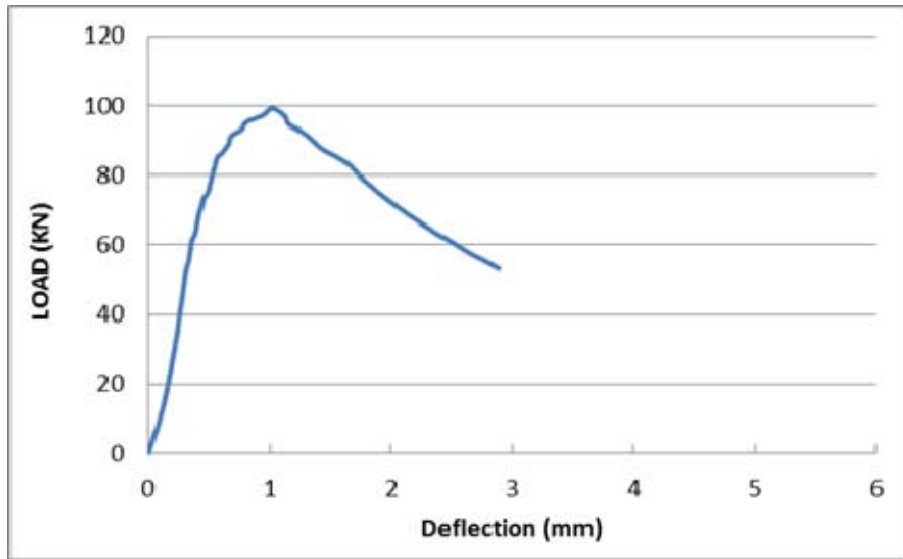


Figure C5: Load-deflection curves for Ductal specimen tested after 28 days water curing (6.2% fibers)

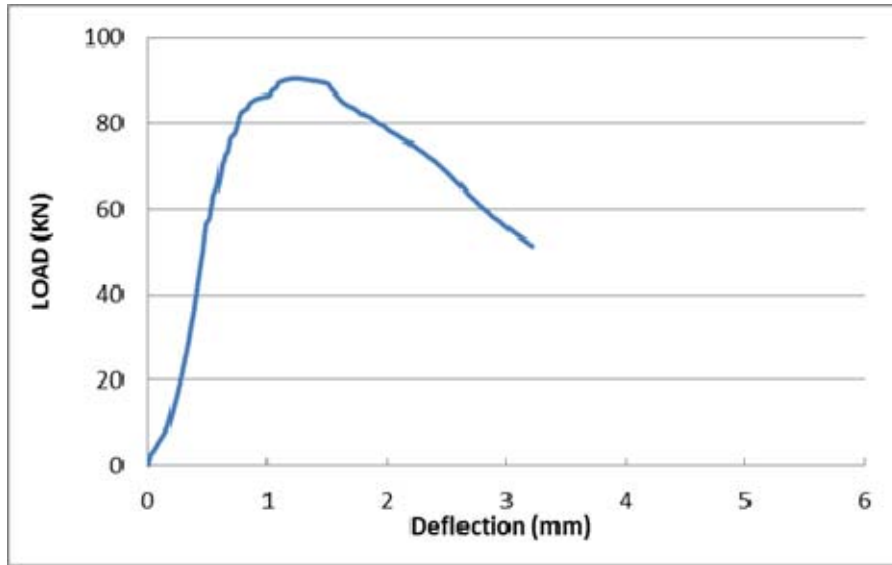


Figure C6: Load-deflection curves for Ductal specimen tested after 28 days water curing (6.2% fibers)

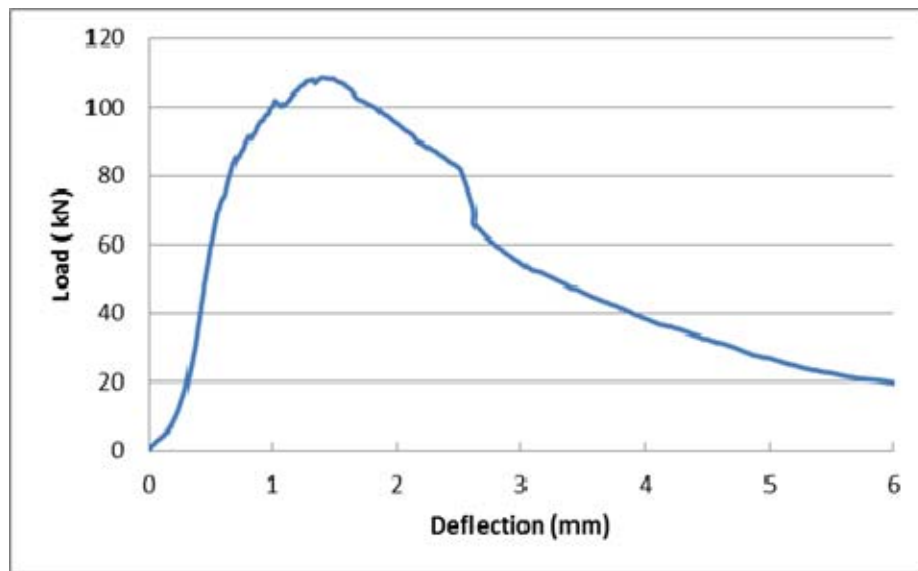


Figure C7: Load-deflection curves for Ductal specimen tested after 28 days water curing (6.2% fibers)

C-III) EXPOSURE CONDITIONS OF DUCTAL AFTER 6 MONTHS

i) Control Specimens of Ductal after 6 Months (6.2% Fibers)

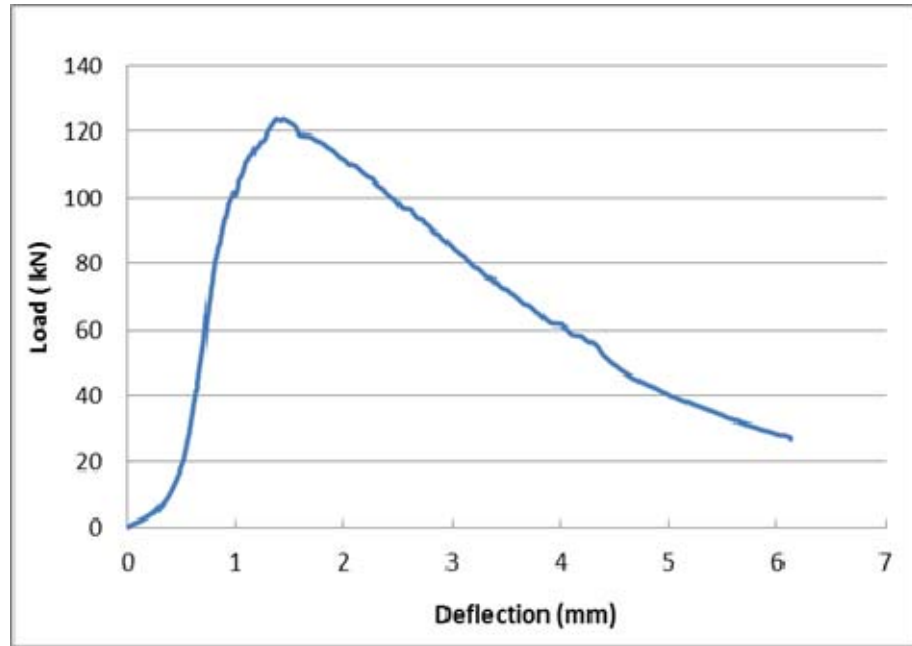


Figure C8: Load-deflection curves for Ductal specimen tested after 6 months of normal exposure (control) (6.2% fibers)

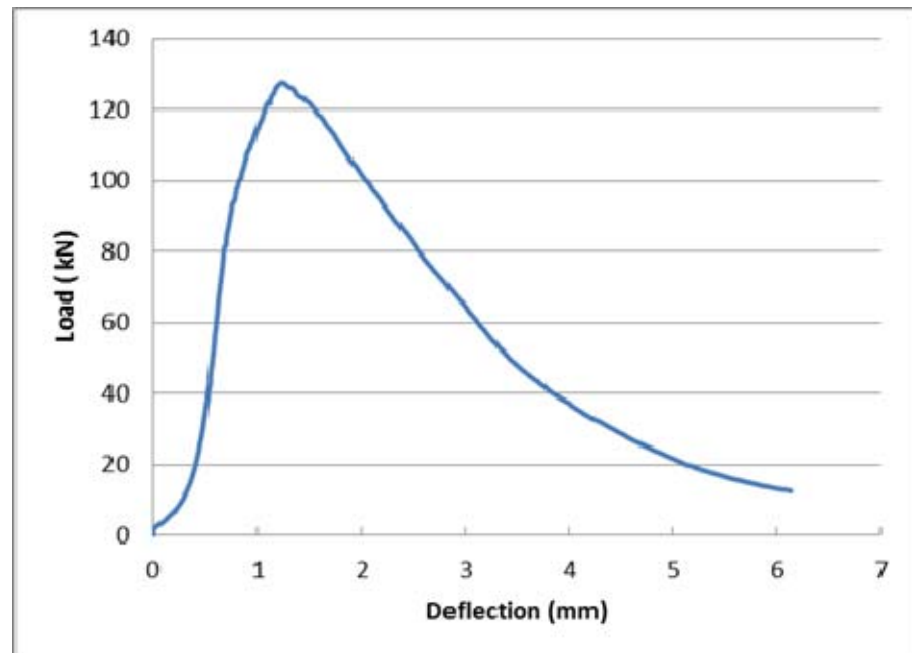


Figure C9: Load-deflection curves for Ductal specimen tested after 6 months of normal exposure (control) (6.2% fibers)

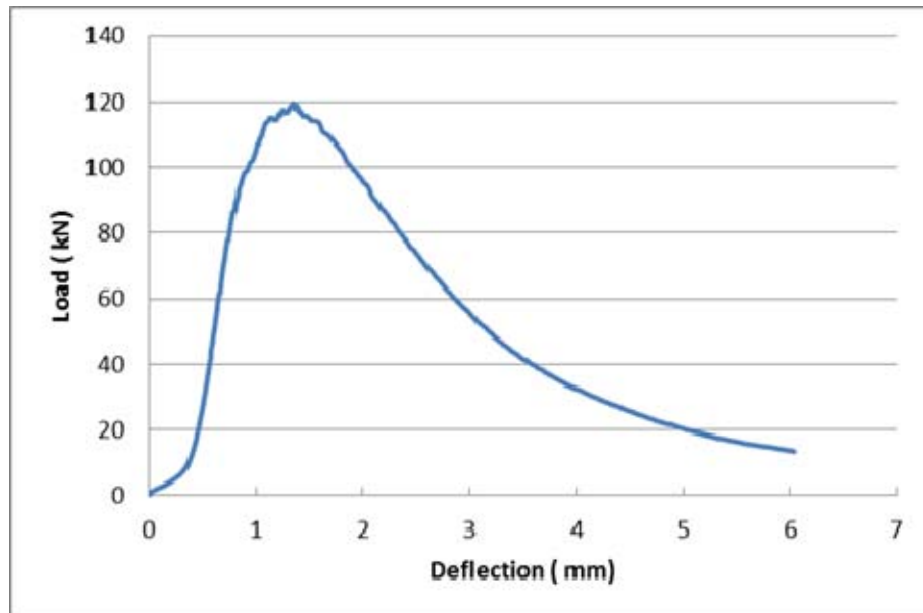


Figure C10: Load-deflection curves for Ductal specimen tested after 6 months of normal exposure (control) (6.2% fibers)

ii) Heat-Cool Cycles Specimens of Ductal after 6 Months (6.2% Fibers)

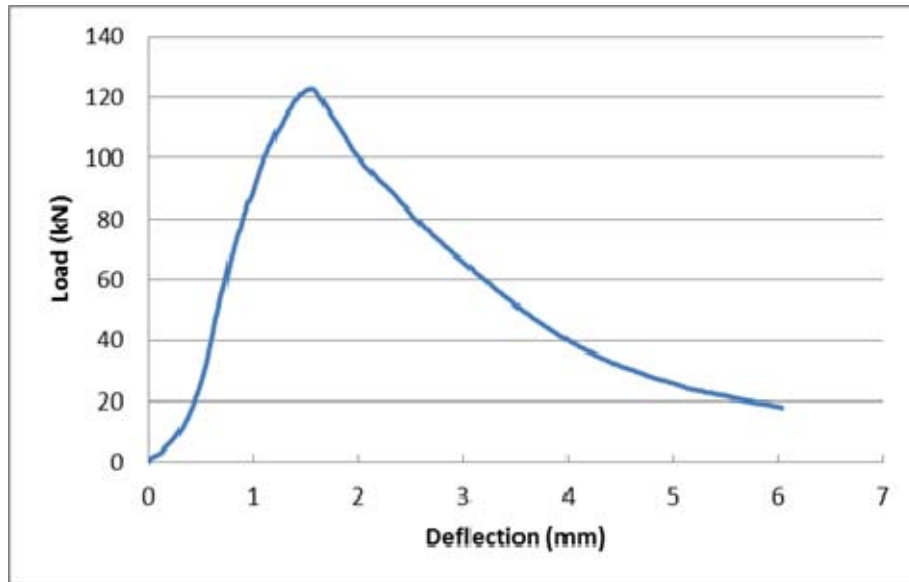


Figure C11: Load-deflection curves for Ductal specimen tested after 6 months of heat-cool cycles (6.2% fibers)

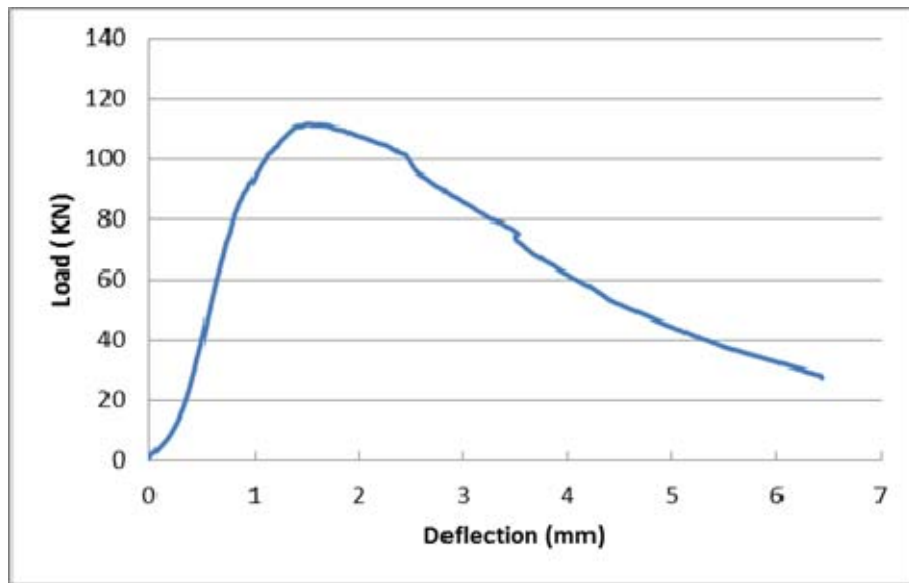


Figure C12: Load-deflection curves for Ductal specimen tested after 6 months of heat-cool cycles (6.2% fibers)

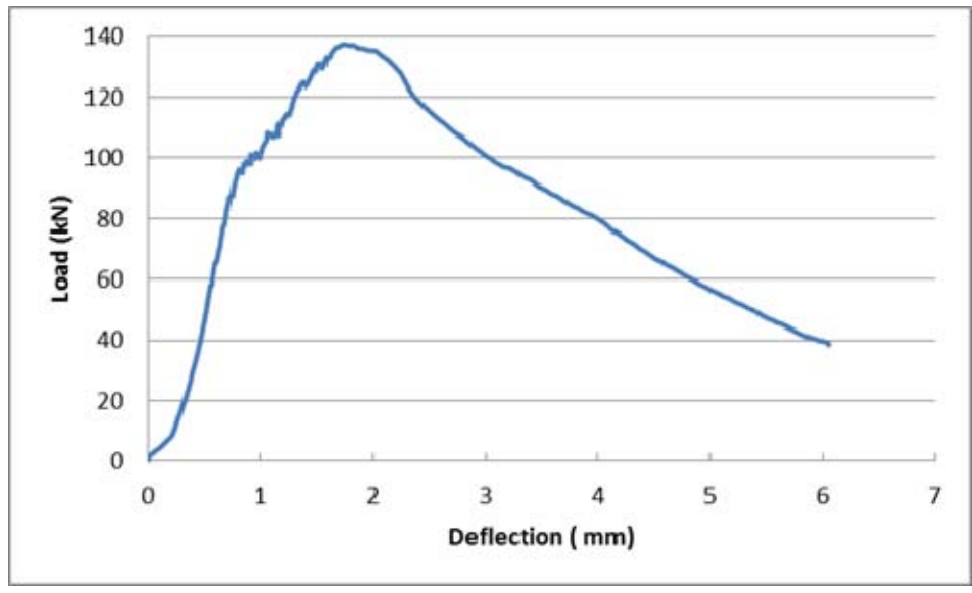


Figure C13: Load-deflection curves for Ductal specimen tested after 6 months of heat-cool cycles (6.2% fibers)

iii) Wet-Dry Cycles Specimens of Ductal after 6 Months (6.2% Fibers)

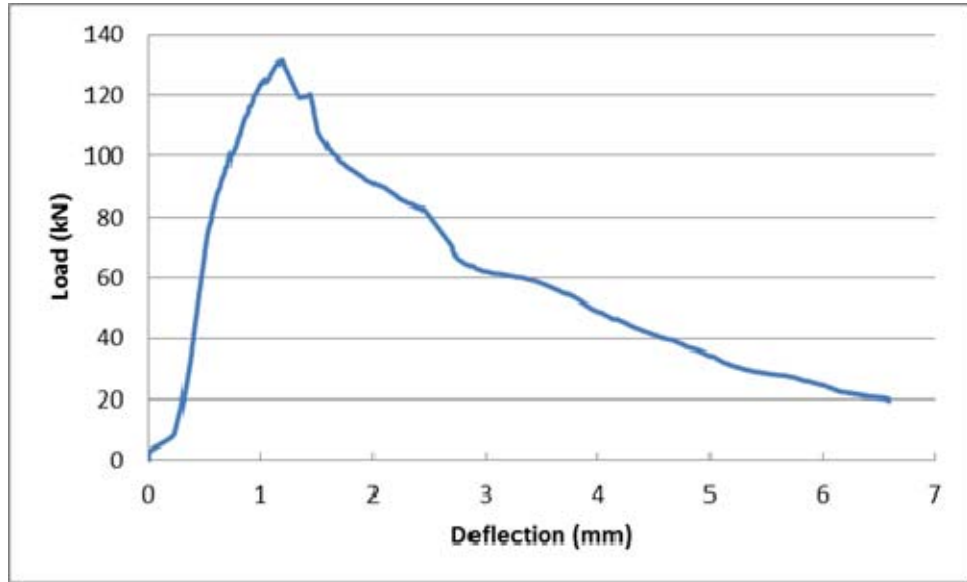


Figure C14: Load-deflection curves for Ductal specimen tested after 6 months of wet-dry cycles (6.2% fibers)

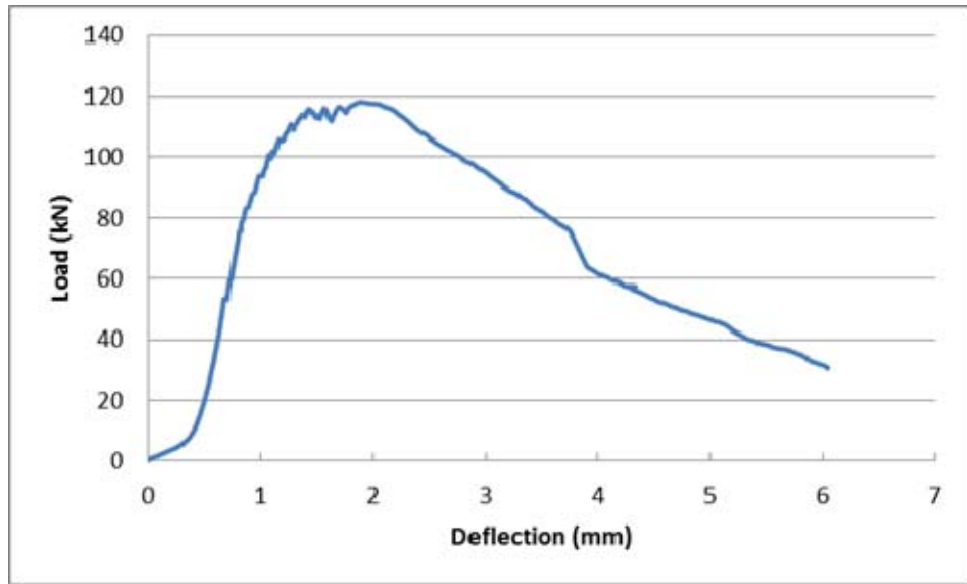


Figure C15: Load-deflection curves for Ductal specimen tested after 6 months of wet-dry cycles (6.2% fibers)

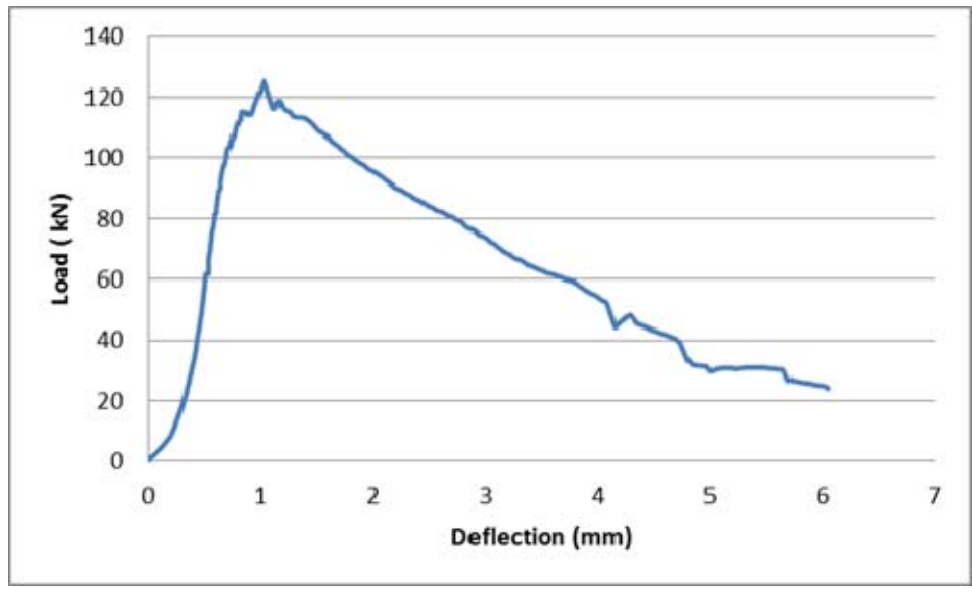


Figure C16: Load-deflection curves for Ductal specimen tested after 6 months of wet-dry cycles (6.2% fibers)

C-IV) 28 DAYS WATER CURING OF DUCTAL (3.1% FIBERS)

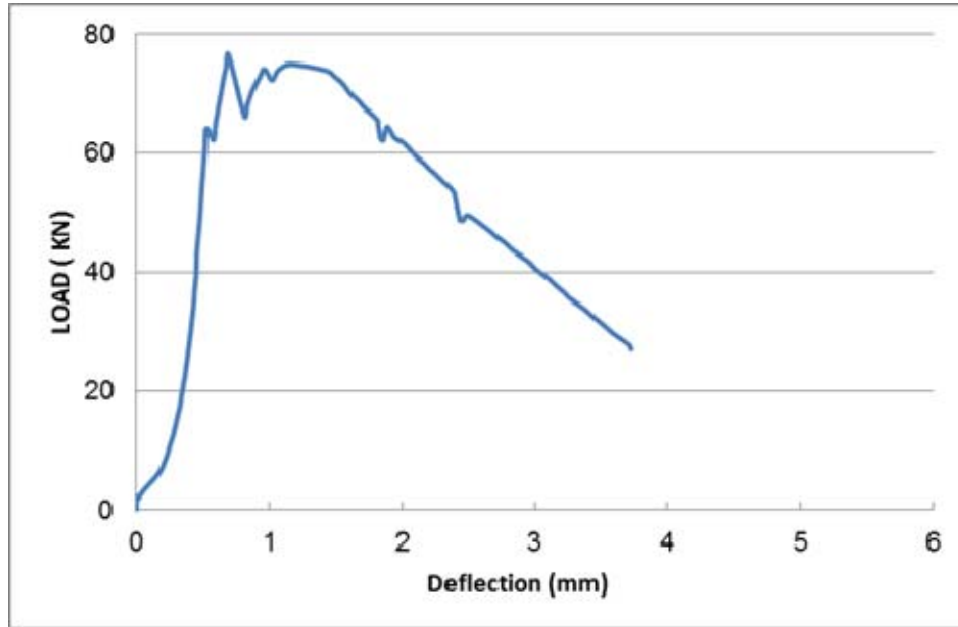


Figure C17: Load-deflection curves for Ductal specimen tested after 28 days water curing (3.1% fibers)

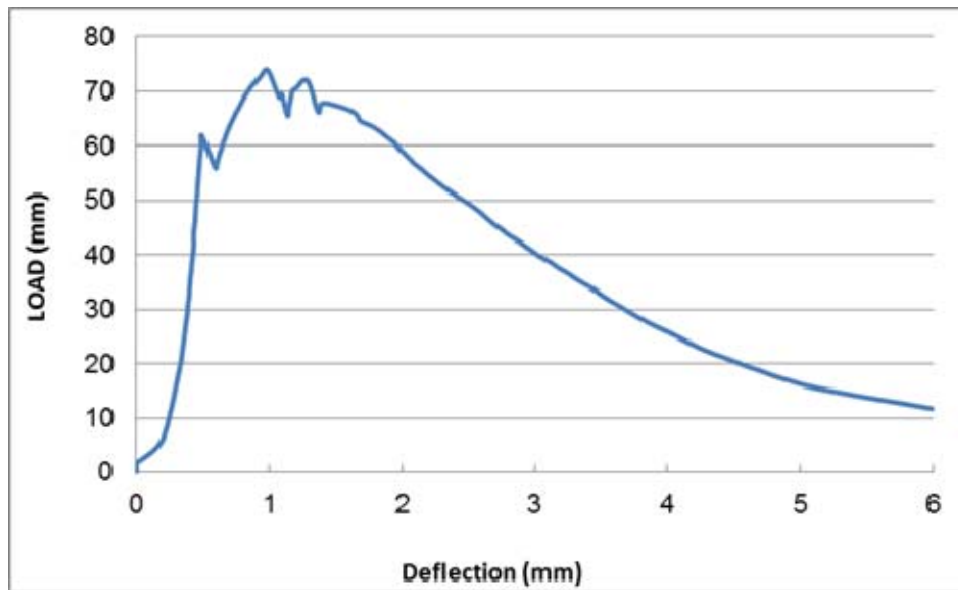


Figure C18: Load-deflection curves for Ductal specimen tested after 28 days water curing (3.1% fibers)

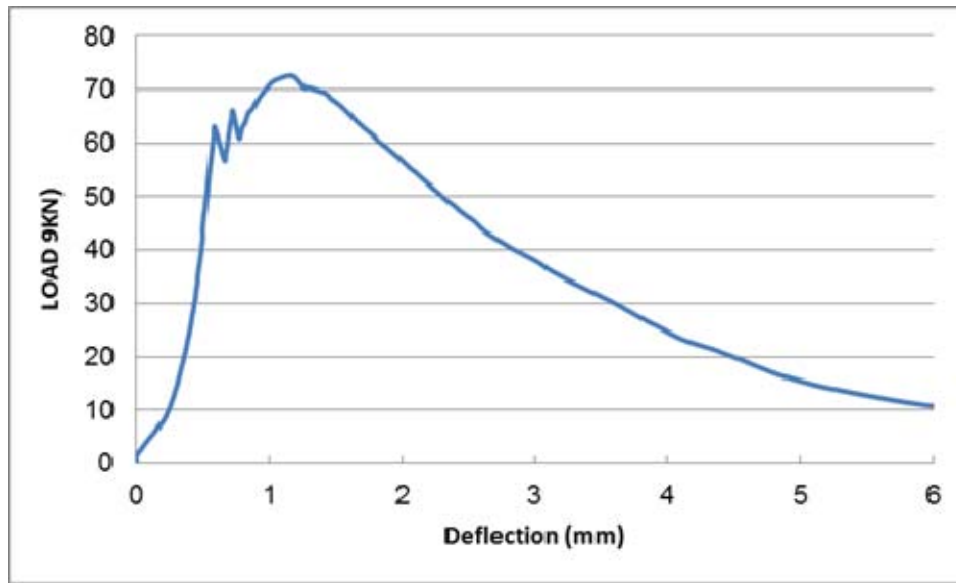


Figure C19: Load-deflection curves for Ductal specimen tested after 28 days water curing (3.1% fibers)

C-V) 28 DAYS WATER CURING OF DUCTAL (0 % FIBERS)

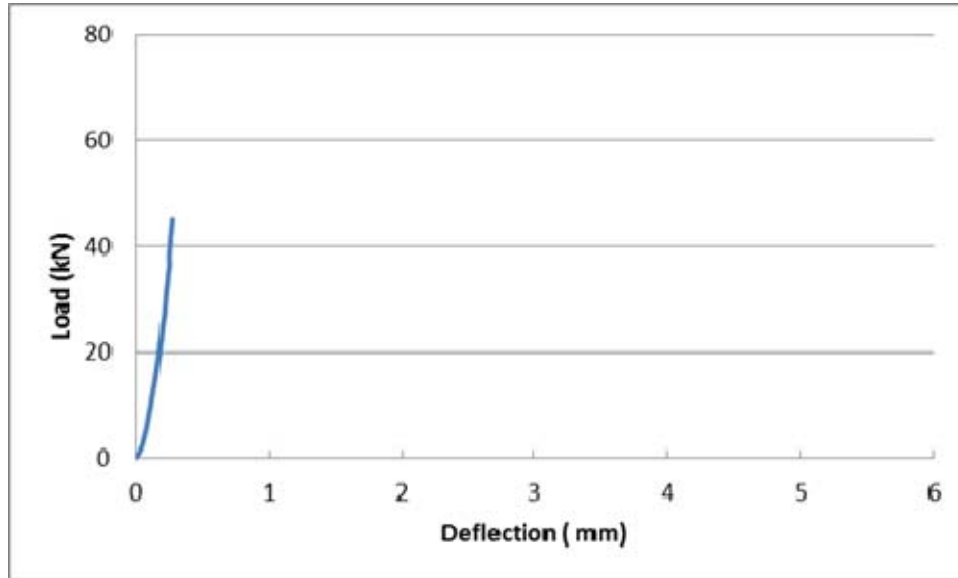


Figure C20: Load-deflection curves for Ductal specimen tested after 28 days water curing (0% fibers)

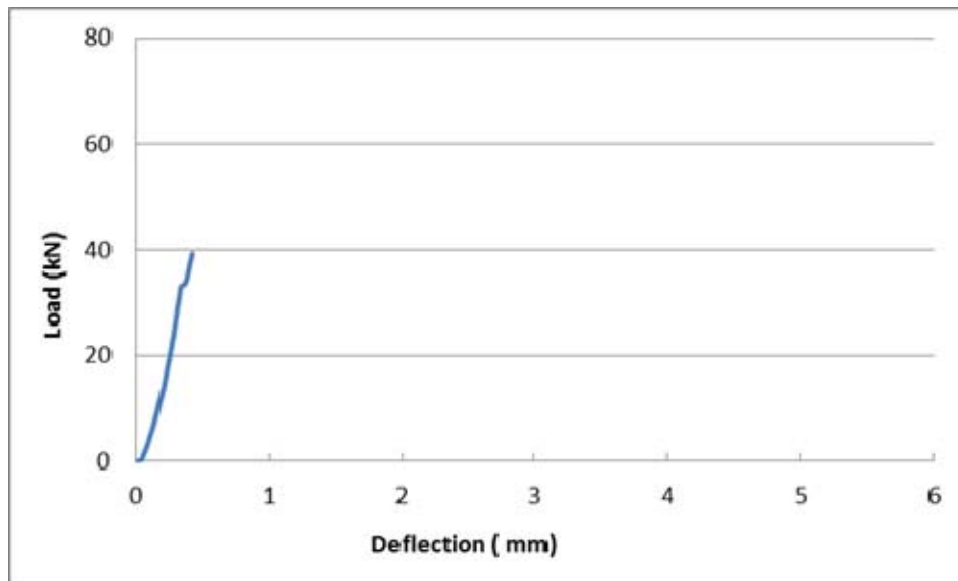


Figure C21: Load-deflection curves for Ductal specimen tested after 28 days water curing (0% fibers)

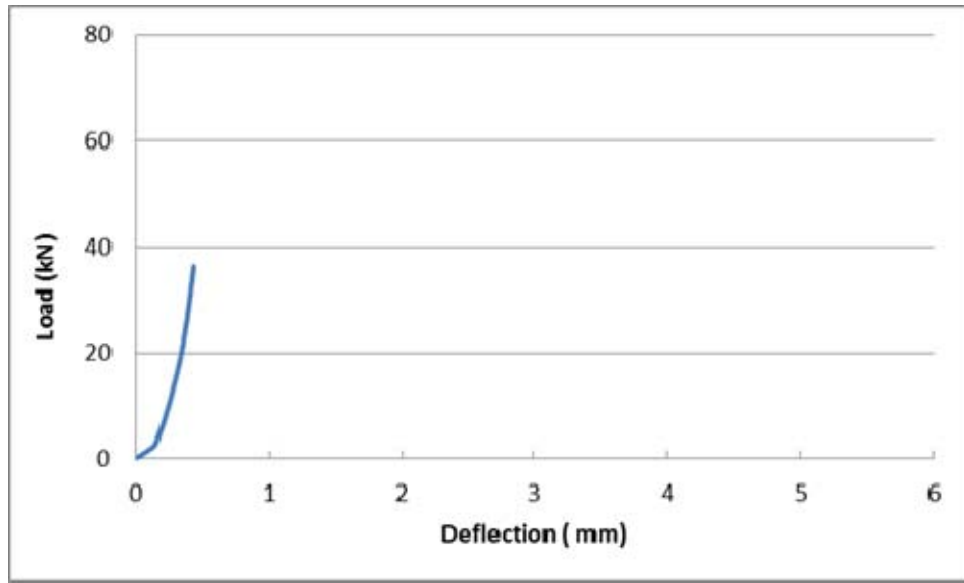


Figure C22: Load-deflection curves for Ductal specimen tested after 28 days water curing (0% fibers)

VITAE

Name : **Ibrahim Yahya Ahmed Hakeem**

Nationality : Yemeni

Date of Birth : 23 January 1975

Education :

- Graduated from the Industrial Technical Institute in 1995, Civil Engineering Department, Aden, Yemen (**first rank with honor**).
- Graduated from Aden University with B.Sc. degree in the civil engineering, in 2001 with **excellent grade (4.62/5) (Received First Honor Awards in all the semesters in the BS program)**.
- Received a scholarship from the Ministry of Higher Education at Aden University to study MS degree at KFUPM in 2007.
- M.S (Structures) from King Fahd University of Petroleum and Minerals, June 2011, **GPA (3.88/4)**

Work Experience:

- * In 2001, appointed as a graduate assistant at Aden University, college of engineering and I am still working there as a faculty member.
- * During the period from 2002 right 2006, I worked as a supervisor and engineer designer for a lot of reinforced concrete projects in both the national and private sectors in Yemen.

Present Address: KFUPM, Dhahran, Saudi Arabia, T.L: 0569584746

E-mail: ibrahimhakeem75@yahoo.com

